Rapporter och meddelanden 141

Geology of the Northern Norrbotten ore province, northern Sweden

Paper 2 (13)

Editor: Stefan Bergman

SGU
Sveriges geologiska undersökning
Geological Survey of Sweden

Rapporter och meddelanden 141

Geology of the Northern Norrbotten ore province, northern Sweden

Editor: Stefan Bergman

Sveriges geologiska undersökning
2018

ISSN 0349-2176
ISBN 978-91-7403-393-9

Cover photos:
Upper left: View of Torneälven, looking north from Sakkaravaara, northeast of Kiruna. ***Photographer:*** Stefan Bergman.
Upper right: View (looking north-northwest) of the open pit at the Aitik Cu-Au-Ag mine, close to Gällivare. The Nautanen area is seen in the background. ***Photographer:*** Edward Lynch.
Lower left: Iron oxide-apatite mineralisation occurring close to the Malmberget Fe-mine. ***Photographer:*** Edward Lynch.
Lower right: View towards the town of Kiruna and Mt. Luossavaara, standing on the footwall of the Kiruna apatite iron ore on Mt. Kiirunavaara, looking north. ***Photographer:*** Stefan Bergman.

Head of department, Mineral Resources: Kaj Lax
Editor: Stefan Bergman

Layout: Tone Gellerstedt och Johan Sporrong, SGU
Print: Elanders Sverige AB

Geological Survey of Sweden
Box 670, 751 28 Uppsala
phone: 018-17 90 00
fax: 018-17 92 10
e-mail: sgu@sgu.se
www.sgu.se

Table of Contents

Introduktion (in Swedish) **6**

Introduction **7**

1.Regional geology of northern Norrbotten County **9**
References 14

2. Geology, lithostratigraphy and petrogenesis of c. 2.14 Ga greenstones in the Nunasvaara and Masugnsbyn areas, northernmost Sweden **19**
Abstract 19
Introduction 20
Regional setting of Norrbotten greenstone belts 21
Geology of the Nunasvaara and Masugnsbyn greenstone successions 23
Petrogenesis of the greenstones: Preliminary U-Pb geochronology, lithogeochemistry and Sm-Nd isotopic results 52
Summary and conclusions 68
Acknowledgements 69
References 70

3. Stratigraphy and ages of Palaeoproterozoic metavolcanic and metasedimentary rocks at Käymäjärvi, northern Sweden **79**
Abstract 79
Introduction 80
General geology 80
Structure and stratigraphy of the Käymäjärvi area 81
Sample description 89
Analytical methods 90
Analytical results 91
Discussion 96
Conclusions 100
Acknowledgements 101
References 101

4. Petrological and structural character of c. 1.88 Ga meta-volcanosedimentary rocks hosting iron oxide-copper-gold and related mineralisation in the Nautanen–Aitik area, northern Sweden **107**
Abstract 107
Introduction 108
Regional setting 108
Geology of the Nautanen–Aitik area 110
Structural geology and deformation 132
Summary and Conclusions 144
Acknowledgements 144
References 145

5. Age and lithostratigraphy of Svecofennian volcanosedimentary rocks at Masugnsbyn, northernmost Sweden – host rocks to Zn-Pb-Cu- and Cu ±Au sulphide mineralisations **151**
Abstract 151
Introduction 152
Geological overview 153
Discussion and preliminary conclusions 194
Acknowledgements 197
References 198

6.Folding observed in Palaeoproterozoic supracrustal rocks in northern Sweden 205
Abstract 205
Introduction 205
Geological setting 207
Structural geological models 209
Geophysical data 212
Discussion and Conclusions 251
References 255

7. The Pajala deformation belt in northeast Sweden:
Structural geological mapping and 3D modelling around Pajala 259
Abstract 259
Geological setting 259
Structural analysis 263
2D regional geophysical modelling and geological interpretation 272
Local and semi-regional 3D models 274
Discussion 280
Conclusions 283
ReferenceS 284

8. The Vakko and Kovo greenstone belts north of Kiruna:
Integrating structural geological mapping and geophysical modelling 287
Abstract 287
Introduction 287
Geological setting 289
Geophysical surveys 291
Results 296
Discussion 306
Conclusions 308
References 309

9. Geophysical 2D and 3D modelling in the areas around
Nunasvaara and Masugnsbyn, northern Sweden 311
Abstract 311
Nunasvaara 312
2D modelling of profile 1 and 2 316
Masugnsbyn 321
Regional modelling 329
Conclusion 338
References 339

10. Imaging deeper crustal structures by 2D and 3D modelling of geophysical data.
Examples from northern Norrbotten 341
Abstract 341
Introduction 341
Methodology 342
Geological setting 342
Results 345
Conclusion 358
Outlook 358
Acknowledgements 358
References 359

11. Early Svecokarelian migmatisation west of the Pajala deformation belt, northeastern Norrbotten province, northern Sweden 361
Abstract 361
Introduction 362
Geology of the Masugnsbyn area 362
Discussion 372
Conclusions 374
Acknowledgements 375
References 376

12. Age and character of late-Svecokarelian monzonitic intrusions in northeastern Norrbotten, northern Sweden 381
Abstract 381
Introduction 381
Geological setting 382
Analytical methods 387
Analytical results 388
Discussion 393
Conclusions 396
Acknowledgements 396
References 397

13. Till geochemistry in northern Norrbotten –regional trends and local signature in the key areas 401
Abstract 401
Introduction 401
Glacial geomorphology and quaternary stratigraphy of Norrbotten 403
Samples and methods 406
Results and discussion 407
Conclusions 426
Acknowledgements 427
References 427

Introduktion

Stefan Bergman & Ildikó Antal Lundin

Den här rapporten presenterar de samlade resultaten från ett delprojekt inom det omfattande tvärvetenskapliga Barentsprojektet i norra Sverige. Projektet initierades av Sveriges geologiska undersökning (SGU) som ett första led i den svenska mineralstrategin. SGU fick ytterligare medel av Näringsdepartementet för att under en fyraårsperiod (2012–2015) samla in nya geologiska, geofysiska och geokemiska data samt för att förbättra de geologiska kunskaperna om Sveriges nordligaste län. Det statligt ägda gruvbolaget LKAB bidrog också till finansieringen. Projektets strategiska mål var att, genom att tillhandahålla uppdaterad och utförlig geovetenskaplig information, stödja prospekterings- och gruvindustrin för att förbättra Sveriges konkurrenskraft inom mineralnäringen. Ny och allmänt tillgänglig geovetenskaplig information från den aktuella regionen kan hjälpa prospekterings- och gruvföretag att minska sina risker och prospekteringskostnader och främjar därigenom ekonomisk utveckling. Dessutom bidrar utökad geologisk kunskap till en effektiv, miljövänlig och långsiktigt hållbar resursanvändning. All data som har samlats in i projektet lagras i SGUs databaser och är tillgängliga via SGU.

Syftet med det här delprojektet var att få en djupare förståelse för den stratigrafiska uppbyggnaden och utvecklingen av de mineraliserade ytbergarterna i nordligaste Sverige. Resultaten, som är en kombination av ny geologisk kunskap och stora mängder nya data, kommer att gynna prospekterings- och gruvindustrin i regionen i många år framöver.

Norra Norrbottens malmprovins står för en stor del av Sveriges järn- och kopparmalmsproduktion. Här finns fyra aktiva metallgruvor (mars 2018) och mer än 500 dokumenterade mineraliseringar. Fyndigheterna är av många olika slag, där de viktigaste typerna är stratiforma kopparmineraliseringar, järnformationer, apatitjärnmalm av Kirunatyp och epigenetiska koppar-guldmineraliseringar. En vanlig egenskap hos de flesta malmer och mineraliseringar i Norr- och Västerbotten är att de har paleoproterozoiska vulkaniska och sedimentära bergarter som värdbergart. För undersökningarna valdes ett antal nyckelområden med bästa tillgängliga blottningsgrad. De utvalda områdena representerar tillsammans en nästan komplett stratigrafi i ytbergarter inom åldersintervallet 2,5–1,8 miljarder år.

Rapporten består av tretton kapitel och inleds med en översikt över de geologiska förhållandena, som beskriver huvuddragen i de senaste resultaten. Översikten följs av fyra kapitel (2–5) som huvudsakligen handlar om litostratigrafi och åldersbestämningar av ytbergarterna. Huvudämnet för de därpå följande fem kapitlen (6–10) är 3D-geometri och strukturell utveckling. Därefter kommer två kapitel (11–12) som fokuserar på U-Pb-datering av en metamorf respektive intrusiv händelse. Rapporten avslutas med en studie av geokemin hos morän i Norra Norrbottens malmprovins (kapitel 13).

Introduction

Stefan Bergman & Ildikó Antal Lundin

This volume reports the results from a subproject within the Barents Project, a major programme in northern Sweden. The multidisciplinary Barents Project was initiated by SGU as the first step in implementing the Swedish National Mineral Strategy. SGU obtained additional funding from the Ministry of Enterprise and Innovation to gather new geological, geophysical and till geochemistry data, and generally enhance geological knowledge of northern Sweden over a four-year period (2012–2015). The state-owned iron mining company LKAB also helped to fund the project. The strategic goal of the project was to support the exploration and mining industry, so as to improve Sweden's competitiveness in the mineral industry by providing modern geoscientific information. Geological knowledge facilitates sustainable, efficient and environmentally friendly use of resources. New publicly available geoscientific information from this region will help exploration and mining companies to reduce their risks and exploration costs, thus promoting economic development. All data collected within the project are stored in databases and are available at SGU.

This subproject within the Barents Project aims to provide a deeper understanding of the stratigraphy and depositional evolution of mineralised supracrustal sequences in northernmost Sweden. The combined results in the form of new geological knowledge and plentiful new data will benefit the exploration and mining industry in the region for many years to come.

The Northern Norrbotten ore province is a major supplier of iron and copper ore in Sweden. There are four active metal mines (March 2018) and more than 500 documented mineralisations. A wide range of deposits occur, the most important types being stratiform copper deposits, iron formations, Kiruna-type apatite iron ores and epigenetic copper-gold deposits. A common feature of most deposits is that they are hosted by Palaeoproterozoic metavolcanic or metasedimentary rocks. A number of key areas were selected across parts of the supracrustal sequences with the best available exposure. The areas selected combine to represent an almost complete stratigraphic sequence.

This volume starts with a brief overview of the geological setting, outlining some of the main recent achievements. This is followed by four papers (2–5) dealing mainly with lithostratigraphy and age constraints on the supracrustal sequences. 3D geometry and structural evolution are the main topics of the next set of five papers (6–10). The following two contributions (11–12) focus on U-Pb dating of a metamorphic event and an intrusive event, respectively. The volume concludes with a study of the geochemical signature of till in the Northern Norrbotten ore province (13).

Authors, paper 2:
Edward P. Lynch
Geological Survey of Sweden
Department of Mineral Resources
Uppsala, Sweden

Fredrik A. Hellström
Geological Survey of Sweden
Department of Mineral Resources
Uppsala, Sweden

Hannu Huhma
Geological Survey of Finland,
Espoo, Finland

Johan Jönberger
Geological Survey of Sweden
Department of Mineral Resources
Uppsala, Sweden

Per-Olof Persson
Swedish Museum of Natural History,
Department of Geosciences,
Stockholm, Sweden

George A. Morris
Geological Survey of Sweden
Department of Mineral Resources
Uppsala, Sweden

2. Geology, lithostratigraphy and petrogenesis of c. 2.14 Ga greenstones in the Nunasvaara and Masugnsbyn areas, northernmost Sweden

Edward P. Lynch, Fredrik A. Hellström, Hannu Huhma, Johan Jönberger,
Per-Olof Persson & George A. Morris

ABSTRACT

Two Palaeoproterozoic greenstone successions in the Nunasvaara and Masugnsbyn areas of north-central Norrbotten (northernmost Sweden) have been investigated to (1) characterise their primary depositional features; (2) establish lithostratigraphic correlations between both areas; and (3) gain insights into the petrogenesis of greenstone-type volcano-sedimentary successions in this sector of the Fennoscandian Shield.

In the Nunasvaara area (*Vittangi greenstone group*), a partly conformable, polydeformed, approximately 2.4 km thick greenstone sequence mainly consists of basaltic (tholeiitic) metavolcanic and metavolcaniclastic rocks (amygdaloidal lava, laminated tuff). Intercalated metasedimentary units include graphite-bearing black schist, and pelite. The uppermost part consists of amphibolitic pelite with intercalated metacarbonate layers and rare meta-ironstone, metachert and meta-ultrabasic horizons. Numerous metadoleritic sills occur throughout the package.

In the Masugnsbyn area (*Veikkavaara greenstone group*) a relatively conformable approximately 3.4 km thick greenstone sequence displays lithological, geochemical and geophysical characteristics similar to that at Nunasvaara. This succession consists of a dominant basaltic metatuff sequence overlain by metasedimentary units towards the top (e.g. meta-ironstone, metachert, amphibolitic schist, calcitic and dolomitic marbles). Minor metadolerite sills occur in the metatuffs. Near the base of the metatuff package, a graphitic black schist horizon occupies a similar stratigraphic position to a prominent black schist layer at Nunasvaara (here named the *Nunasvaara member*). This unit is a key marker horizon providing lateral correlation between both successions and also acts as a useful strain marker for reconstructing deformational events.

Both greenstone successions record the effects of overprinting syn- to late-orogenic (Svecokarelian) tectonothermal events. These include complex, polyphase ductile deformation (D1 to D3 events at Nunasvaara, forming the *Nunasvaara dome*), peak amphibolite facies metamorphism, metasomatic-hydrothermal alteration and late-stage retrogression and brittle faulting (composite D4 at Nunasvaara). Locally, these overprinting processes formed metamorphic graphite, skarn-related Fe ± Cu and hydrothermal Cu ± Pb ± Mo mineralisation.

U-Pb SIMS zircon dating of a metadolerite dyke from Nunasvaara and a metadolerite sill from Masugnsbyn have yielded mean weighted $^{207}Pb/^{206}Pb$ ages of 2 144 ±5 Ma (2σ, *n* = 10) and 2 139 ±4 Ma (2σ, *n* = 5) Ma, respectively. These precise dates constrain the timing of hypabyssal mafic magmatism, provide a minimum age for the deposition of the volcanic and sedimentary rocks, and identify a new approximetly 2.14 Ga episode of tholeiitic magmatism in this sector of the Fennoscandian Shield. Whole-rock initial εNd values for greenstone meta-igneous units range from +0.4 to +4.0 at Nunasvaara (*n* = 11) and +0.4 to +3.7 at Masugnsbyn (*n* = 7). These data indicate a juvenile depleted to partly enriched mantle (asthenospheric or lithospheric) as a major source of the tholeiitic melts. Corresponding trace element systematics have enriched mid-ocean ridge (E-MORB)-type signatures, and indicate minor assimilation of Archaean continental crust (i.e. Norrbotten craton) during magma ascent and storage. Overall, the combined geological, geochemical and isotopic characteristics of the greenstones are consistent with protolith formation within an incipient oceanic basin (epieric *Norrbotten Seaway*) during approximetly 2.14 Ga rifting and sagging of the Norrbotten craton.

INTRODUCTION

The Palaeoproterozoic bedrock of northernmost Sweden (i.e. northern Norrbotten) predominantly comprises supracrustal and intrusive rocks formed 1.90–1.78 Ga during the composite Svecokarelian orogeny (the name *Svecofennian* is also used). Historically, geological investigations in northern Norrbotten have focused on synorogenic rocks (and associated structures), since these preserve evidence of Palaeoproterozoic orogenesis and crustal accretion (e.g. Skiöld et al. 1993, Talbot & Koyi 1995, Wikström et al. 1996, Öhlander et al. 1999, Talbot 2001, Bergman et al. 2006, Lahtinen et al. 2015). Similarly, metallogenic studies of Svecokarelian-related supracrustal and intrusive rocks have been favoured because they preferentially host economically important mineral deposits, including "Kiruna-type" iron oxide-apatite (IOA), iron oxide-copper-gold (IOCG) and "modified" or "hybrid" deposits such as the Aitik porphyry Cu + IOCG and Tjårrojåkka IOA + IOCG systems (e.g. Cliff et al. 1990, Romer et al. 1994, Edfelt et al. 2005, Smith et al. 2007, Smith et al. 2009, Billström et al. 2010, Wanhainen et al. 2012).

In contrast, supracrustal and intrusive rocks in northern Norrbotten formed before the Svecokarelian orogeny (i.e. "Karelian" successions and associated mafic-ultramafic intrusions > c. 2.0 Ga) have received less attention in terms of their petrographic, geochemical, structural or metallogenic characteristics (cf. Martinsson 1997). Consequently, knowledge about the petrogenesis and subsequent modification of these rocks remains limited, particularly when compared with analogous successions in other sectors of Fennoscandia (cf. Hanski & Huhma 2005, Hanski 2012, Melezhik & Hanski 2012). Additionally, given that Karelian rocks in northern Finland, Sweden and Norway host known Fe, Cr, Ni, Cu, PGE, Au and graphite mineralisation (e.g. Bergman et al. 2001, Weihed et al. 2005, Eilu 2012, Sandstad et al. 2012), geological studies of Karelian greenstone belts in northern Norrbotten may enhance the prospectivity of these units for undiscovered base, precious and critical raw materials (cf. Sarapää et al. 2015).

In this account we present an investigation of two Palaeoproterozoic greenstone successions (i.e. metamorphosed mafic volcanic-sedimentary sequences) located in the Nunasvaara and Masugnsbyn areas, north-central Norrbotten. Field mapping, structural measurements and geophysical investigations have been integrated with U-Pb SIMS zircon dating, lithogeochemistry and Sm-Nd isotopic analysis to reassess the lithostratigraphy of both successions, establish lateral correlations, review deformation and mineralisation events, and provide constraints for greenstone petrogenesis as part of the broader Palaeoproterozoic evolution of the Fennoscandia Shield.

A note on Norrbotten greenstone nomenclature

Various informal geographical, geological and stratigraphic names (or a combination of them) have been used to label and subdivide greenstone-type volcanic-sedimentary successions in Norrbotten, either collectively or for individual sequences. Numerous local names exist for individual successions or belts (e.g. Bergman et al. 2001, Table 2), often designated at the stratigraphic "group" level and typically subdivided into informal formations (e.g. Eriksson & Hallgren 1975; cf. Öhlander et al. 1992). Examples of informal collective names include *Greenstone group* (Frietsch 1984, Witschard 1984, Bergman et al. 2001) *Norrbotten greenstone belt* (Gustafsson 1993) and *Kiruna greenstone group* (Martinsson 2004, Martinsson et al. 2016). The latter name, or simply *Kiruna greenstones*, has also been used in a local sense for greenstones in the immediate Kiruna area (e.g. Ambros 1980, Skiöld 1986, Martinsson 1997, Masurel 2011; cf. Fig. 1B). Additional collective names applied in a broader, regional sense have included *Nordkalott tholeiitic province* (Pharoh et al. 1987) and *Karelian supracrustal rocks* (Welin 1987). Thus, a clearly defined, formally adopted and consistently used stratigraphic or descriptive nomenclature for the greenstones is somewhat lacking. Likewise, rigorous application of stratigraphic principles has been hampered by relatively poor exposure, the effects of multiple deformation events, a lack of marker horizons to establish lateral correlations, and apparent minimal formal stratigraphic oversight.

In this chapter we retain the previously established informal stratigraphy and unit names for the Nunasvaara and Masugnsbyn successions, with some modification mainly at the "formation" stratigraphic level, in particular for the latter area (cf. Padget 1970, Eriksson & Hallgren 1975). Our approach provides a degree of continuity with the previously established systems and aims to minimise the introduction of new unit names without clear geological or practical justification. Additionally, we use the name *Norrbotten greenstone belts* (without any stratigraphic connotation) to refer collectively to all greenstone-related rocks in Norrbotten (cf. Gustafsson 1993).

REGIONAL SETTING OF NORRBOTTEN GREENSTONE BELTS

Palaeoproterozoic greenstone belts occur only in the most northerly and northeasterly parts of Norrbotten (Fig. 1; Bergman et al. 2001, 2012). Compared with analogous belts in Norway and Finland, greenstone successions in northern Sweden tend to form smaller, disconnected "inlier" domains enclosed by younger Palaeoproterozoic rocks (Fig. 1A). Collectively, the greenstones combine to form an approximately 100 × 400 km northwest-trending discontinuous zone comprised of individual north–northeast and north–northwest-orientated, 5–15 km wide, curvilinear zones (Fig. 1B).

From a regional perspective, the Norrbotten greenstone belts represent the northwestern margin of a major northwest–southeast-trending, approximately 800 × 1,500 km lithotectonic domain stretching from Tromsö (Norway) in the northwest to beyond Petrozavodsk (Russia) in the southeast (Fig. 1A). This domain mainly consists of mafic-ultramafic rocks formed during lithospheric-scale intraplate rifting and break-up of the composite Fennoscandian Shield between approximetly 2.5 and 2.0 Ga (e.g. Lahtinen et al. 2008, Melezehik & Hanski 2012, Melezhik et al. 2012). Before this major phase of continental dispersal, the Fennoscandian Shield formed part of a composite supercontinent called Kenorland (e.g. Reddy & Evans 2009, Melezhik et al. 2012).

In northern Norrbotten, greenstone belts and other Palaeoproterozoic metasupracrustal rocks are underlain by the *Norrbotten craton* (Lahtinen et al. 2005), a partly hidden Meso- to Neoarchaean continental basement terrane extending roughly from Luleå in the south to Sweden's northernmost border (e.g. Öhlander et al. 1987b, Mellqvist et al. 1999). The greenstones are typically separated by younger syn- to late-orogenic metasupracrustal and intrusive rocks (Fig. 1B), while isolated greenstone blocks are also known from the northernmost Swedish Caledonides (e.g. Romer & Boundy 1988).

Lithologically, the greenstone sequences predominantly comprise basaltic (tholeiitic) metavolcanic and meta-intrusive rocks (e.g. Pharaoh & Pearce 1984, Pharaoh & Brewer 1990, Martinsson 1997).

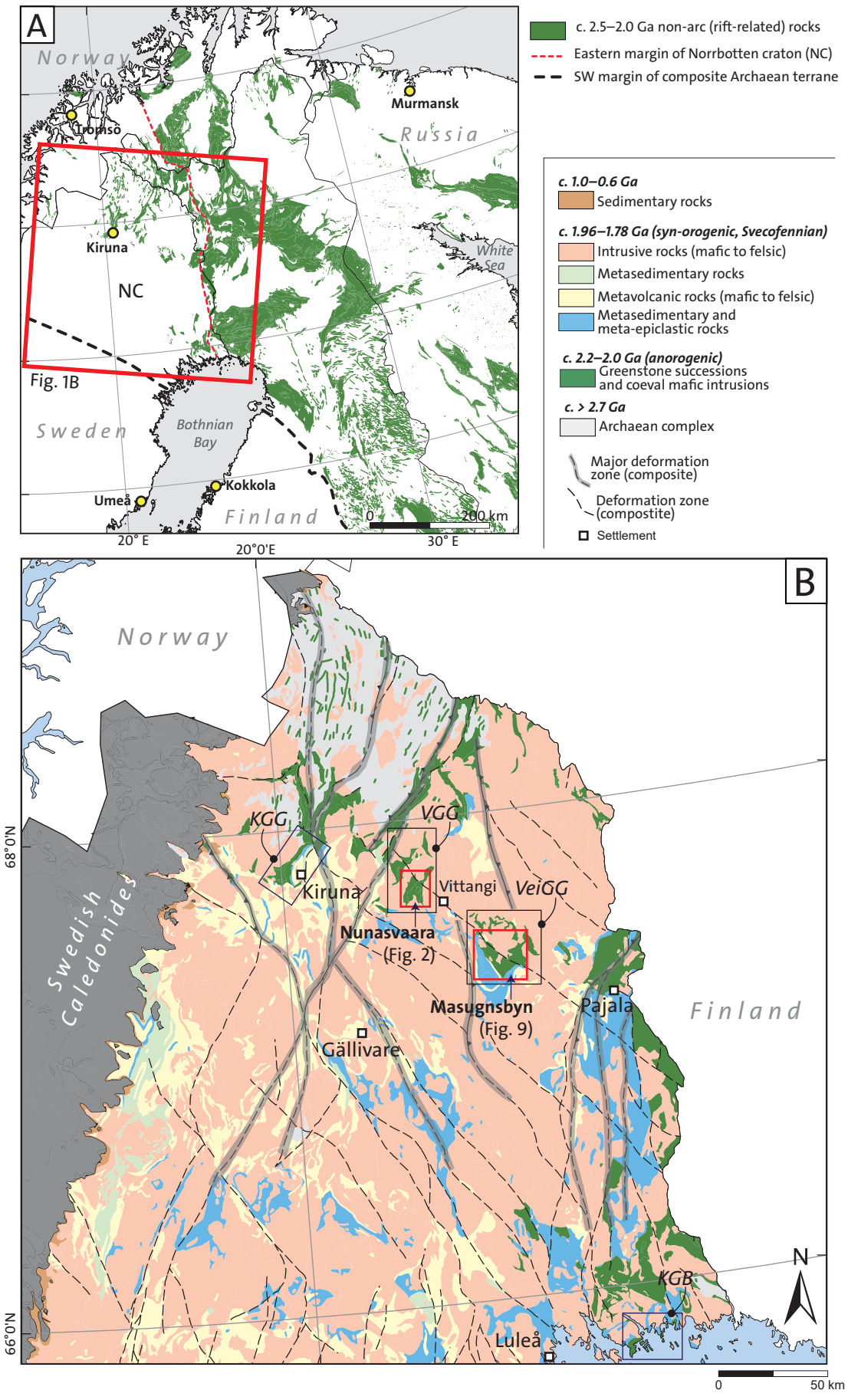
A
Norway
Murmansk
Tromsö
Russia
Kiruna
White Sea
NC
Fig. 1B
Sweden
Bothnian Bay
Kokkola
Umeå
Finland
0
200 km
20° E
20°0'E
30° E
c. 2.5–2.0 Ga non-arc (rift-related) rocks
Eastern margin of Norrbotten craton (NC)
SW margin of composite Archaean terrane
c. 1.0–0.6 Ga
Sedimentary rocks
c. 1.96–1.78 Ga (syn-orogenic, Svecofennian)
Intrusive rocks (mafic to felsic)
Metasedimentary rocks
Metavolcanic rocks (mafic to felsic)
Metasedimentary and meta-epiclastic rocks
c. 2.2–2.0 Ga (anorogenic)
Greenstone successions and coeval mafic intrusions
c. > 2.7 Ga
Archaean complex
Major deformation zone (composite)
Deformation zone (compostite)
Settlement
B
Norway
KGG
VGG
Kiruna
Vittangi
VeiGG
Nunasvaara
(Fig. 2)
Masugnsbyn
(Fig. 9)
Pajala
Finland
Gällivare
Swedish Caledonides
68°0'N
66°0'N
KGB
Luleå
N
0
50 km

◄ Figure 1. **A.** Map of northern Fennoscandia highlighting the distribution of undifferentiated volcanic, sedimentary and intrusive rocks associated with continental rifting events that affected the composite Archaean craton between c. 2.5 and 2.0 Ga. Base geology is taken from Koistinen et al. (2001). NC = Norrbotten craton. **B.** Precambrian geology of northernmost Sweden (Norrbotten), showing the location of the Nunasvaara and Masugnsbyn areas (red rectangles). Geology modified from Bergman et al. (2012). Major deformation zones (grey) are taken from Bergman et al. (2001). Black rectangles outline the approximate location of major greenstone successions discussed in the main text. KGG = Kiruna greenstone group, VGG = Vittangi greenstone group, VeiGG = Veikkavaara greenstone group, KGB = Kalix greenstone belt.

Most of these rocks contain intercalations of metasedimentary rocks such as amphibolitic pelite to schist, marble, black schist and banded meta-ironstones. In some areas, greenstone-related metasedimentary rocks are more abundant than metavolcanic units (e.g. the Pajala area and Kalix greenstone belt, northeastern Norrbotten, Fig. 1B; Gustafsson 1993, Martinsson 1993, Wanke & Melezhik 2005). This feature may reflect facies variation, stratigraphic position or erosional level (cf. Martinsson 2004).

Greenstone-related mafic intrusions mainly consist of doleritic to gabbroic dykes and sills, and their orientation tends to mimic the trends of the main greenstone belts. Details about the character and age of these intrusive units and their genetic association with mafic extrusive suites are presently lacking (cf. Bergman et al. 2001). In the Kiruna area (*Kiruna greenstone group*), komatiitic lavas occur in the lower part of the greenstone sequence (e.g. Martinsson 1997).

From a stratigraphic perspective, Norrbotten greenstone successions represent the upper part of a 2.4–2.1 Ga Karelian metasupracrustal sequence resting unconformably on the Norrbotten craton (Bergman et al. 2001). The basal part of the Karelian sequence is mainly represented by continental-derived flysch deposits (metaconglomerate, meta-arenite) formed during early continental rifting (e.g. *Kovo group,* Martinsson 1997). More abundant 1.9–1.8 Ga (syn-orogenic) metavolcanic and metasedimentary sequences lie unconformably above the greenstones (Fig. 1B). Regionally, the Norrbotten greenstones mostly correlate with Jatulian (Rhyacian) 2.3–2.06 Ga volcanic-sedimentary successions located to the north and east in northern Finland and Norway, and in northwest Russia (e.g. Hanski 2012, Bingen et al. 2016).

GEOLOGY OF THE NUNASVAARA AND MASUGNSBYN GREENSTONE SUCCESSIONS

Previous geological descriptions and reviews of the studied areas have been presented by Eriksson (1969), Padget (1970), Eriksson & Hallgren (1975), Lynch et al. (2014) and Hellström & Jönsson (2014, 2015).

The lithostratigraphic descriptions that follow present new minimum thicknesses for the various stratigraphic units. These estimates are based on the thickness of steeply dipping (0–90°) volcanic-sedimentary units (excluding hypabyssal rocks) occurring along profiles X–X' and Y–Y' at Nunasvaara (Fig. 2A–B), and profiles A and B at Masugnsbyn (Fig. 9A–B). In general, estimating exact true thicknesses of the stratigraphic units in both successions is complicated by (1) the polydeformed nature of the bedrock; (2) the presence of metadoleritic intrusions (often emplaced concordantly along unit boundaries); (3) the truncation of both packages by younger intrusions; and (4) likely preservation and exposure gaps (cf. Gustafsson 1993).

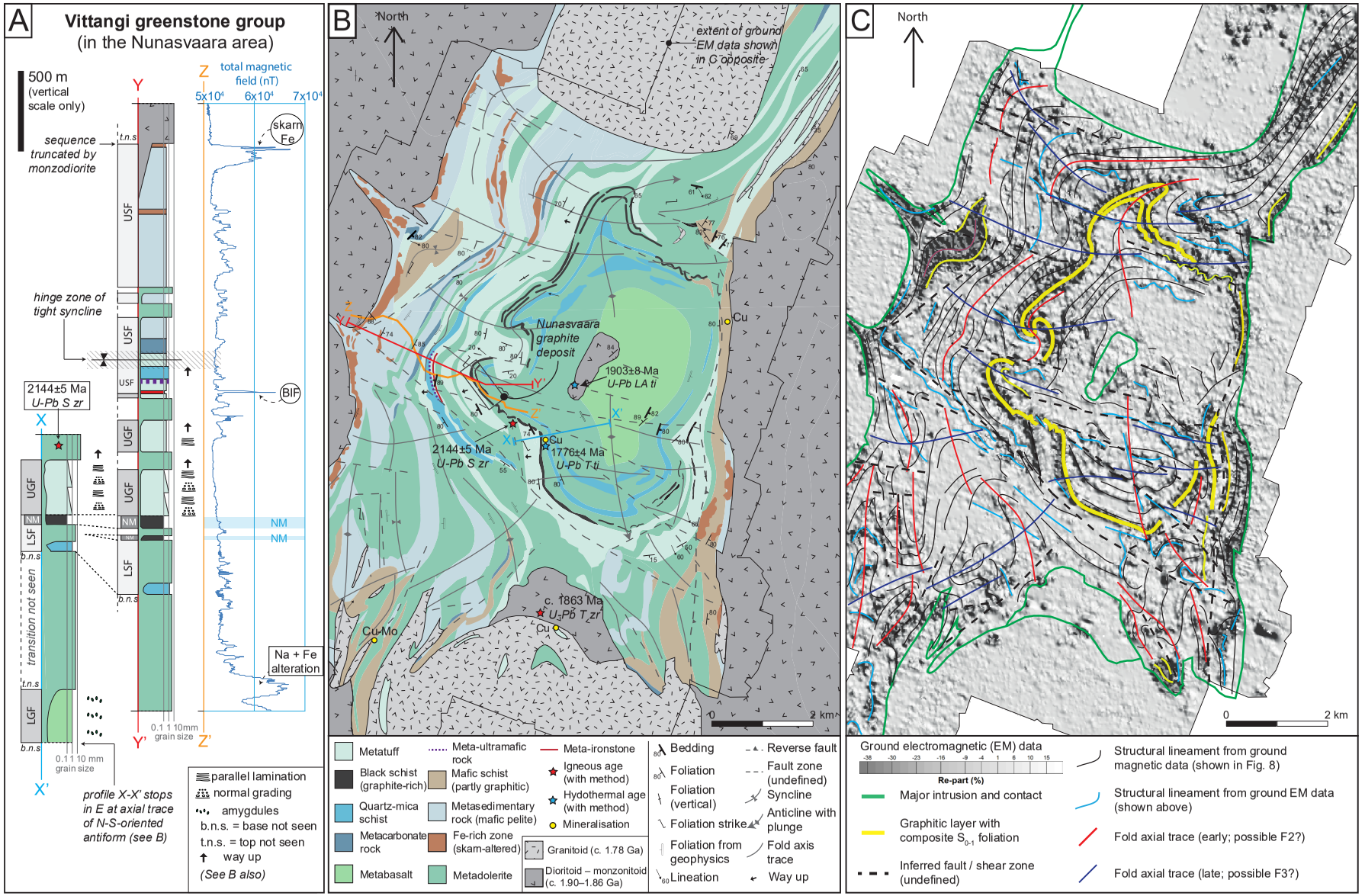
A
Vittangi greenstone group
(in the Nunasvaara area)
500 m
(vertical
scale only)
total magnetic
field (nT)
5x10⁴
6x10⁴
7x10⁴
sequence
truncated by
monzodiorite
t.n.s
USF
hinge zone of
tight syncline
2144±5 Ma
U-Pb S zr
skarn
Fe
BIF
UGF
NM
LSF
b.n.s
transition not seen
LGF
Na + Fe
alteration
0.1 1 10mm
grain size
profile X-X' stops
in E at axial trace
of N-S-oriented
antiform (see B)
parallel lamination
normal grading
amygdules
b.n.s. = base not seen
t.n.s. = top not seen
way up
(See B also)
B
North
extent of ground
EM data shown
in C opposite
Nunasvaara
graphite
deposit
1903±8 Ma
U-Pb LA ti
2144±5 Ma
U-Pb S zr
Cu
1776±4 Ma
U-Pb T-ti
c. 1863 Ma
U-Pb T zr
Cu-Mo
0
2 km
Metatuff
Black schist
(graphite-rich)
Quartz-mica
schist
Metacarbonate
rock
Metabasalt
Meta-ultramafic
rock
Mafic schist
(partly graphitic)
Metasedimentary
rock (mafic pelite)
Fe-rich zone
(skarn-altered)
Metadolerite
Meta-ironstone
Igneous age
(with method)
Hydothermal age
(with method)
Mineralisation
Granitoid (c. 1.78 Ga)
Dioritoid – monzonitoid
(c. 1.90–1.86 Ga)
Bedding
Foliation
Foliation
(vertical)
Foliation strike
Foliation from
geophysics
Lineation
Reverse fault
Fault zone
(undefined)
Syncline
Anticline with
plunge
Fold axis
trace
Way up
C
North
0
2 km
Ground electromagnetic (EM) data
Re-part (%)
Major intrusion and contact
Graphitic layer with
composite S0-1 foliation
Inferred fault / shear zone
(undefined)
Structural lineament from ground
magnetic data (shown in Fig. 8)
Structural lineament from ground EM data
(shown above)
Fold axial trace (early; possible F2?)
Fold axial trace (late; possible F3?)

◀ Figure 2. Geology of the Nunasvaara area (part of Vittangi greenstone group). **A.** Schematic stratigraphy of the Nunasvaara area based on profile lines X–X', Y–Y' and Z–Z' shown in B. LGF = Lower greenstone formation, LSF = Lower sedimentary formation, NM = Nunasvaara member (of the LSF), UGF = Upper greenstone formation, USF = Upper sedimentary formation. Unit thicknesses represent minimum estimates. **B.** Geological map highlighting greenstone-related lithologies (based on Eriksson & Hallgren 1975, with additional mapping from this study). Radiometric age sources are: Skiöld 1981 for U-Pb TIMS zircon age (U-Pb T zr), Smith et al. 2009 for U-Pb LA-ICP-MS titanite age (U-Pb LA ti) and Martinsson et al. 2016 for U-Pb TIMS titanite age (U-Pb T ti). U-Pb SIMS zircon age (U-Pb S zr) is from this study. C. Ground-based electromagnetic (slingram) map (in-phase, real component) showing anomalous zones of relatively high conductivity (darker shade) corresponding to graphite-rich layers, fracture zones and skarn-related alteration. Additional structural lineaments (black lines) are based on magnetic anomalies shown in Figure 8A. Fold axial traces from C are also plotted in B and suggest at least two folding events.

Geology and lithostratigraphy at Nunasvaara (Vittangi greenstone group)

The Nunasvaara area is located about 10 km west of Vittangi village (Fig. 1). Here, a polydeformed succession of mafic metavolcanic rocks, hypabyssal intrusions (metadoleritic sills, minor dykes) and metasedimentary rocks form a rectangular, approximately 9 × 11 km, north-northeast-orientated, metasupracrustal inlier (Fig. 2). The sequence extends a further 9 km or so from the northeastern corner of the study area, along a narrow, linear belt toward the north-northeast (cf. Eriksson & Hallgren 1975). In the study area, important examples of skarn-related iron and metamorphic graphite mineralisation occur (e.g. Frietsch 1997, Pearce et al. 2015).

At Nunasvaara the greenstone succession is bordered and truncated by extensive syn- to late-orogenic intrusions (Fig. 2B–C). These consist of (1) generally deformed c. 1.89 Ga gabbros, dioritoids and granitoids assigned to the regional *Haparanda suite*; (2) less abundant c. 1.87 Ga syenitoids and granitoids belonging to the regional *Perthite-monzonite suite*; and (3) weakly deformed to massive c. 1.80 Ga granitic plutons, stocks and dykes assigned to the regional *Lina suite* (cf. Ahl et al. 2001).

Stratigraphically, the greenstones form part of the *Vittangi greenstone group* (VGG, Fig. 1B; Eriksson & Hallgren 1975, Gustafsson 1993). Historically, the VGG has been subdivided into five informal formations (see Eriksson & Hallgren 1975, p. 5). For our study (and in the interests of consistency), we retain the informal stratigraphic subdivisions and unit names proposed by Eriksson & Hallgren (1975), with some minor modifications. A schematic stratigraphic column for the sequence is presented in Figure 2A.

The lowermost stratigraphic unit of the VGG, named the *Tjärro quartzite formation* (TQF), has not been seen at Nunasvaara and is not considered further in this account. In their regional compilation, Bergman et al. (2001) re-assigned the TQF to the regionally extensive and inferred stratigraphically lower *Kovo group*, based on lithological considerations (cf. Kumplulainen 2000).

Lower greenstone formation

The lowermost VGG unit occurring at Nunasvaara is the *Lower greenstone formation* (LGF, Fig. 2A). Contact between the LGF and its bounding formations are not preserved in the area. Thus, a tentative minimum thickness of approximately 300 m is estimated for this unit (Profile X–X', Fig 2A). In contrast, Gustafsson (1993) indicated a minimum thickness of approximately 900 m, while Eriksson & Hallgren (1975) reported a thickness of approximately 5 km for a more completely exposed section about 35 km to the northwest of Nunasvaara (Saivo–Leppäkoski area).

The LGF predominantly consists of effusive mafic metavolcanic rock (*basaltic lava* of Eriksson & Hallgren 1975). Rare ultramafic dykes (Mg-rich, olivine-bearing serpentinite) have also been assigned to this unit (Eriksson & Hallgren 1975). The metabasalt is dark grey to greenish-grey, aphanitic (< 0.5 mm) and locally amygdaloidal. It crops out across several flat-lying exposures in the centre of the study area (Figs. 2 & 3A). In general, it is massive to weakly foliated, without conspicuous banding or layering and consists of granoblastic hornblende and plagioclase feldspar, with minor biotite, clinopyroxene (diopside?), titanite, magnetite and late-stage epidote.

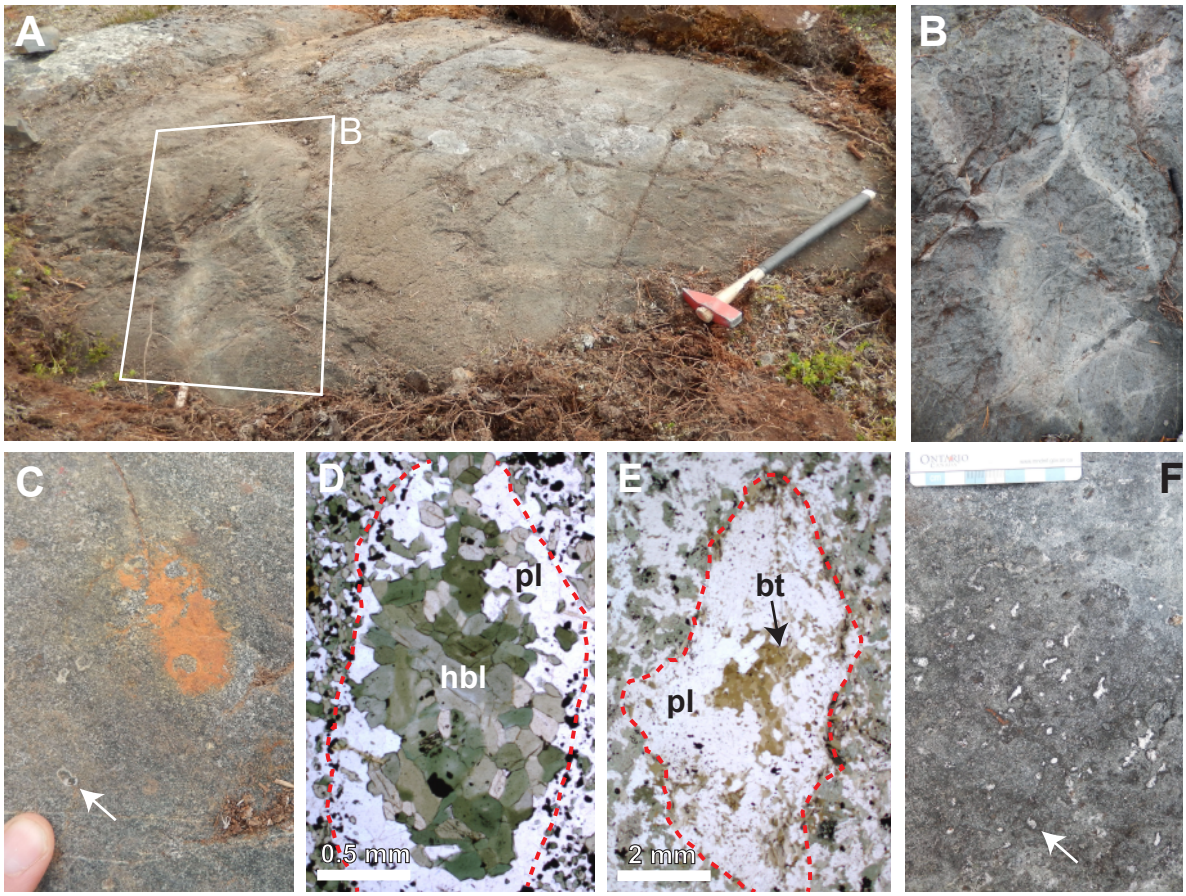

Figure 3. **A.** Outcrop view of metabasalt (orthoamphibolite) of the Lower greenstone formation, Nunasvaara. The hammer head is 15 cm long. **B.** Close-up view from A showing possible cross-section through a deformed tube-like structure (i.e. tube-fed pahoehoe lava flow). Curvilinear, pale green zones (actinolite-chlorite altered?) delineate the outer rim of the lobe. **C.** Oblate, hornblende-rich amygdales (arrow) in metabasalt. **D.** Thin section, plane polarised light (PPL) view of an amygdale (dashed outline), with an outer zone of plagioclase (pl) and a core of hornblende (hbl). **E.** PPL view of irregular and stretched amygdale with an outer zone of plagioclase (pl) and a core of biotite (bt). **F.** Outcrop view of elongate-irregular (pipe vesicle?) amygdales in metabasalt (arrow).

Although bedding contacts are not well exposed, some outcrops display bulbous, tabular forms, suggesting flow bed thicknesses of 0.7–2 m. Rare polygonal shapes, delineated by curvilinear, pale green bands (actinolite ± chlorite?), may represent cross-sectional views of tube-like flow lobes or deformed pillows (Fig. 3A–B). Where present, these structures consist of dense, vesicle-free interiors, which grade outwards to an external vesicular zone (1–3 cm wide), and then to an outermost rind or margin (1–2 cm wide), typically devoid of vesicles. These features are suggestive of the types of flow lobes and channels associated with pahoehoe-type lava extrusion (e.g. Self et al. 1998, Oze & Winter 2005). Thicker and better preserved sequences of pillowed metabasalt occur to the northwest of Nunasvaara (cf. Eriksson & Hallgren 1975).

A more conspicuous feature of the metabasalt at Nunasvaara is the variable presence of amygdales, which impart a spotted, variolitic appearance to the rock (Fig. 3C–F). Amygdales are generally oblate to elongate or irregular and typically range from 0.2 cm to 1.5 cm in length. They mainly contain hornblende or biotite cores with plagioclase ± scapolite rims (Fig. 3C–E). Examples of sericite-altered K-feldspar cores that grade into plagioclase margins also occur. Locally, some cores have a pale green appearance, suggesting chlorite ± actinolite replacement, while fine-grained subhedral magnetite may be disseminated around rims (Fig. 3E). Rarely, amygdales consist of creamy white scapolite ± albite without the darker amphibole-rich cores (Fig. 3F).

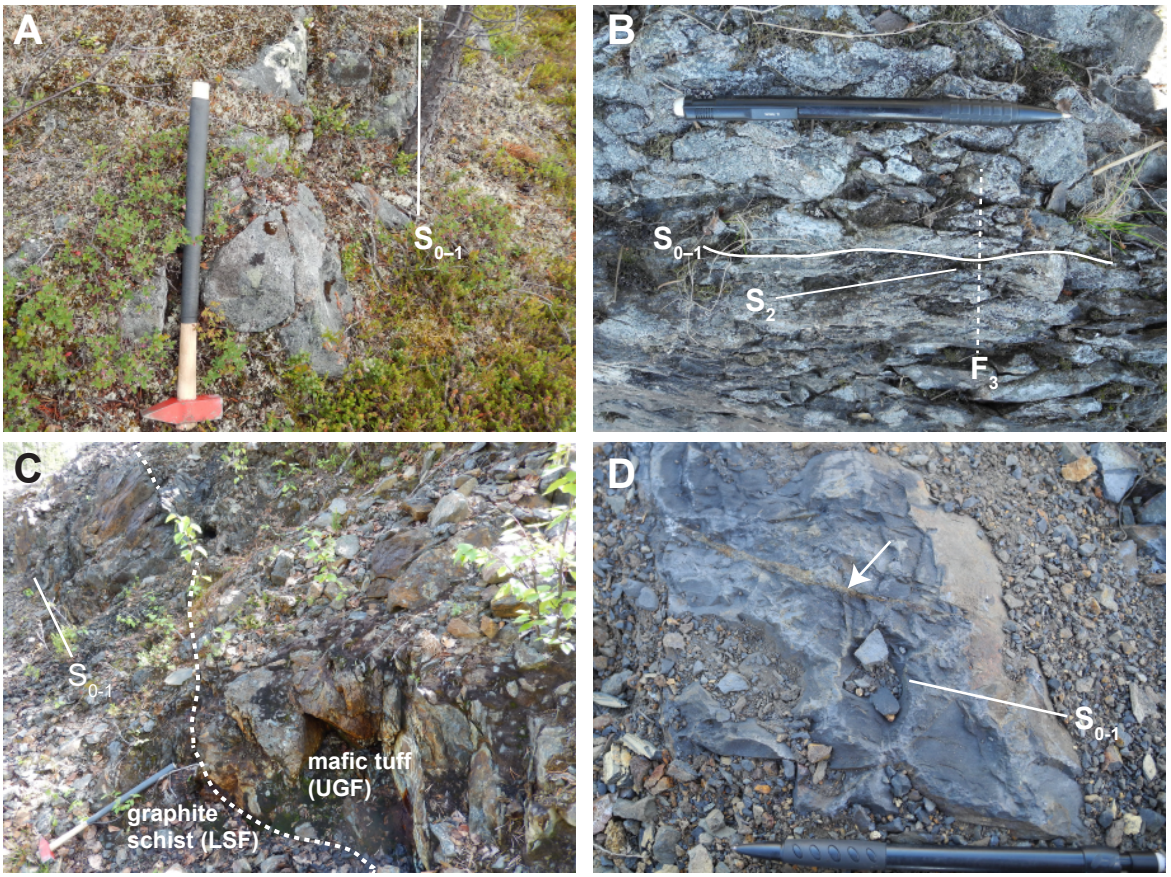

Figure 4. Lower sedimentary formation rocks at Nunasvaara. **A.** Along-strike view to the north of sub-vertical, mafic to intermediate metasedimentary rock (amphibole-mica schist). The hammer head is 15 cm long. **B.** Horizontal surface view to the east–northeast of Nunasvaara member graphite schist. The rock displays a weak S-C-fabric with a crenulation cleavage formed at an acute angle (approximately < 15°) to the main schistosity. The schist is also affected by east-northeast-orientated and steeply plunging gentle F2 folds. The pencil is 15 cm long. **C.** View to the southeast of the hanging wall contact zone at the Nunasvaara graphite deposit showing steeply southwest-dipping graphite-rich schist (LSF, left) overlain by metatuff of the Upper greenstone formation (UGF, right). **D.** Horizontal surface view to the southwest of graphite-rich schist at the Nunasvaara deposit (Nunasvaara member). A weak $S_{0–1}$ foliation is developed. The arrow indicates a weathered, sulphide-bearing veinlet. The pencil is 15 cm long.

Lower sedimentary formation

The next overlying stratigraphic unit at Nunasvaara is the *Lower sedimentary formation* (LSF, Fig. 2A). It consists of basal quartz-mica schist and an uppermost graphitic black schist horizon (Fig. 4). The lower contact with the underlying LGF is not seen in the Nunasvaara area. The top of the LSF is marked by a distinctive, graphite-rich schist horizon (*graphite schist* of Eriksson & Hallgren 1975). This layer hosts the Nunasvaara graphite deposit and several other named graphite prospects along strike (cf. Shaikh 1972). A minimum thickness estimate for the LSF is 200 m. Gustafsson (1993) reports a minimum thickness of 450 m for this formation.

The lithologically distinctive nature of the black schist layer (relatively abundant flake and amorphous graphite), its stratified, semi-continuous character, and its potential use as a strain marker, provide a basis for this unit to act as a correlative stratigraphic horizon in the Nunasvaara and broader north-central Norrbotten areas. We therefore formally introduce the name *Nunasvaara member* for this graphitic black schist horizon. A brief, systematic description of this unit now follows.

The Nunasvaara member (NM) refers to a 10–50 m thick graphite schist horizon (black schist) that forms the stratigraphically uppermost part of the Lower sedimentary formation of the Vittangi greenstone group at Nunasvaara (Vittangi area, northern Norrbotten). A suggested stratotype locality is the old Nunasvaara quarry (Nunasvaara graphite deposit; SWEREF99 TM: N7524309, E0770109, and

general area). Here, the unit is in conformable contact with an overlying laminated metatuff (i.e. Upper greenstone formation, Fig. 4C). The basal contact with underlying mafic to intermediate schist is not exposed and is intruded by a metadoleritic sill, which locally entrains the graphite schist, creating two sub-parallel horizons (e.g. Shaikh 1972). The NM extends along strike toward the northeast and southwest and intermittently continues as a polydeformed, discontinuous, sub-circular horizon with a total length of approximately 14 km.

In general, the graphite schist is dark grey, fine-grained (0.01–1 mm) and foliated, containing lepidoblastic feldspar, amphibole (actinolite-tremolite), scapolite, graphite, mica, titanite and pyrite. Locally, microcrystalline graphite abundances are relatively high (25–45 modal %; Shaikh 1972, Bergström 1987). The schist has a dark metallic blue-grey appearance and is massive to weakly foliated (Fig. 4D). Historical lithogeochemical analyses indicate that graphitic carbon concentrations for the NM range 10–45 wt. % (e.g. Shaikh 1972, Eriksson & Hallgren 1975, Bergström 1987; cf. Table 3).

Stable carbon isotope analysis of Nunasvaara graphite has yielded $\delta^{13}C_{graphite}$ values within a narrow range of approximately -23 to -22‰ that are consistent with a biogenic source for the precursor carbonaceous material (Pearce et al. 2015; cf. Luque et al. 2012). These data are similar to $\delta^{13}C_{graphite}$ values from the "C zone" black schist horizon of the *Viscaria formation* (Kiruna greenstone group), located southwest of Kiruna (Martinsson et al. 1997). They also fall within the range of approximately -27.0 to -19.2‰ for graphite-bearing metasedimentary rocks from elsewhere in north-central Norrbotten (Gavelin 1957). Deposition of an inferred black shale protolith for the Nunasvaara graphitic schist at c. 2.14 Ga corresponds with a known global increase in organic carbon production and burial at c. 2.1 Ga during a major period of continental dispersal (Condie et al. 2001).

Upper greenstone formation

The next overlying unit in the sequence is the *Upper greenstone formation* (UGF, Fig. 2A). It predominantly consists of fine-grained, laminated, mafic metavolcaniclastic rock (*amphibolitic tuff* of Eriksson & Hallgren 1975). The upper and lower contacts of the UGF and its bounding formations appear to be transitional-conformable. At Nunasvaara, the UGF has a minimum thickness of approximately 600 m. Gustafsson (1993) indicated a minimum thickness of approximately 800 m for this unit. About 30 km to the northwest (Sautusvaara area) the UGF comprises intercalated mafic metavolcaniclastic and effusive metavolcanic rocks (including local pillowed horizons in the latter), with subordinate meta-epiclastic and marble layers (Eriksson & Hallgren 1975).

In general, UGF metatuff is dark grey to medium grey, fine- to medium-grained (0.1–2 mm) and forms parallel, laterally continuous and planar, thin to medium beds (approximately 3 cm and 50 cm thick, Fig. 5A). Within individual beds, the metatuff has a stratified appearance and contains planar to wavy, parallel to sub-parallel, laterally continuous, 0.1–1 cm thick laminae (Fig 5B). Locally, it contains thicker (2–10 cm), alternating mafic and intermediate bands, resulting in an overall interlayered, compositionally variable volcaniclastic sequence (Fig. 4C–D). Likewise, relatively thin argillaceous seams (often micaceous and iron oxide-stained) occur, suggesting variable input of terrigeneous sedimentary material (Fig. 5C–D). Higher in the sequence, the metatuff is more crystalline (hornfelsed?) with a non-laminated appearance.

Along the mapped profile Y–Y' shown in Figure 2A & B UGF metatuffs dip steeply (80–90°) towards the west-southwest and contain laminated, fining upward sequences (i.e. normal grading), which indicate younging toward the southwest (Fig. 5E; cf. Eriksson & Hallgren 1975). Rarely, lensoidal, channel-like features are also developed, indicative of sub-aqueous, climbing ripple deposition (Fig. 5F).

Mineralogically, the metatuff consists of lepidoblastic hornblende (± actinolite) and plagioclase, with minor biotite, muscovite, magnetite, pyrite and garnet (e.g. Fig. 5E–G). The latter mineral is generally subhedral to euhedral, dark red to greyish-red (almandine), fine- to medium-grained (0.2–0.8 cm) and appears to occur preferentially within darker brown to rust-brown horizons with a more clay-like

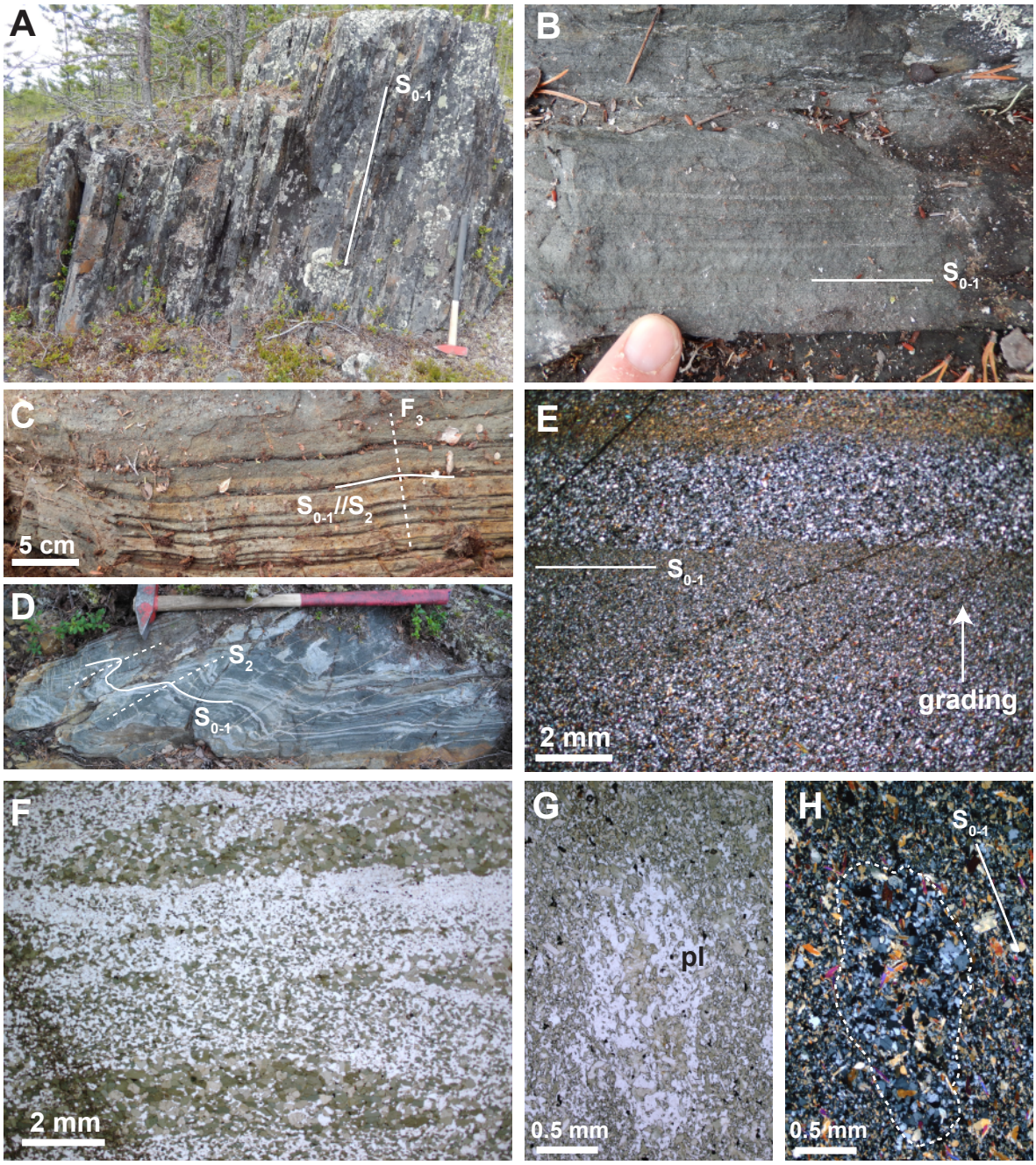

Figure 5. Mafic metatuff of the Upper greenstone formation at Nunasvaara. **A.** Outcrop view to the northwest of steeply southwest-dipping, medium- to thickly-bedded, metatuff. This sequence forms part of the hanging wall rocks of the Nunasvaara graphite deposit. The hammer is 65 cm long. **B.** Sub-horizontal, bedding orthogonal view (to the southwest) of fine-grained and well-sorted laminated tuff. **C.** Sub-horizontal view (to the southwest) of thin- to medium-bedded, compositionally banded metatuff. Locally, bands and laminae display gentle, steeply southwest-plunging upright F2 folds, typically orientated orthogonally to a composite So-1 foliation. **D.** Sub-horizontal view (to the northeast) of compositionally banded and folded metatuff. The hammer is 65 cm long. **E.** Thin section cross-polarised light (XPL) view of fine-grained, well-sorted, laminated metatuff, displaying fining upwards, normal grading, indicating younging toward the west-southwest. **F.** Thin section plane polarised light (PPL) view of lensoidal, channel-like features in metatuff. **G and H.** PPL and XPL views (respectively) of a possible remnant lithic clast in metatuff (dashed outline). The clast consists of an aggregate of relatively coarse plagioclase feldspar (pl) and amphibole and is stretched parallel to the main So-1 foliation.

appearance. Other features of the metatuff include the presence of chert-like nodules and bands, and granular lapilli-like horizons, with elongate, sub-rounded to oblate feldspar aggregates, possibly representing previously consolidated volcaniclastic material (i.e. lithic metatuff, Fig. 5G–H).

Upper sedimentary formation

The uppermost stratigraphic unit at Nunasvaara is the *Upper sedimentary formation* (USF, Fig. 2A). It consists of intercalated mafic to intermediate pelite to schist (Fig. 6A–B), graphitic black schist (Fig. 6C), metacarbonate rocks (Fig. 6E–F), minor banded quartz-rich horizons (metachert, Fig. 6G) and laminated iron-rich seams (meta-ironstone or BIF, Fig. 6H). In the last-mentioned unit, magnetite grains display fining upward textures that indicate younging toward the west-northwest (Fig. 6I).

A prominent feature of the USF at Nunasvaara is the occurrence of curvilinear zones of metasomatised, iron-rich and locally sulphide-bearing "skarn-"-altered rocks (i.e. amphibole + pyroxene + magnetite ± sulphide horizons, e.g. Frietsch 1997). These areas, locally containing relatively abundant stratabound iron mineralisation, are typically associated with upper metacarbonate and metasedimentary layers. The skarn metasomatic alteration zones also appear to be spatially focused along the margins of c. 1.89 Ga mafic to intermediate intrusions in the west and east of the study area (Fig. 2B).

Gustafsson (1993) reported that the UGF–USF contact is not preserved in the general Vittangi area. For this study, we have assigned the base of the USF to a thin seam (< 1 m) of banded meta-ironstone located approximately 985 m west-northwest of the Nunasvaara graphite deposit (Fig. 2A–B). Although poorly exposed, this laminated, magnetite-rich horizon is identifiable using ground-based magnetic measurements, and is illustrated in Figure 2A as a relatively narrow and intense (approximately 6.4×10^4 nT) magnetic anomaly on profile Z–Z'.

The basal part of the USF is inferred to represent the hinge zone of a northeast-trending upright syncline (Fig. 2A–B). Here, the greenstone sequence has mixed metasedimentary-metavolcanic characteristics, marking a transitional (conformable?) zone between the UGF and USF. The area contains intercalations of mafic metatuff and a rare, relatively thin (approximately < 5 m), meta-ultramafic horizon with a picritic geochemical signature (Table 3, Fig. 15C). A similar meta-ultramafic unit occurs in the Masugnsbyn area.

The stratigraphic top of the USF is not exposed in the study area and in the west the formation is truncated by an inferred c. 1.89 Ga quartz monzodiorite (Fig. 2A–B; e.g. Lynch et al. 2014). An estimated minimum thickness of the USF at Nunasvaara is approximately 1.3 km, similar to that indicated by Gustafsson (1993).

In summary, Palaeoproterozoic greenstones at Nunasvaara represent a discontinuous, partly conformable sequence of predominantly basaltic metavolcanic, metavolcaniclastic and metasedimentary rocks. The entire package may be divided into four informal lithostratigraphic formations (including one member), which have an estimated total minimum thickness of approximately 2.4 km (cf. Martinsson 1993, Gustafsson 1993).

Greenstone-related mafic intrusions at Nunasvaara

Metadoleritic intrusions occur throughout the volcanic-sedimentary sequence at Nunasvaara (*metadiabase* of Eriksson & Hallgren 1975). Typically, they form discontinuous, sub-parallel to lenticular sills, ranging 25–150 m maximum thickness (locally up to approximately 450 m, Fig. 2A–B). Minor discordant dykes (apophyses) associated with larger bodies also occur (Eriksson & Hallgren 1975). While distinct intrusive contacts are only rarely exposed, their sub-volcanic nature is most apparent from intrusive contacts seen in drill cores and their general petrographic characteristics (cf. Eriksson 1969, Gerdin et al. 1990).

Metadolerite at Nunasvaara is typically dark greenish-grey, fine- to medium-grained (0.3–4 mm), weakly to moderately foliated, and displays an intergranular (granoblastic) texture (Fig. 7A–C). Scapolite ± albite alteration commonly imparts a medium grey speckled or knobbly appearance to exposed surfaces (Fig. 7A). Mineralogically, they consist of ophitic hornblende and plagioclase feldspar (andesine to labradorite; Eriksson & Hallgren 1975), with minor biotite, zircon, titanite and magnetite (Fig. 7C–D). The latter mineral may be relatively abundant (10–15 vol. %) and is typically associated with disseminated pyrite,

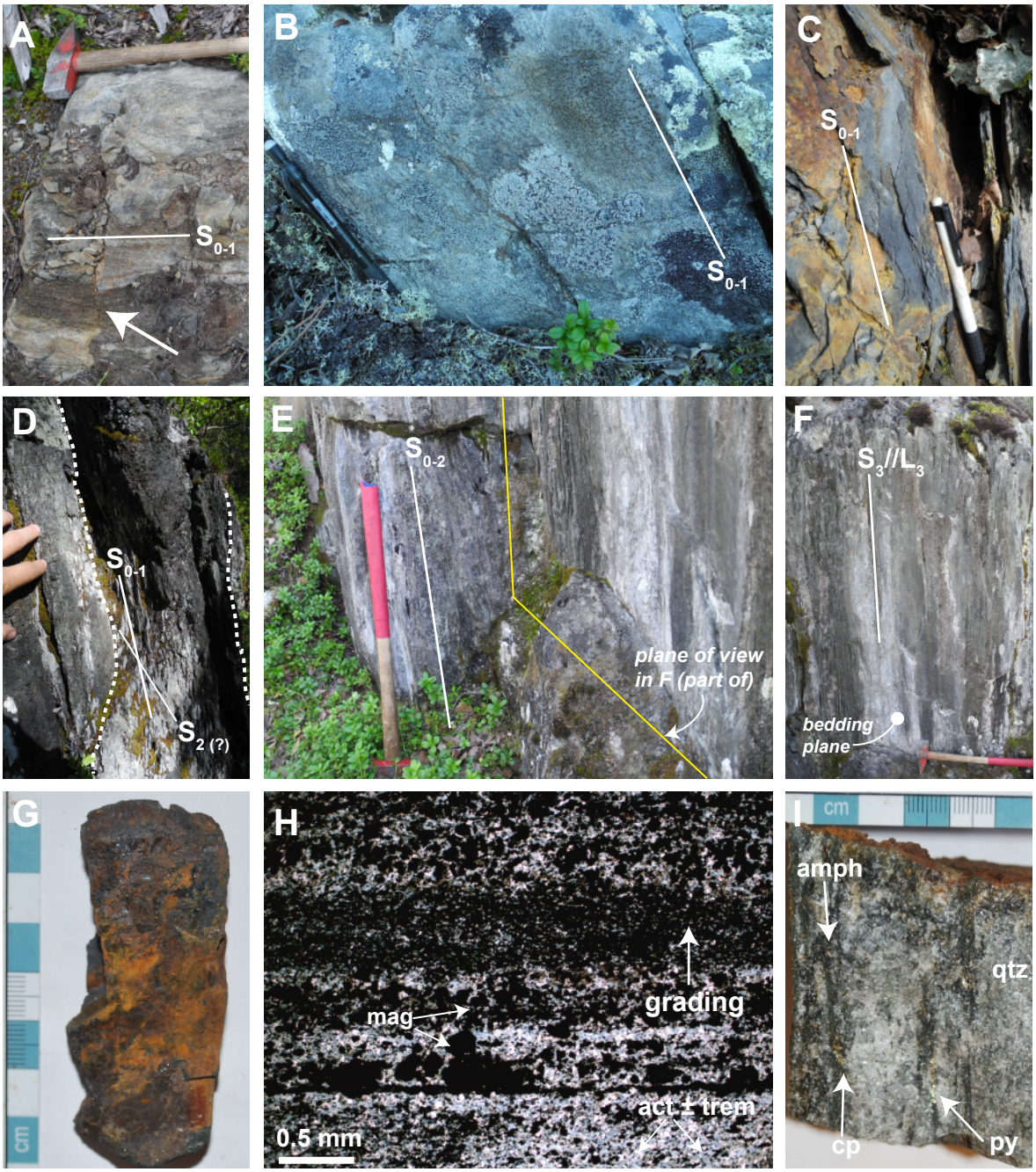

Figure 6. Upper sedimentary formation rocks at Nunasvaara. **A.** Argillaceous layer (arrow) in mica schist. The hammer head is 15 cm long. **B.** Sub-vertical, bedding plane view of fine-grained, mafic metasedimentary rock (possible greywacke). **C.** Sub-vertical, along-strike view of graphitic schist. The pencil is 15 cm long. **D.** Sub-vertical, along-strike view of approximately 20 cm thick, planar to undulose metacarbonate horizon (calc-silicate rock) in a metasedimentary rock. **E.** Sub-vertical view of laminated meta-carbonate rock showing a composite So-2 foliation. **F.** Sub-vertical view of bedding plane surface (approximately orthogonal to strike) shown in E with L3 intersection lineations. **G.** Hand specimen of laminated meta-ironstone. **H**. Thin section plane polarised light view of laminated meta-ironstone showing grading. **I.** Hand specimen view of amphibole and sulphide-bearing quartz-rich horizon (possible metachert).

chalcopyrite and titanite, or occurs in hornblende ± actinolite veinlets (Figs. 7C & 7E). Rarely, relict clino-pyroxene occurs, typically as anhedral and fragmented crystals, enclosed or partly replaced by hornblende aggregates (Fig. 7E). Plagioclase is commonly replaced by scapolite (Figs. 7B & 7D) while late-stage (retro-gressive) minerals include chlorite (replacing hornblende), sericite (replacing plagioclase) and hematite (replacing magnetite). Irregular amphibole ± magnetite veinlets are also a fairly common feature (Fig. 7A).

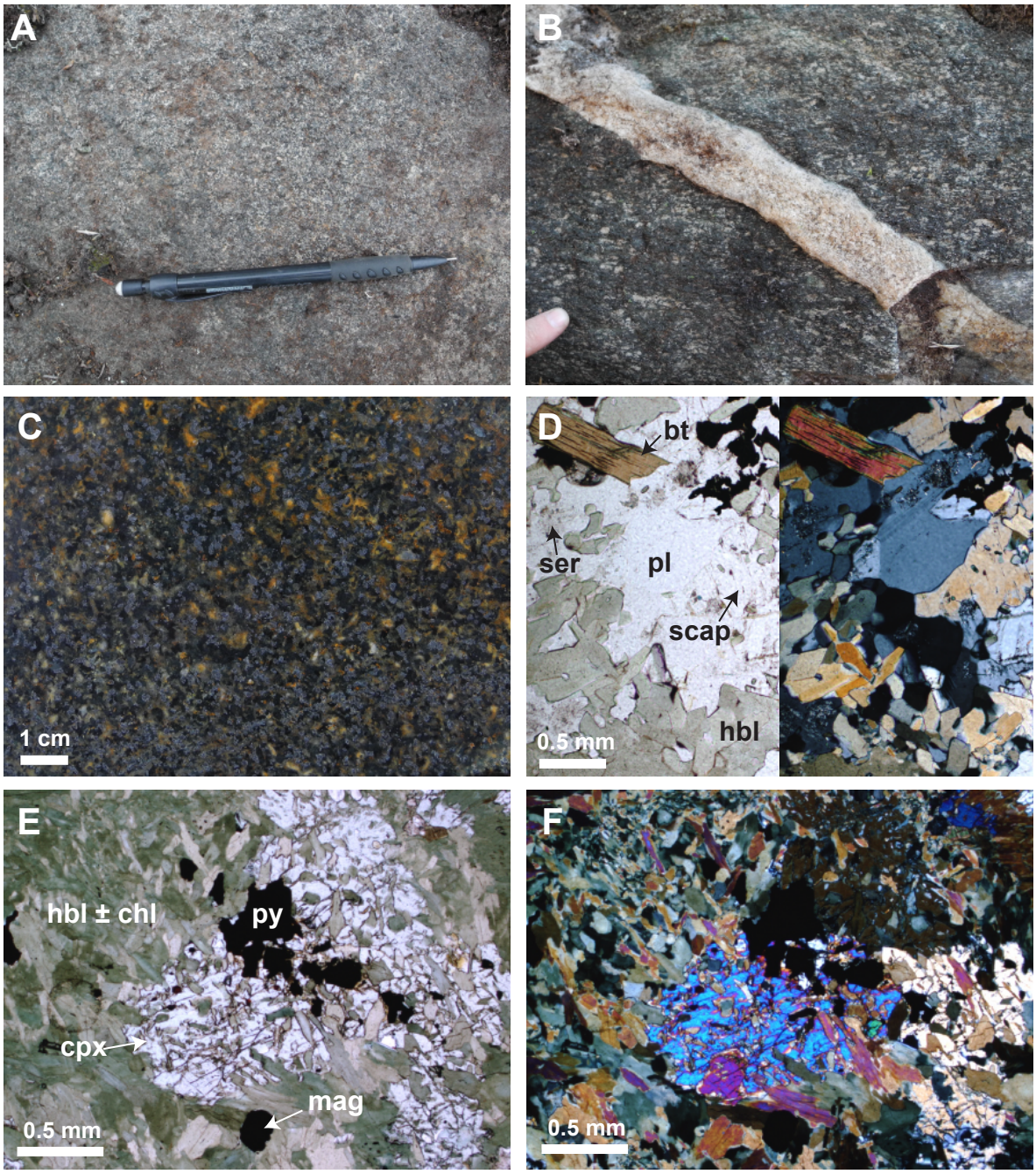

Figure 7. Metadolerite at Nunasvaara. **A.** Outcrop view of weakly foliated, weakly to moderately scapolite ± albite-altered, metadolerite. Dark grey, amphibole-rich veinlets also seen. The pencil is 15 cm long. **B.** Outcrop view of a foliated metadolerite cut by an aplite dyke. **C.** Cut hand sample surface showing medium-grained, intergranular (granoblastic), amphibole-plagioclase feldspar matrix with abundant disseminated magnetite (medium grey, anhedral grains). Patchy orange staining is fine-grained hematite (after magnetite) overprinting plagioclase. **D.** Split thin section plane-polarised light (PPL, left) and cross-polarised light (XPL, right) views of ophitic and xenoblastic hornblende–plagioclase feldspar matrix. Subhedral biotite (top left) may be a late metasomatic phase (replacing hornblende?). **E and F.** Thin section PPL and XPL views of granoblastic to decussate hornblende associated with relict clinopyroxene grain (second-order blue, purple). Mineral abbreviations: bt = biotite, chl = chlorite, hbl = hornblende, mag = magnetite, pl = plagioclase feldspar, py = pyrite, cpx = clinopyroxene, scap = scapolite, ser = sericite.

Throughout the sequence the metadolerite sills are variably deformed and display folding patterns that conform to the general ductile deformation trends seen across the area (Fig. 2B). Based on magnetic anomaly data, folded sills partly correspond to curvilinear zones, with relatively high magnetic

signatures (Fig. 8A). In general, the folded nature of the sills attests to their emplacement as part of the broader greenstone sequence before the onset of Svecokarelian-cycle orogenesis and deformation.

Based on geological and petrographic considerations, Eriksson & Hallgren (1975) considered the metadolerite to represent the hypabyssal equivalent of *Vittangi greenstone group* mafic metavolcanic rocks. Alternatively, the prevalence of sill-like bodies crosscutting the volcanic-sedimentary sequence suggests that the metadolerite may represent a compositionally similar but younger phase of mafic magmatism. However, given the lack of chilled margins in the sills, the comparable mineralogy of both units, their close spatial proximity and similar deformation history, a comagmatic link between the metadolerite and mafic metavolcanic rocks seems plausible (e.g. Eriksson & Hallgren 1975). Lithogeochemical and isotopic results reported here support the contention that both units form part of a broadly contemporaneous suite of tholeiitic mafic magmatism.

Deformation and structures at Nunasvaara

The greenstone sequence at Nunasvaara has been affected by episodic, polyphase deformation (Eriksson 1969, Eriksson & Hallgren 1975). Overprinting folding events have imparted a striking "basin and dome"-type pattern, indicative of refold interference (cf. Thiessien 1986). Asymmetric fold patterns, localised shearing and strain partitioning of structurally incompetent layers has developed a broad, roughly northeast-trending ductile shear zone, in which meta-volcanosedimentary units "wrap around" a central, relatively more competent mainly meta-igneous core. In addition, numerous crosscutting fault and fracture zones suggest one or more episodes of late-stage brittle or brittle-ductile deformation.

The most commonly observed structure in the Nunasvaara area is a penetrative planar fabric (S1) in layered metavolcanic and metasedimentary rocks that locally parallels inferred bedding (S0). Based on this premise and the general observation that layered rocks display large-scale folding patterns formed by subsequent deformation events, the composite bedding–foliation fabric (S0-1) is inferred to represent the earliest deformation event in the area (i.e. D1) and to have formed before the major folding episodes.

Two major folding systems are recognised at Nunasvaara (cf. Eriksson & Hallgren 1975). These are (1) asymmetric, approximately north-northwest to north-northeast-orientated, moderate to tight, gently to moderately-plunging, upright folds; and (2) symmetric, east-southeast to east-northeast-orientated, open to gentle, steeply plunging (sub-vertical) folds (Fig. 8). Eriksson & Hallgren (1975) tentatively suggested the latter folds represent the earlier phase of folding. Based on refold patterns derived from structural lineament analysis of reprocessed ground geophysical data and outcrop structural features (Fig. 8A–E), we preliminarily interpret the north-trending folds as the earlier fold system, here designated F2 (D2 event), whereas the gentler, east-trending and steeply plunging folds formed later (F3 folds during D3). However, the possibility that F2 folds have refolded earlier, approximately E–W-aligned, upright and horizontal F1 folds, is suggested by the domical, non-cylindrical nature of some F2 folds (Fig. 8B–C). Overall, the interaction and overprinting of F2 and F3 folds (and potential earliest F1 folds) developed numerous fold interference patterns across the area. The largest expression of this is an approximately 5 × 6 km, antiformal domical structure, here named the *Nunasvaara dome* (Fig. 8A).

The Nunasvaara dome has an elongate, north–south-orientated oblate form, centred on a doubly-plunging, non-cylindrical, F2 antiform (Figs. 2 & 8). The domical outline is clearly delineated by folding patterns on geophysical anomaly maps and is reinforced by compositional and rheological contrasts between metasedimentary and meta-igneous rock layers (e.g. Figs. 2C & 8A). In particular, the graphite schist horizon hosting the Nunasvaara graphite deposit (i.e. *Nunasvaara member*) acts as an important strain "marker horizon", which discontinuously curves around the domical body, highlighting its oblate form (Fig. 8A). Moreover, moderately to steeply plunging F2 and F3 fold axes and mineral lineations from across the study area highlight how linear structures generally record axial-type symmetry, concomitant with a radiating, dome-like pattern following fold interference (Fig. 8C).

Locally, the domical shape is disrupted in the west and north by distinct refold patterns (Figs. 2 & 8).

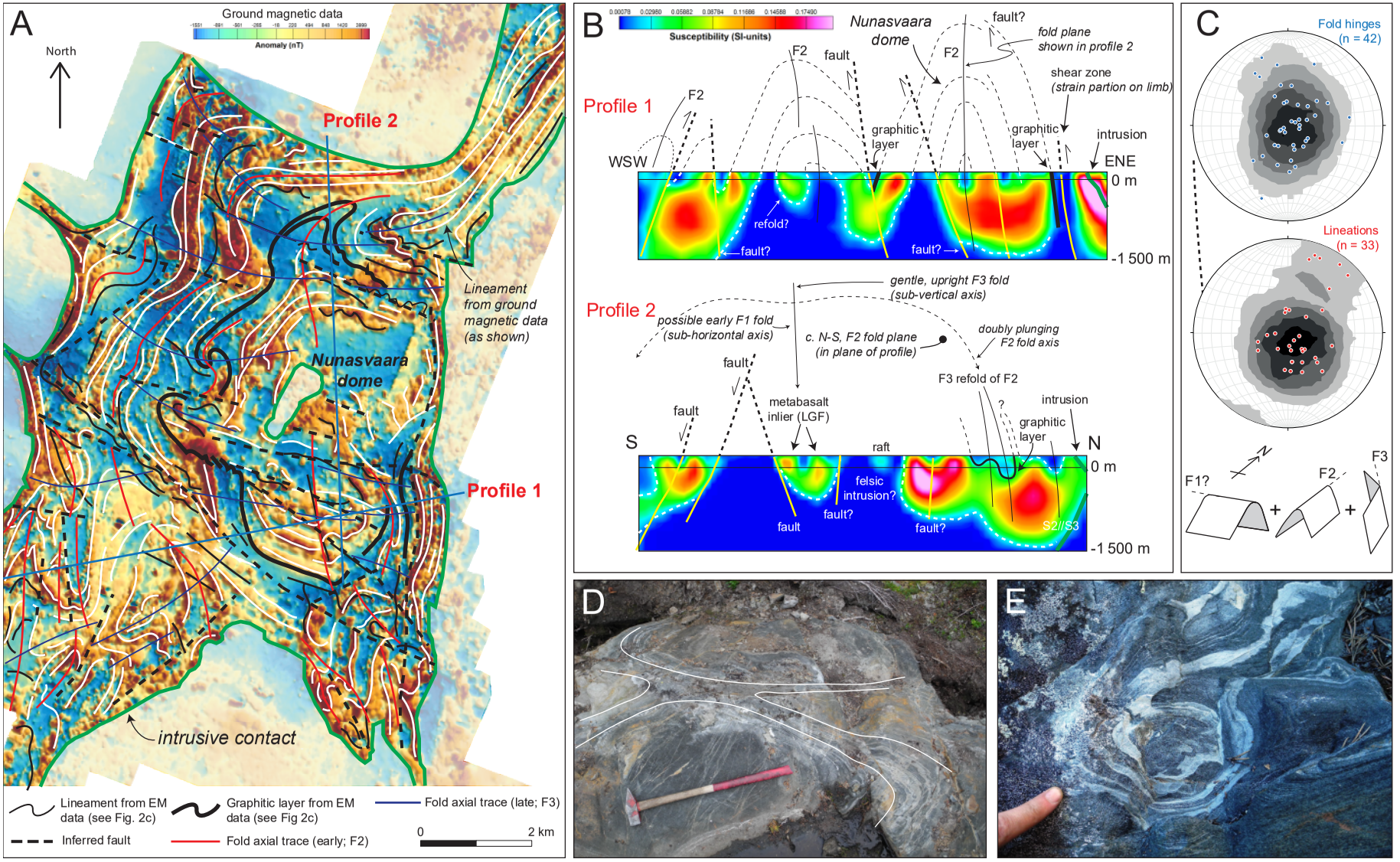
A
Ground magnetic data
Anomaly (nT)
North
Profile 2
Profile 1
Nunasvaara dome
Lineament from ground magnetic data (as shown)
intrusive contact
Lineament from EM data (see Fig. 2c)
Graphitic layer from EM data (see Fig 2c)
Fold axial trace (late; F3)
Inferred fault
Fold axial trace (early; F2)
0
2 km
B
Susceptibility (SI-units)
Nunasvaara dome
fault?
fold plane shown in profile 2
shear zone (strain partion on limb)
Profile 1
F2
fault
graphitic layer
intrusion
WSW
ENE
0 m
refold?
fault?
-1 500 m
Profile 2
gentle, upright F3 fold (sub-vertical axis)
possible early F1 fold (sub-horizontal axis)
c. N-S, F2 fold plane (in plane of profile)
doubly plunging F2 fold axis
F3 refold of F2
metabasalt inlier (LGF)
S
N
raft
felsic intrusion?
S2//S3
C
Fold hinges (n = 42)
Lineations (n = 33)
F1?
F2
F3
D
E

◀ Figure 8. Structural geology of the Nunasvaara area. **A.** Ground magnetic anomaly map with interpreted structural lineaments. Solid black lines and graphitic layers are derived from the slingram data shown in Figure 2C. **B.** Two-dimensional magnetic susceptibility models along profiles lines 1 and 2 (shown in A), with associated structural interpretations. Profile 2 highlights the position of metabasaltic rocks of the Lower greenstone formation (LGF) in the core of an approximately N–S-aligned, antiformal dome-type structure. **C.** Equal-area stereonets with plotted points for fold axis and lineation orientations from across the study area. These data, displaying axial-like symmetry, corroborate the presence of non-cylindrical, domical structures, formed by the interaction of two or three overprinting folding events (sketch). **D.** Outcrop view to the south-southeast of an "egg box"-type fold interference pattern in a laminated metatuff. The hammer head is 15 cm long. E. View of dome-like pattern preserved in a laminated metatuff. Top is to the northeast.

In the west, a west-northwest-orientated, steeply west to northwest-plunging F2 fold hosts the Nunasvaara graphite deposit along its hinge area and southwest limb (Fig. 8A). In the north, the axis of a northward-plunging F2 fold is deflected towards the northeast by an east-trending F3 fold. Beyond the tightening hinge zone of the refolded F2 fold, the greenstones become stretched and transposed into a curvilinear, northeast-trending composite deformation zone (Fig. 8A–B). Overall, bedding appears squeezed and channelled between two large intrusions, while locally, bedding and F2 fold traces appear deflected, indented and locally truncated by a c. 1.8 Ga granite (Figs. 2B & 8A). In contrast, F3 fold traces tend to curve parallel to the contact with the granitoid. This suggests F3 folding may have been synchronous with, or slightly predate, the c. 1.8 Ga phase of granitic magmatism. Further refolding patterns are evident in the southwest of the study area (e.g. Type I of McClay 1987) from structural lineament patterns derived from magnetic anomalies (Fig. 8A).

The layered greenstone sequence (including metadoleritic sills) extends outward along the western and eastern flanks of the Nunasvaara dome. On the western limb, the most continuous stratigraphic sequence is preserved (corresponding to the stratigraphy determined along profile lines X–X', Y–Y' and Z–Z', Fig. 2A–B). In contrast, the eastern limb is truncated by a steeply east-dipping, north to north-northeast-trending, composite deformation zone (Fig. 8A–B). Here, shearing and faulting have juxtaposed a narrow zone of graphitic schist (*Upper sedimentary formation*) against a tapering slice of metatuff (*Upper greenstone formation*). This apparent superimposition, combined with asymmetric lineament patterns and magnetic anomaly dip orientations (Fig. 8A–B), indicates mainly top-to-the-west thrusting, with a possible dextral-oblique component (i.e. reverse-oblique shearing or faulting). Strain partitioning along the eastern limb of the dome may have contributed to the focused deformation occurring along this relatively narrow, localised zone. An additional aspect is how bedding on the eastern limb is intruded and partly deflected by a foliated, c. 1.9 Ga, gabbroic to dioritic pluton (Fig. 8A). Syn-tectonic emplacement of this intrusion may have contributed to focused zones of deformation along its western margin.

Magnetic susceptibility inversion modelling (to a depth of 1.5 km) and structural lineament analysis of geophysical anomaly data have facilitated further assessment of the nature and geometry of the Nunasvaara dome (Fig. 8A–B). A preliminary interpretation of Profile 1 (west-southwest-aligned, Fig. 8A) indicates steeply east-northeast-dipping anomalies in the east and steeply west-southwest-dipping anomalies in the west. Correspondingly, the southern part of the dome consists of an asymmetric, weakly west-verging, upright F2 fold. In contrast, at the western end of the profile, lower amplitude upright F2 folds verge to the east. The narrow deformation zone along the eastern limb of the Nunasvaara dome is steeply east-dipping (Fig. 8B, Profile 1).

Profile 2 (north-aligned, Fig. 8A) transects the length of the Nunasvaara dome, sub-parallel to a major F2 axial plane. This profile highlights fold interference patterns in the north, where an F2 fold is refolded and transposed into a composite S2-3 foliation (Fig. 8B, Profile 2). Where the profile transects the central part of the dome, a fault-bounded anomaly corresponds to an inlier block of mafic metavolcanic rocks (metabasalt), and is inferred to represent the base of the stratigraphy at Nunasvaara

(i.e. *Lower greenstone formation*). Two adjacent zones of low magnetic susceptibility (that have no known surface exposures) may represent intermediate to felsic intrusions in this central area (Fig. 8B, Profile 2).

In summary, ductile deformation patterns observed across the study area suggest the succession forms part of a broader, roughly northeast-trending composite shear zone. Locally, asymmetric F2 folding of layered units indicates shearing was mainly dextral-oblique. A conspicuous feature of the deformation geometry is the strongly distorted and partly sinuous nature of areas underlain by layered meta-volcanosedimentary rocks. These units appear to "wrap around" the core of the Nunasvaara dome, imparting a large-scale, somewhat "augen"-type pattern to the sequence. This geometry suggests the core of the dome (mainly comprising metadolerite and metabasalt) may have acted as a more competent or rigid block within the larger shear zone.

Numerous faults and fracture zones transect the Nunasvaara area, and represent a composite phase of brittle deformation (i.e. D4 event, Fig. 2A). The faults are mainly west-northwest-aligned, are subvertical, and their general orientation parallels the roughly east–west trace of F3 fold axes. Locally, D4 faults displace and truncate both F2 and F3 axial traces (e.g. southwest study area, Fig. 8). Based on structural lineament patterns (Figs. 2B & 8A), lateral fault displacements are not strongly developed and the steeply dipping faults may have facilitated mainly vertical displacements.

A major northwest-trending fault zone occurs to the south of the Nunasvaara graphite deposit and transects the southern part of the Nunasvaara dome (Fig. 2B). A fault splay of this zone trends close to and partly overlaps the southeastern extension of the Nunasvaara graphite deposit. Given that numerous graphite-bearing veins occur within the deposit, localised brittle or brittle-ductile deformation may have played an important role in enhancing the degree of graphite mineralisation at Nunasvaara (cf. Pearce et al. 2015).

Structural analysis of similar graphite mineralisation in northern Norway (Western Troms Basement Complex) indicates that complex folding and composite brittle-ductile shearing and faulting are important controls on graphite mineralisation in Palaeoproterozoic metasupracrustal rocks (Henderson & Kendrik 2003).

Geology and lithostratigraphy at Masugnsbyn (Veikkavaara greenstone group)

The Masugnsbyn area is located approximately 90 km east-southeast of Kiruna and approximately 60 km northwest of Pajala (Fig. 1B). Here, greenstones of the *Veikkavaara greenstone group* are overlain by a package of Svecofennian metasedimentary and subordinate metavolcanic rocks assigned to the *Pahakurkio* and *Kalixälv groups* (Padget 1970). The supracrustal sequence is folded into large scale anticlinal and synclinal structures. The area is best known for its skarn-type iron mineralisation and dolomite, which occur in the uppermost part of Veikkavaara greenstone group. Minor Cu-Zn-Pb, Cu-Au and graphite mineralisation also occurs in the Masugnsbyn area (e.g. Geijer 1929, Padget 1970, Witschard et al. 1972, Grip & Frietsch 1973, Niiniskorpi 1986, Frietsch 1997, Martinsson et al. 2013, 2016, Zaki 2015).

Rocks of the Veikkavaara greenstone group, predominantly consisting of mafic volcaniclastic rocks, form a V-shaped area between the villages of Masugnsbyn, Saittarova and Junosuando (Fig. 9). This distinctive pattern developed on the opposing limbs of a large-scale, roughly north-trending, upright fold, named the Saitajärvi anticline (Padget 1970). Additional folding and faulting with variable orientations developed across the area during protracted, polyphase deformation (cf. Grigull et al. 2018).

Outcrop exposure of greenstone-related units at Masugnsbyn is generally poor (< 1% by area). The greenstone sequence is clearly outlined as a high-magnetic and banded sequence on the aeromagnetic map (Fig. 10A). The alternating high and low magnetic anomalies probably reflect depositional features, further accentuated by secondary-growth magnetite in distinct layers, associated with overprinting metamorphic and metasomatic alteration events.

Low-resistivity, graphite-bearing horizons in the greenstones are discernible from airborne electro-

magnetic measurements (Fig. 10B). A relatively conductive graphitic horizon at the stratigraphic top of the sequence marks the contact zone with overlying Svecofennian rocks, and can be traced continuously around the V-shaped structure (Fig. 8B). Locally, the graphitic horizons coincide with stratiform Masugnsbyn skarn iron mineralisation. The iron mineralisation north of Masugnsbyn forms a relatively continuous, approximately 8 km long curvilinear zone, coinciding with the uppermost part of the greenstone stratigraphy (e.g. Witschard et al. 1972, Frietsch 1997).

Supracrustal rocks at Masugnsbyn are intruded by c. 1.88 Ga early and 1.80 Ga late orogenic intrusions of mainly granitic to syenitic composition. At Masugnsbyn village a perthitic granite is in direct contact with skarn iron mineralisation (Fig. 9, Padget 1970). In the central part of the Veikkavaara greenstones a homogeneous, low-conductive rectangular area is inferred to represent intrusive rocks of gabbroic composition (Figs. 9 & 10).

The stratigraphy of the Veikkavaara greenstone group has previously been assessed by Padget (1970). In that account, three broad, informal subdivisions were proposed. They are (1) a lowermost approximately 2000 m thick unit of massive, basaltic greenstones (named Unit 1a); (2) an approximately 100 m thick middle unit comprising pelitic schist and quartzite (Unit 1b); and (3) an uppermost, approximately 1500 m thick composite unit of basaltic tuffs with overlying graphite schist and metacarbonate horizons (Unit 1c). Given the lack of exposure and degree of deformation, the thickness estimates proposed by Padget (1970) are probably approximations.

As part of this study, we have reassessed the stratigraphy of the Veikkavaara greenstone group. Detailed geological mapping along two profiles that equate to approximately 2000 m of stratigraphy provides the basis for our re-examination (Profiles A and B, Fig. 9). Additionally, new interpretations of reprocessed airborne magnetic and electromagnetic data (Fig. 10A–B) have been integrated with geological observations to construct a new composite stratigraphy for the area.

In summary, four new subdivisions at the stratigraphic formation level are recognised for the Veikkavaara greenstone group at Masugnsbyn. Detailed descriptions of these units incorporating new minimum thickness estimates are presented in the following subsections. As part of this work, we officially abandon the alphanumeric names used by Padget (1970) for subunits of the Veikkavaara greenstone group, and here propose new informal names that combine geographical (i.e. stratotype location) and stratigraphic unit or rank components. This approach is more consistent with formal stratigraphic nomenclature and procedures (e.g. Salvador 1994). Two of the proposed informal names retain geological qualifiers, however. The lowermost unit (previously 1a) is referred to as the *Nokkokorvanrova greenstone formation*, the middle unit (1b) as the *Suinavaara formation*; while the uppermost unit (1c) is now split into the lower *Tuorevaara greenstone formation* and upper *Masugnsbyn formation*.

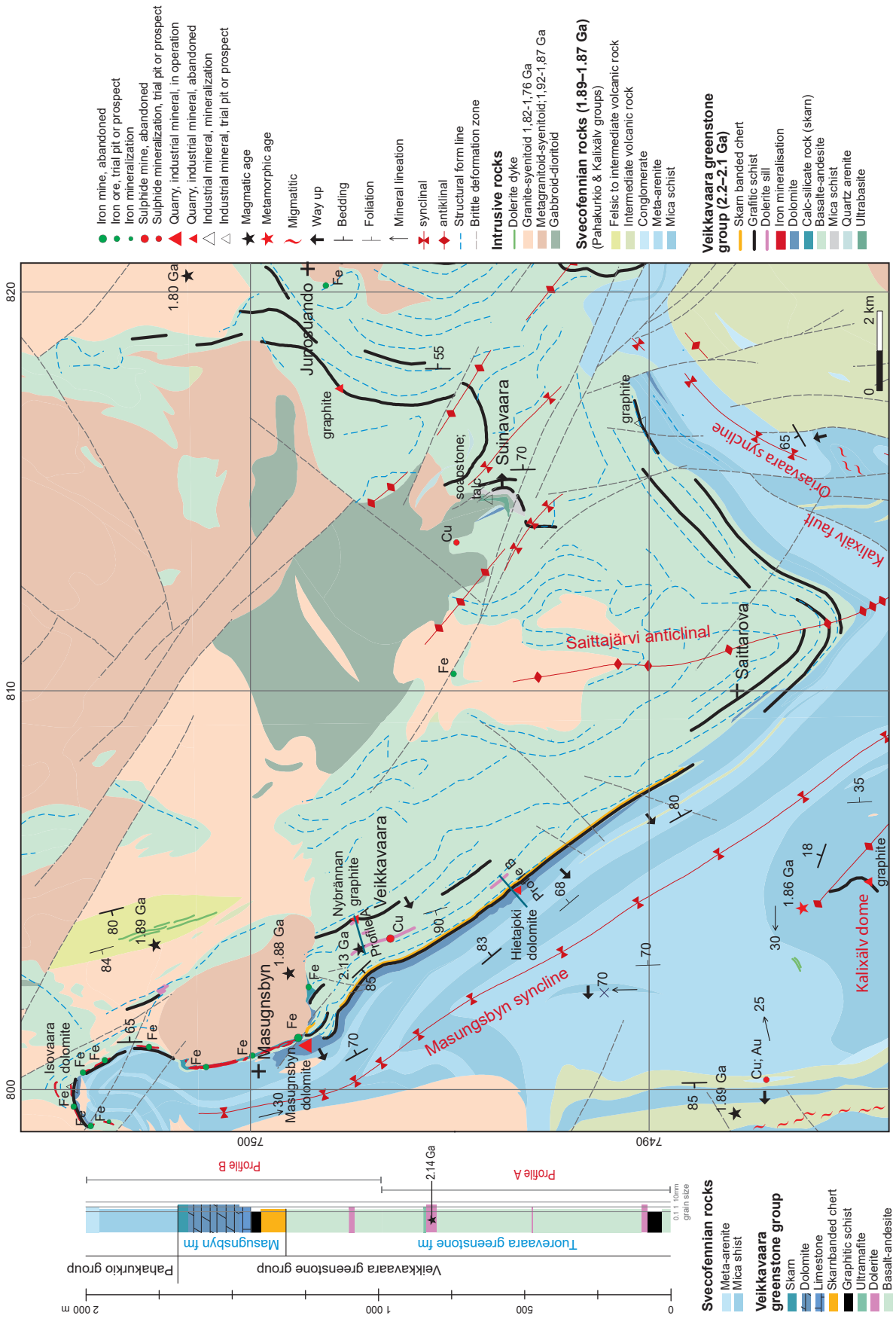

Figure 9. Geology of the Masugnsbyn area with a composite schematic stratigraphy of the Veikkavaara greenstone group, based on profiles A and B. Radiometric age determinations are from Bergman et al. (2001, 2006), Hellström et al. (2018), and this study.

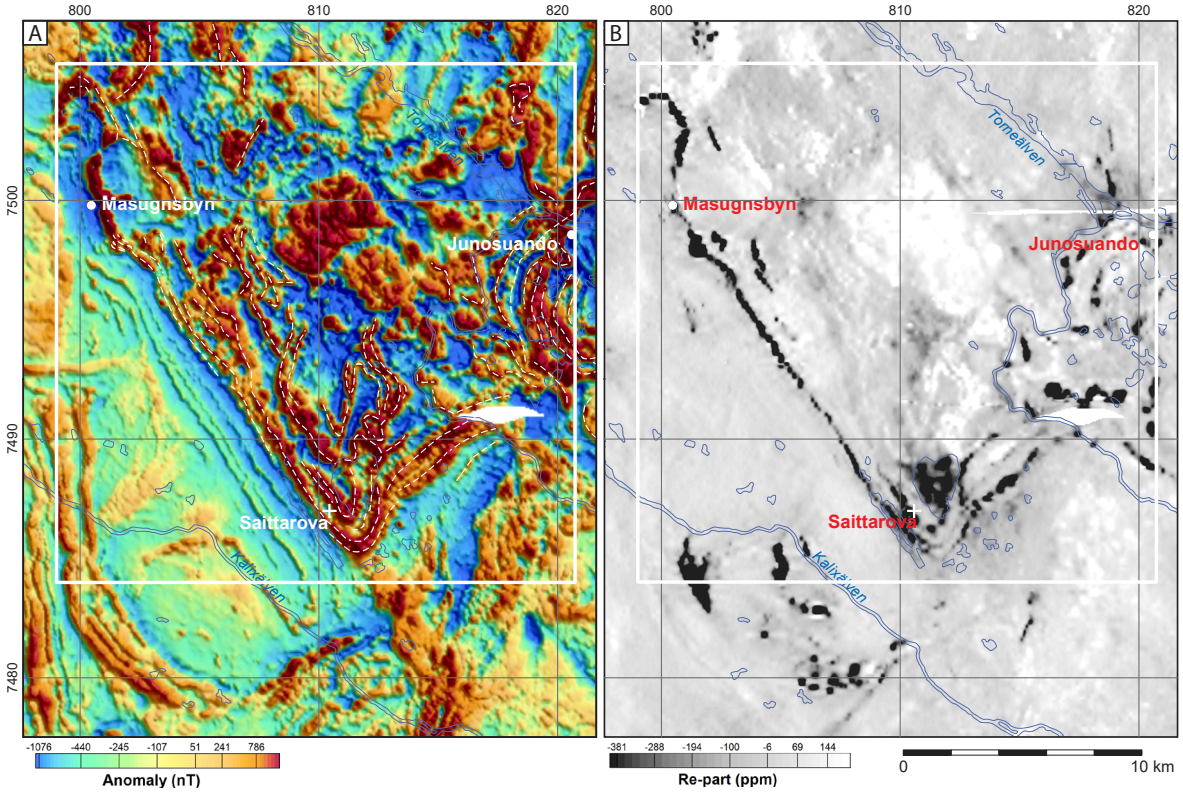

Figure 10. **A.** Airborne magnetic anomaly map for the Masugnsbyn area. It is suggested that structural form lines (broken white lines) in the Veikkavaara greenstones represent bedding in the basaltic tuffs. The white rectangle shows the extent of the geological map in Figure 9. **B.** Grey-scale, airborne electromagnetic (slingram) anomaly map (in-phase, real component) of the Masugnsbyn area. Black areas represent relatively conductive, graphite- and sulphide-rich rocks. The white rectangle shows the extent of the geological map in Figure 9.

Nokkokorvanrova greenstone formation

Mafic rocks assigned to the Nokkokorvanrova greenstone formation (NGF) are only exposed north of Suinavaara (eastern Masugnsbyn area), along the banks of the river Tärendöälven (Fig. 9, unit 1a of Padget 1970). This area represents the eastern limb of the Saitajärvi anticline. This lowermost formation predominantly consists of dark green, fine-grained, massive units, resembling mafic lavas or possibly intrusive rocks.

Banded magnetic anomaly patterns seen on the Masugnsbyn aeromagnetic map (Fig 10A) suggest the NGF extends to the west and north of Tärendöälven, but no outcrops are known from that area. Based on this interpretation, Padget (1970) estimated the (minimum) thickness of the NGF to be approximately 2 km. But a homogenous, low-conductive area in the core of the Saitajärvi anticline (Fig. 10B) suggests that parts of the core area may consist of intrusive rocks, highlighting a degree of uncertainty about the thickness estimate.

Suinavaara formation

Padget (1970) described an approximately 100 m thick metasedimentary sequence at Suinavaara (unit 1b, eastern Masugnsbyn area, Fig. 9). The sequence mainly consists of a clastic quartzite horizon with lesser pelite and metacarbonate rocks. The pelitic rocks (partly graphitic) occur at the same horizon or slightly above the quartzite. Locally, at Suinavaara, the quartzite is in contact with a marble horizon (Padget 1970).

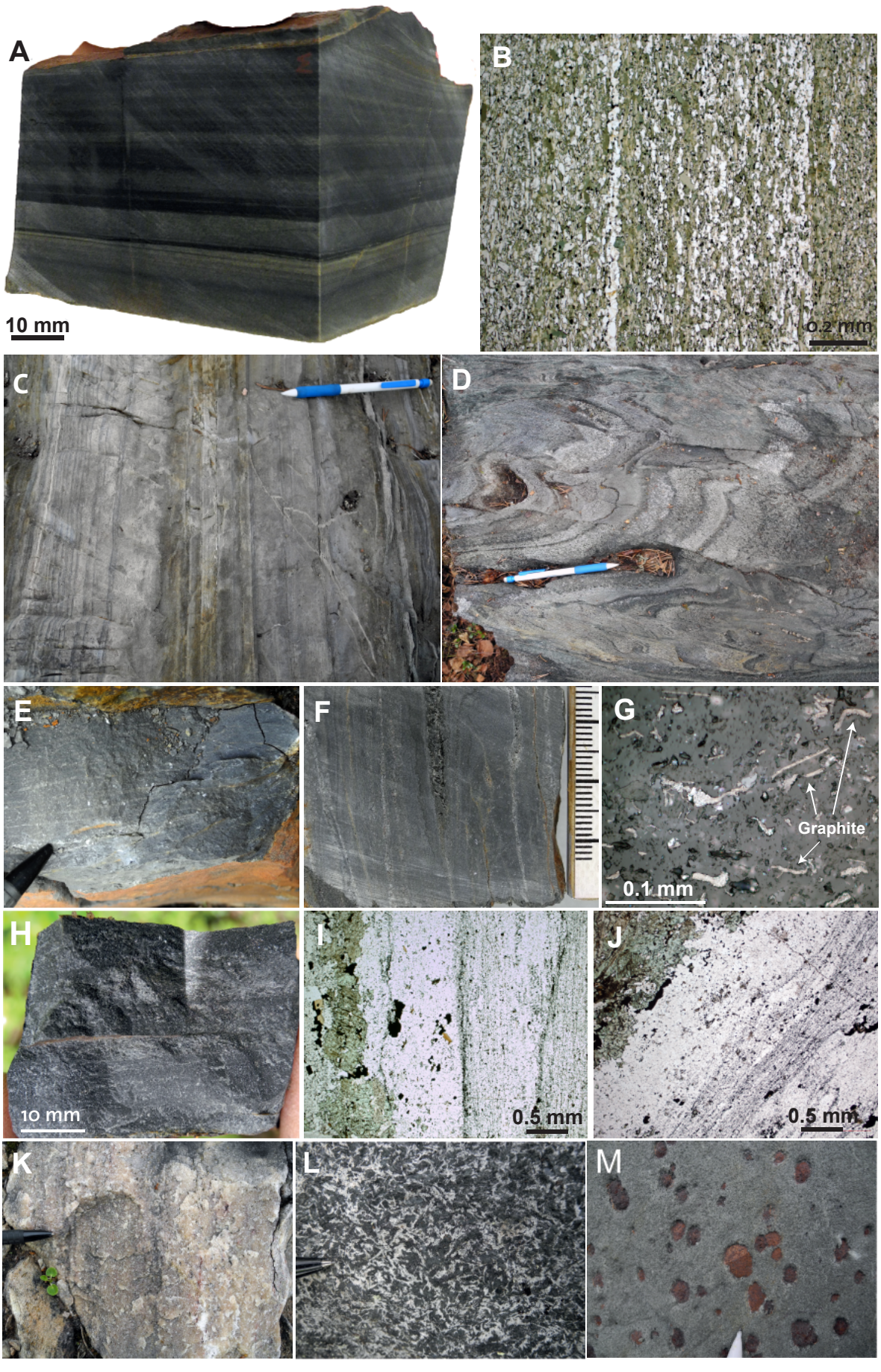
A
10 mm
B
0.2 mm
C
D
E
F
G
Graphite
0.1 mm
H
10 mm
I
0.5 mm
J
0.5 mm
K
L
M

◀ Figure 11. Rock types of the Veikkavaara greenstone group. **A.** Sawn rock sample of laminated metatuff taken from the western wall rock of the Veikkavaara Cu prospect (Tuorevaara greenstone formation) (7496490/803773). **B.** Thin section plane-polarised light (PPL) view of the laminated metatuff shown in A, predominantly consisting of layered amphibole and plagioclase feldspar. **C.** Outcrop showing the laminated to layered character of Tuorevaara greenstone formation metatuff. The pen is 15 cm long (7497085/803714). **D.** Folded mafic metatuff at Suinavaara (Tuorevaara greenstone formation), from the eastern limb of the Saitajärvi anticline (7494094/815621). **E.** Graphite schist at the Nybrännan graphite quarry, basal part of the Tuorevaara greenstone formation (7497394/804271). **F.** Graphitic schist of the Masugnsbyn formation (7498403/801505). **G.** Thin section reflected-light view of graphitic schist shown in F. **H.** Skarn-banded chert with very fine-grained, dark quartz bands alternating with diopside-rich bands (Masugnsbyn formation). **I.** Thin section cross-polarised light view of skarn-banded chert. Granular quartz (grey, right) is variably very fine- to fine-grained. **J.** PPL view of skarn-banded chert. Band of green diopside (left), alternating with quartz bands (colourless, right). **K.** Dolomitic marble from the Hietajoki quarry (7493321/805002, Masugnsbyn formation). **L.** Fine- to medium-grained metadolerite with relict subophitic texture (7497276/803517). **M.** Ultramafite with orthopyroxene megacrysts in an amphibole-rich matrix (7497209/803517). Coordinates are given in SWEREF99 TM.

Stratigraphically, the metasedimentary sequence at Suinavaara, here named the Suinavaara formation (equivalent to Unit 1b of Padget 1970), has been placed between the Nokkokorvanrova greenstone formation and Tuorevaara greenstone formation (Padget 1970). Cross-bedding in the basaltic tuffs above the Suinavaara formation indicates way-up to the east and thus support this stratigraphic interpretation (Padget 1970). Occurrence of marble and graphitic schist is otherwise a characteristic feature of the uppermost part of the Veikkavaara greenstone group. Complex folding of the metatuffs at Suinavaara probably complicates the interpretation of way-up indicators in the sequence (e.g. Fig. 11D).

Tuorevaara greenstone formation

The Tuorevaara greenstone formation (TGF) is primarily exposed in the Veikkavaara–Tuorevaara area and forms the western limb of the Saitajärvi anticline (Fig. 9). Here, the sequence mainly consists of mafic metatuffs with minor graphitic schist and metadolerite sills. The formation has an estimated thickness of approximately 1 km (cf. Padget 1970).

The metatuffs typically display planar, parallel laminae or compositionally variable layering at the mm- to cm-scale (Fig. 11A–D). Locally, subordinate cm- to m-scale layers have a more massive appearance and resemble lava flows or mafic intrusive rocks. While cross-bedded tuffaceous rocks are known at Suinavaara in the eastern Masugnsbyn area (Padget 1970), metatuffs at Veikkavaara are predominantly planar, with a parallel, laminated structure. Locally, grain size grading indicates way-up to the west-southwest.

Mineralogically, the metatuffs consist of plagioclase feldspar ($An_{10–50}$, Padget 1970) and green, pleochroic hornblende. Locally, elongate actinolite-tremolite crystals are the predominant amphibole phase. Minor and accessory minerals include brown, pleochroic biotite, and magnetite, pyrite, chalcopyrite and rare quartz.

Intercalated graphitic schist horizons are known from the TGF, primarily from electromagnetic surveys and exploration trenching. At Veikkavaara (Fig. 9), a layer of graphite schist is exposed at the Nybrännan graphite quarry in the easternmost part of the mapping profile at Veikkavaara (Figs. 9 & 11E). This unit possibly constitutes the same stratigraphic level as the Suinavaara formation, thus forming the upper part of a predominantly metasedimentary sequence. This interpretation provides a correlation between the graphite schist at Nybrännan and the Nunasvaara member of the Lower sedimentary formation at Nunasvaara. East of the Nybrännan quarry there are no known outcrops, but the banded magnetic anomaly pattern suggests that the greenstones continue for approximately 3 km (Fig. 10A).

The Nybrännan graphitic schist unit, estimated to be at least 50 m thick, is bordered by an approximately 20 m thick dolerite sill to the west. Locally, the horizon is inter-layered with plagioclase-rich light grey tuffite containing subordinate biotite, pale green actinolite and accessory titanite and pyrrhotite. Gerdin et al. (1990) describe the graphite-rich horizon at Nybrännan as an approximately 20 m thick, northwest-trending and sub-vertical layer containing up to approximately 40% graphite. Graphite is typically very fine-grained (approximately 0.005 mm, amorphous) and disseminated within a groundmass of microcline, quartz, plagioclase, biotite, titanite and rutile. Locally, graphite occurs in aggregates and veins of more variable grain size. Amphibole porphyroblasts (0.5–2 mm) also occur. No greenstone-type outcrops are known east of Nybrännan.

Masugnsbyn formation

The Masugnsbyn formation constitutes the uppermost part of the Veikkavaara greenstone group in the Masugnsbyn area. It mainly consists of chemically deposited metasedimentary rocks such as skarn-banded metachert (BIF-related) and calcitic to dolomitic marble with lesser graphitic schist. The thickness of the formation is estimated to be 370 m (see Profile B, Fig. 9).

The stratigraphically lowest rock unit is an approximately 80 m thick skarn-banded chert. It is dark grey and consists of alternating bands of very fine-grained to fine-grained polygonal quartz and fine- to medium-grained clinopyroxene or amphibole (Fig. 11H–J). Relatively abundant disseminated pyrrhotite and pyrite also occur (2.4 wt % S, Table 3), which are coarser within skarn bands. Minor magnetite and flakey graphite are disseminated in quartz-rich zones and locally enriched in thin seams, imparting a banded appearance. The whole-rock iron content is 17.5 wt. % Fe_2O_3t (Table 3).

A 20–30 m thick graphitic schist horizon occurs above the skarn-banded chert (Fig. 9). The unit does not crop out along Profile B (Fig. 9), but is known from electromagnetic measurements (slingram), historical exploration trenching (Fig. 10B, e.g. Gerdin et al. 1990), recent core drilling at Masugnsbyn (Zaki 2015) and a newly discovered outcrop east of the Masugnsbyn quarry. Based on these data, the graphitic unit forms a fairly continuous, approximately 10 km long, conductive layer from the Masugnsbyn dolomite quarry in the north to the village of Saittarova to the southeast (Figs. 9 & 10). Sulphide minerals and graphite associated with the underlying chert horizon may also contribute to this geophysical anomaly. In general, the graphitic schist is very fine-grained and laminated, and locally contains veins of coarser quartz, mica and amphibole, as well as thin calcite layers (Fig. 11F). It predominantly consists of quartz, feldspar, biotite, muscovite and amphibole. Accessory minerals include graphite, carbonates, Fe-oxides, sulphides and titanite. Graphite typically occurs as disseminated, very fine flakes (Fig. 11G). Historical geochemical analyses indicate whole-rock C and S concentrations ranging from 1.1 to 5.1 wt % and 1.8 to 5.2 wt %, respectively (Gerdin et al. 1990). Fairly thin layers of calcitic marble occur locally within the graphitic schist (Zaki 2015).

Stratigraphically above the graphitic schist lies a 150–250 m thick metacarbonate unit (dolomitic marble, Fig. 11K), which is exposed along Profile B at the Hietajoki dolomite quarry (e.g. Bida 1979). This unit marks the top of the Veikkavaara greenstone group. It is suggested that it forms a more or less continuous layer from Hietajoki northwards to the Masugnsbyn dolomite quarry (Fig. 9). In the latter area the dolomite horizons widens to approximately 300 m, possibly due the effects of folding (Zaki 2015). Further to the north, at Isovaara, the dolomitic horizon also crops out (Fig. 9). To the west, above the carbonate rocks, there is an andalusite-bearing mica schist of the *Pahakurkio group*, which seems to be concordant with the carbonate rocks.

At Hietajoki (Fig. 9) the metacarbonate sequence from east to west consists of (1) a 20–25 m thick lowermost unit of fine- to medium-grained calcitic marble with intercalations of fine-grained schist and skarn bands; (2) a 150–200 m thick dolomitic marble; and (3) an uppermost 30–40 m wide skarn-altered rock with tremolite and calcite. In general, bedding strikes northwest and dips steeply to the east (80–85°). The dolomitic marble is pinkish or yellowish to greyish-white. Some layers are dark grey,

attributable to disseminated graphite. Mineralogically, the dolomitic marble consists of medium- to coarse-grained, polygonal to granular dolomite with minor quartz, tremolite, pyrite and limonite (after pyrite). Rare diopside, sericite, chlorite, serpentine and scapolite also occur (Bida 1979). Late-stage calcite fills fractures. The main components of the dolomite are rather constant, with 21 wt. % MgO and 30 wt. % CaO, together with some impurities resulting in 0.5–3.0 wt % SiO_2 and 0.5–1.5 wt % Fe_2O_3 (Bida 1979).

Andalusite-bearing mica schist assigned to the Svecofennian Pahakurkio group occurs to the west at Hietajoki (Fig. 9), stratigraphically above the metacarbonate rocks of the Masugnsbyn formation. In general, the attitude and orientation of this younger supracrustal sequence is concordant with the Masugnsbyn formation (cf. Hellström et al. 2018).

In summary, a mainly mafic metavolcaniclastic sequence occurs at Masugnsbyn, containing subordinate metasedimentary horizons located predominantly near the top of the stratigraphy. The package may be divided into four informal formations, and has a total thickness of approximately 3.4 km.

Greenstone-related mafic intrusions at Masugnsbyn

Like Nunasvaara, metadoleritic rocks form part of the greenstone sequence at Masugnsbyn and most commonly occur as relatively thin sills, concordant to bedding in the Tuorevaara greenstone formation (Fig. 9). Typically, they are fine- to medium-grained (0.5–5 mm), and are variably deformed and altered. Locally, metadolerites are isotropic and display relict igneous, intergranular to subophitic textures (Fig. 11L). They predominantly consist of uralitic hornblende aggregates, which fill the interstices between randomly orientated plagioclase laths. The latter are commonly recrystallised into a polygonal granoblastic texture. Subordinate minerals include biotite, magnetite and quartz.

The largest known metadolerite sill at Masugnsbyn occurs approximately 800 m along Profile A and is estimated to be 35–40 m thick (Fig. 9). Within this body, a medium-grained (1–5 mm) gabbroic pegmatite pod occurs, which was sampled for U-Pb geochronology. At the western margin of the doleritic sill, an approximately 10 m wide meta-ultramafic rock occurs. This rock consists of rounded, up to 2 cm orthopyroxene megacrysts in a fine-grained, amphibole-rich (anthophyllite) matrix (Fig. 11M). The relationship between the metadolerite and the meta-ultramafic rock is unclear.

Deformation and structures at Masugnsbyn

Metasupracrustal rocks at Masugnsbyn preserve large-scale, upright folds and steeply dipping fault zones, which mainly have northeast or northwest trends (Fig. 9, Padget 1970). A detailed assessment of geological structures and deformation events in the Masugnsbyn area is presented by Grigull et al. (2018). Hence, only a brief outline of some key structural features is given here.

In general, fold axial planes have northwest to north-northwest orientations, are steeply inclined to upright, and verge toward the west (Fig. 9). One exception is the northeast-orientated and east-verging Oriasvaara syncline, which is bounded to the northwest by the parallel-trending Kalixälv fault. Dip-slip movements along the Kalixälv fault have down-thrown the southeastern block, resulting in a major tectonic contact between the Pahakurkio and Kalixälv groups.

In the Kalixälv dome (Fig. 9), inferred bedding has low to moderate dips, which increase progressively outwards from the centre of the structure. The dome is thought to have formed by the interaction and overprinting of at least two folding events (Padget 1970, Grigull et al., 2018). Insights into polyphase folding at Masugnsbyn are best derived from magnetic anomaly patterns, which reveal a complexly folded internal structure for both the Veikkavaara greenstones and younger Svecofennian rocks (Fig. 10A). Tight to isoclinal folding, with mainly north-northwest-orientated axial planes within the Veikkavaara greenstones may possibly represent an earlier phase of folding.

Metamorphism and metasomatism

The greenstone successions in both study areas have undergone peak regional metamorphism to approximately lower amphibolite facies conditions, based on observed metamorphic mineral assemblages (cf. Padget 1970, Eriksson & Hallgren 1975). Green, pleochroic hornblende is ubiquitous in metamorphosed mafic rocks and typically forms granoblastic, blasto-ophitic and lepidoblastic intergrowths with plagioclase feldspar ± biotite (Fig. 12A–C). Commonly, it is retrogressed to actinolite, chlorite and oxyhornblende (Fig. 12B–C).

In mafic metatuffs, subhedral almandine porphyroblasts with randomly orientated inclusions (muscovite) occur locally as disseminated seams in more biotite-rich (argillaceous?) layers (Fig. 12D). Individual garnets symmetrically deflect a composite S_{0-1} fabric, while weakly developed asymmetric tails indicate limited sinistral-oblique lateral shearing and suggest overall pre- to syn-tectonic garnet growth (Fig. 12E). Additionally, compositionally banded metatuff alternates locally between darker, hornblende- or biotite-rich layers and lighter, cummingtonite ± actinolite-bearing zones (Fig. 12F).

Other key metamorphic minerals include porphyroblastic andalusite, sillimanite and cordierite in more micaceous metasedimentary units (e.g. Lower sedimentary formation, Nunasvaara; cf. Eriksson & Hallgren 1975), while carbonaceous horizons (black schist) record locally significant graphitisation (Fig. 12G). Partial dolomitisation of metalimestone horizons is probably a by-product of syn-deformation metasomatic effects as well.

At Masugynsbyn, Svecofennian meta-volcanosedimentary rocks also contain porphyroblasts of andalusite, sillimanite and cordierite consistent with lower to mid amphibolite facies metamorphism (Padget 1970). However, localised zones of migmatitic paragneiss in the south of the area suggest that possible upper amphibolite facies conditions existed locally. Here, the timing of migmatitisation is constrained to 1878 ±3 Ma (U-Pb SIMs zircon dating), and coincides with the emplacement of voluminous, mafic to felisic, syn-orogenic Svecokarelian intrusive rocks (Hellström 2018).

Quantitative metamorphic pressure-temperature (PT) modelling has not been conducted either at Nunasvaara or Masugnsbyn. However, Bergman et al. (2001) reported PT estimates for several greenstone-related units from across the region, albeit without corresponding metamorphic age constraints. A mafic metatuff (approximately 35 km northwest of Nunasvaara, *Vittangi greenstone group*) yielded PT values of 2.6 ± 0.5 kbars and 510 ± 35°C, while a meta-argillite (approximately 40 km east of Masugnsbyn, Veikkavaara greenstone group) gave values of 3.6 ± 0.6 kbars and 570 ± 20°C. Recently, Pearce et al. (2015) obtained a peak temperature range of 400–500°C for graphitisation at the Nunasvaara graphite deposit, consistent with the regional prograde burial path and the expected thermal regime for successful conversion of carbonaceous matter to graphite (e.g. Buseck & Beyssac 2014).

Overprinting metasomatic alteration affects the greenstones in a variety of styles and with varying degrees of intensity (Lynch et al. 2014). In general, a fairly early (metasomatic) sodic ± calcic assemblage (scapolite ± albite ± actinolite-tremolite) is pervasively developed in broad zones, thin bands and irregular patches and disseminations (Fig. 13). In mafic metatuffs, disseminated and aggregate scapolite porphyroblasts (≤ approximately 1 cm), associated with matrix actinolite, form planar, conformable seams, parallel to primary laminae and bedding (Fig. 13A–B). Relatively intense amphibole + clinopyroxene (diopside) ± garnet alteration (skarn) associated with stratiform–stratabound magnetite-rich horizons and metacarbonate layers is found within the upper stratigraphy (Fig. 13H).

Sodic ± calcic alteration of metadoleritic bodies locally imparts a leucocratic, speckled appearance to the rock, defining a pseudomorphic igneous texture, with scapolite typically replacing plagioclase (Fig. 13C). In extreme cases, the obliteration of primary features has produced monomineralic albitites (*leuco-diabase* of Eriksson & Hallgren 1975). Adjacent to metadoleritic bodies, breccia-like zones containing albitised wall-rock clasts in a fine-grained, magnetite + amphibole ± albite matrix are locally developed (Fig. 13D). In mafic metatuffs these features are associated with more massive (non-laminated), hornfelsed wall rock and suggest mobilisation of magnetite during localised fluid-rock interaction.

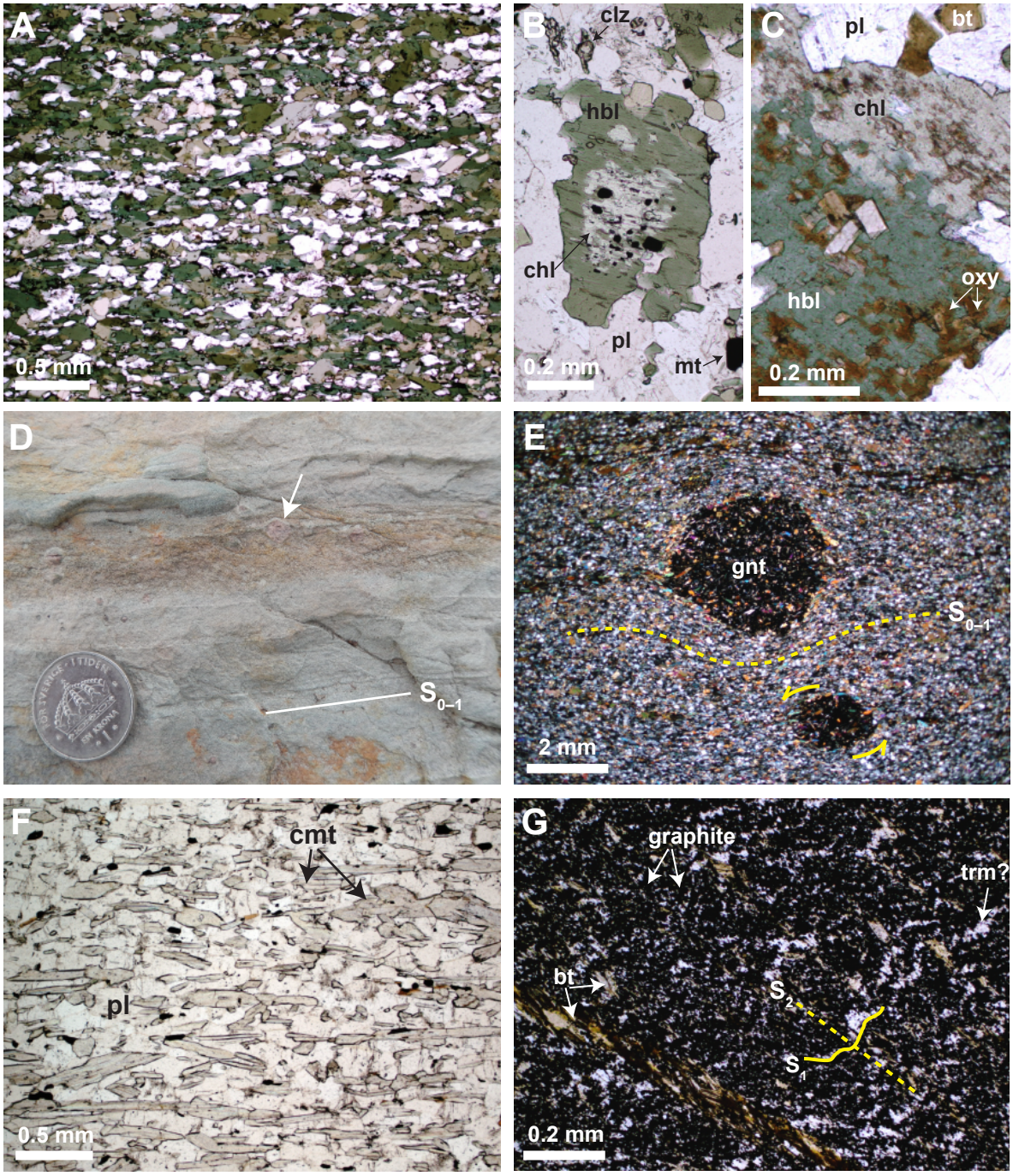

Figure 12. Representative metamorphic minerals (amphibolite facies) in greenstone units. **A.** Thin section plane-polarised light (PPL) view of lepidoblastic hornblende-plagioclase matrix in mafic metavolcanic rock. **B.** PPL view of hornblende crystaloblast retrogressed to chlorite in amphibolitic lava. **C.** PPL view of granoblastic hornblende-plagioclase ± biotite matrix in metadoleritic intrusion. Hornblende is retrogressed to chlorite and oxyhornblende. **D.** Outcrop view (orthogonal to bedding) of laminated, mafic metatuff containing almandine porphyroblasts (arrow). The coin is 25 mm in diameter. **E.** Thin section cross-polarised light view of almandine porphyroblasts in a mafic metatuff. Deflection of a composite S_{0-1} fabric indicates pre- to syn-tectonic garnet growth with a weak sinistral-oblique rotation. **F.** PPL view of lepidoblastic cummingtonite-plagioclase matrix from a more leucocratic band of a metatuff. **G.** PPL view of graphite-rich black schist cut by a biotite veinlet (bottom left corner). Biotite occurs preferentially along an S_2 crenulation cleavage that steeply transects an earlier S_1 foliation. Mineral abbreviations: bt = biotite, chl = chlorite, clz = clinozoisite, cmt = cummingtonite, hbl = hornblende, mt = magnetite, oxy = oxyhornblende, pl = plagioclase feldspar, gnt = garnet, trm = tremolite, amf = amphibole.

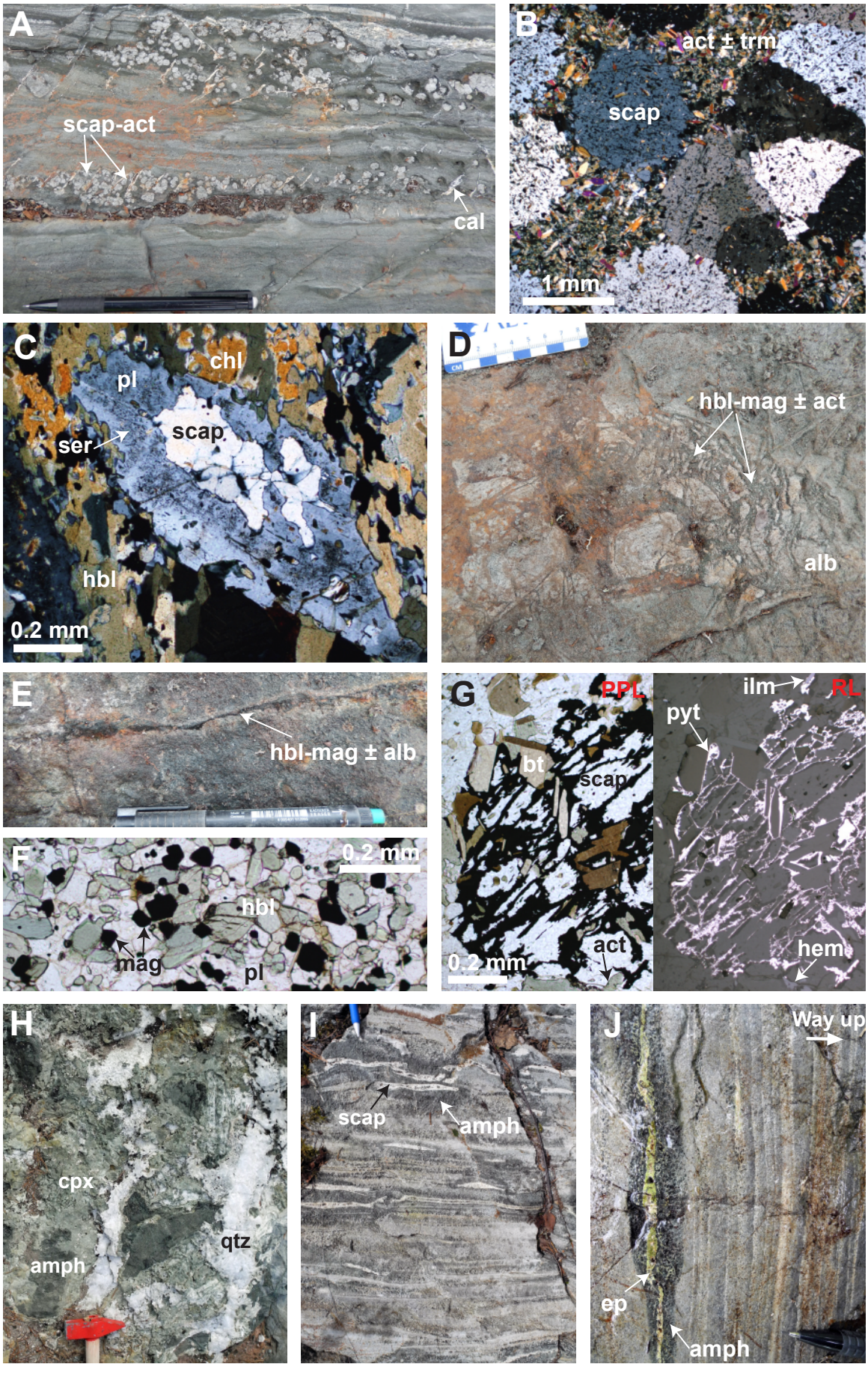
A
scap-act
cal
B
act ± trm
scap
1 mm
C
chl
pl
scap
ser
hbl
0.2 mm
D
hbl-mag ± act
alb
E
hbl-mag ± alb
F
0.2 mm
hbl
mag
pl
G
PPL
bt
scap
act
0.2 mm
ilm
RL
pyt
hem
H
cpx
qtz
amph
I
scap
amph
J
Way up
ep
amph

◀ Figure 13. Representative metasomatic alteration features. **A.** Pervasive, scapolite + actinolite ± albite alteration in a laminated mafic tuffite (Nunasvaara). Locally, scapolite forms relatively coarse, sub-rounded porphyroblasts. Calcite veinlets fill late, high-angle fractures subparallel to an earlier, spaced crenulation cleavage. The pencil is 14 cm long. **B.** Thin section plane polarised light (PPL) view of sub-rounded, scapolite porphyroblasts associated with fine-grained actinolite ± tremolite in a mafic tuffite (Nunasvaara). **C.** PPL view of anhedral scapolite replacing sericitised plagioclase feldspar in a metadolerite (Nunasvaara). **D.** Hornblende + magnetite ± actinolite ± albite breccia in an amphibolitic metatuff near the contact with a metadoleritic intrusion (Nunasvaara). **E.** Hornblende + magnetite veinlet with albite halo in a metabasalt (Nunasvaara). The pen is 14 cm long. **F.** PPL view of subhedral to euhedral hydrothermal magnetite overprinting the hornblende-plagioclase matrix of a mafic tuffite (Nunasvaara). **G.** Split PPL-reflected light views (left and right sides, respectively), showing a pyrite breccia associated with biotite, ilmenite and magnetite (replaced by hematite) in a scapolite ± actinolite-altered metabasalt (Nunasvaara). **H.** Skarn-type amphibole + pyroxene alteration associated with late quartz veins (Masugnsbyn). The hammer head is 15 cm long. **I.** Scapolite veinlets associated with amphibole in a mafic tuff (Masugnsbyn). The pencil is 1 cm thick. **J.** Epidote veinlet (late?) associated with amphibole in a laminated mafic tuff (Masugnsbyn). The pencil is 3 cm long in this view. Abbreviations: act = actinolite, alb = albite, amph = amphibole, bt = biotite, cal = calcite, chl = chlorite, cpx = clinopyroxene, ep = epidote, hem = hematite, hbl = hornblende, ilm = ilmenite, mag = magnetite, pl = plagioclase feldspar, pyt = pyrite, qtz = quartz, scap = scapolite, ser = sericite, trm = tremolite.

The sodic ± calcic assemblage also forms veins and vein-related alteration haloes across both study areas. For example, mafic metavolcanic rocks at Nunasvaara (Lower greenstone formation) contain fairly common hornblende-magnetite ± actinolite veins, with discontinuous albite ± scapolite haloes (Fig. 13E). Locally, these veins grade into relatively intense stockwork and breccia zones. Scapolite ± albite bands and veinlets are particularly abundant in mafic metatuff at Masugnsbyn (Veikkavaara upper greenstone formation). Here they trend parallel to primary laminae or are slightly discordant with en echelon orientations and local folding, suggesting pre- to syn-tectonic formation (Fig. 13I). Late-stage epidote veins bordered by patchy amphibole haloes also occur in mafic metatuffs (Fig. 13J).

A later (overprinting) potassic ± sodic alteration (biotite + magnetite + pyrite + chalcopyrite + titanite ± K-feldspar ± carbonate) also affects the greenstone successions, although it is less pervasively developed than the sodic ± calcic assemblage. It typically occurs as overprinting disseminations or is associated with sulphide-bearing fractures, veins and narrow breccia zones and with thin aplitic veinlets and granitic dykes (Fig. 13F–G). Biotite is typically tabular and subhedral where associated with sulphide and may fill high-angle crenulation cleavages (cf. Fig. 12G). Magnetite is subhedral to euhedral and is locally martitised along irregular fracture planes.

Recent geochronology results provide a temporal framework for the overprinting metasomatism and alteration. For example, Smith et al. (2009) constrained the timing of sodic ± calcic metasomatism at Nunasvaara to 1903 ± 8 Ma (U-Pb LA-ICP-MS method) by dating titanite from a scapolitised metadioritic intrusion (e.g. Fig. 2B). Trace element analysis of the titanite revealed chondrite-normalised REE patterns (LREE-enriched with $[Ce/Lu]N \approx 8–20$, negative Eu anomalies with $[Eu/Eu^*]_N \approx 0.5–0.9$), similar to those for 1.90–1.87 Ga, intermediate to felsic syn-orogenic volcanic and intrusive suites in northern Norrbotten (e.g. Blake 1990, Wanhainen et al. 2006, Edfelt et al. 2006).

Younger metasomatic-hydrothermal events are also recorded in the Nunasvaara and Masugnsbyn areas, suggesting that metasomatism-alteration was both protracted and episodic during orogenesis. For example, Bergman et al. (2006) obtained a U-Pb monazite cooling age of c. 1.86 Ga for Svecofennian andalusite mica schist at Masugnsbyn, while Martinsson et al. (2016) report U-Pb TIMS titanite ages of 1.80–1.77 Ga for sodic ± carbonate alteration associated with epigenetic-style Cu mineralisation in both areas (cf. Billström et al. 2002).

The predominant sodic ± calcic assemblage affecting the greenstones is representative of the regionally pervasive scapolite ± albite alteration that preferentially overprints mafic and intermediate metasupracrustal rocks across northern Norrbotten (e.g. Frietsch et al. 1997). The broad footprint of this

hydrothermal event(s) is also manifested by positive Na, Ba, Cl and Ca anomalies in the glacial overburden (Ladenberger et al. 2012). In general, extensive sodic ± calcic metasomatism is interpreted to have formed via the circulation of halogen-rich, high-salinity basinal ± magmatic brines during early 1.90–1.87 Ga tectonothermal events (Frietsch et al. 1997, Smith et al. 2009, Smith et al. 2013). Subsequent hydrothermal activity during later orogenic stages probably led to additional magmatic and metamorphic-related alteration (cf. Bergman et al. 2006).

At deposit scales in northern Norrbotten, sodic alteration is associated with skarn-related stratabound iron, volcanic-exhalative Cu, Kiruna-type iron oxide-apatite, and hydrothermal Cu-Au mineralisation (e.g. Frietsch 1997, Martinsson et al. 1997, Masurel 2011, Nordstrand 2012). In contrast, potassic alteration is most typically associated with hydrothermal Cu-Au mineralisation (IOCG-style), particularly where links with relatively high-strain deformation zones and related structures have developed (e.g. Edfelt et al. 2005, Smith et al. 2007, Wanhainen et al. 2012, Lynch et al. 2015, Lynch et al. 2018).

Greenstone-hosted mineralisation

Four major types of mineralisation are hosted by greenstone-related rocks in the Nunasvaara and Masugnsbyn areas. These are

1. *Black schist-hosted graphite mineralisation* (e.g. Nunasvaara graphite deposit, Bergström 1987; Nybrännan graphite mineralisation at Veikkavaara, Gerdin et al. 1990).
2. *Stratiform–stratabound iron mineralisation ± sulphides* (e.g. Masugnsbyn iron deposits, Geijer 1929, Witschard et al. 1972, Frietsch 1997; Kuusi Nunasvaara iron deposit, Frietsch 1997).
3. *Stratiform dolomite* (e.g. Masugnsbyn and Hietajoki dolomite deposits; Bida 1979, Zaki 2015).
4. *Hydrothermal vein- and breccia-hosted Cu ± Pb ± Mo mineralisation* (e.g. Jälketkurkkio and Veikkavaara prospects, Martinsson et al. 2016).

(1) Graphite mineralisation: Stratiform black schist horizons containing variable graphite mineralisation form an integral part of the volcanic–sedimentary successions in both study areas. The most important example is the Nunasvaara graphite deposit in west-central Nunasvaara (Fig. 2B). A recent JORC-compliant indicated and inferred resource estimate for this deposit (using a 10% cut-off) is 9.8 Mt grading 25.3 wt. % graphitic carbon (Talga Resources 2016). Based on this assessment, graphite mineralisation at Nunasvaara is considered to be one of the world's highest grade metamorphic graphite deposit (Scogings et al. 2015).

Graphite mineralisation at the Nunasvaara deposit occurs within two subparallel, black schist horizons that form part of the hinge zone and southern limb of an approximately northwest-aligned, subvertical and upright fold (cf. Bergström 1987). The graphitic horizons dip steeply toward the southwest (75–90°) and extend laterally beyond the deposit, forming part of the Nunasvaara member (Fig. 2B). Along the limb section, both graphitic seams are weakly foliated and contain a steeply southwest-dipping, spaced S_1 fracture cleavage that tends to parallel the approximately SE-striking bedding (Fig. 14A–B). Locally, a discordant S_2 crenulation cleavage is also observed (cf. Fig. 12G).

In general, the stratigraphically upper black schist horizon is thicker and more graphite-rich compared to the lower horizon. At the deposit, both seams are divided by a metadolerite sill, which also represents the footwall unit. Where exposed, the contact between the upper black schist horizon and hanging wall mafic metatuffs appears conformable-sedimentary. Finally, a set of apparently younger (Sveckokarelian-related?) mafic dykes of uncertain origin also crosscuts the area.

In general, the mineralisation consists of dark grey, semi-massive to massive (25–50 vol. %), disseminated microcrystalline graphite (< approximately 0.08 mm, or "amorphous"-grade; cf. Taylor 2006), in a granoblastic amphibole-scapolite ± feldspar ± biotite ± pyrite matrix. Typically, graphite has a metallic, dullish blue-grey colour, is well-sorted and forms sub-rounded and tabular anhedral grains (Fig. 14C). Beyond the high-grade zone elsewhere along the Nunasvaara member, slightly

coarser (0.08–0.15 mm) disseminated graphite with a flake-like morphology has developed (Fig. 14D). Relatively abundant graphite-bearing veinlets also occur at the Nunasvaara deposit (Fig. 14C; cf. Pearce et al. 2015). Their presence suggests remobilisation of graphite, producing several depositional generations and that deformation and hydrothermal events may have facilitated secondary enrichment (upgrading) of the deposit (Fig. 14C; cf. Henderson & Kendrick 2003, Pearce et al. 2015). Future research should focus on testing this hypothesis.

At the Nunasvaara deposit, minor pyrite, pyrrhotite and chalcopyrite also occur in amphibole-mica-scapolite ± feldspar ± graphite veinlets and fractures (cf. Fig. 4D). Rarely, pyrite also forms fine-grained nodular disseminations in thin, stringer-like bands. The presence of accessory sulphides associated with metasedimentary graphite mineralisation provides petrographic evidence for a relatively reduced (anoxic to euxinic) depositional environment (e.g. Mitchell 1993, Tice & Lowe 2006).

Graphite mineralisation in the Masugnsbyn area is exemplified by the Nybrännan deposit (e.g. Gerdin et al. 1990). Here, an approximately 20 m thick, roughly northwest-orientated and sub-vertical graphite schist horizon occurs and has similar characteristics to the Nunasvaara deposit (Figs. 9 & 10). The mineralisation consists of stratiform, semi-massive, fine-grained (approximately 0.005 mm) disseminated graphite, or occurs as aggregates and veins of more variable grain size.

(2) Banded and skarn-related iron: Banded iron formations occur in the stratigraphically upper parts of the Masugnsbyn and Nunasvaara greenstones, and contain iron-rich silicates or iron oxide alternating with layers of chert (Frietsch 1997, Martinsson 2004). In places these typically grade into Mg-rich iron zones, traditionally referred to as "skarn iron ores", with Mg-rich silicates typical as gangue minerals (e.g. Grip & Frietsch 1973). The close association between the banded iron formations and Mg-rich skarn iron suggests that the latter represents metamorphosed banded iron (e.g. Frietsch 1997). From a resource perspective, the skarn-style mineralization tends to be more iron-rich than the banded iron-style (Frietsch 1997). The Tornefors iron deposit at Junosuando is one example, where a Mg-rich skarn horizon containing 25–35 wt % Fe is overlain by typical BIF mineralisation with 15–25 wt % Fe (Martinsson et al. 2016). At Tornefors layers of magnetite alternate with layers of actinolite–tremolite diopside and layers of dense, very fine-grained "quartzitic" chert (cf. Damberg et al. 1974).

In general, the skarn-related mineralisation consists of massive stratabound magnetite lenses, layers and seams associated with banded and disseminated amphibole + pyroxene + pyrite + chalcopyrite ± garnet alteration (Fig. 14E–F & H). The Masugnsbyn iron mineralisation occurs in an approximately 8 km long zone, apparently concordant with the stratigraphy in the uppermost part of the Veikkavaara greenstones next to the overlying Svecofennian metasedimentary rocks (Witschard et al. 1972, Frietsch 1997). The southern iron deposits are classified as skarn iron ores, whereas Fe mineralisations to the north have more sedimentary characteristics including mm- to cm-wide, quartz + calc-silicate + magnetite, banded iron indicative of an exhalative origin (Fig. 14G). The southern skarn iron mineralisations, including the Junosuando deposit, contain concentrations of economic interest and were discovered in 1644, the first such discovery in Norrbotten (Geijer 1929, Witschard et al. 1972). The Junosuando deposit has a JORC-compliant indicated and inferred resource of 112 Mt grading 28.6% Fe (Talga Resources 2014).

A significant difference between Fe mineralisations is that the southern part is bordered by a thick dolomitic marble layer and granite, whereas no spatial association with granite or carbonate is present in the north. The close spatial connection between skarn iron ores and granite suggests that the intrusion is responsible for the skarn formation and remobilisation of iron, with higher grade and coarser grain size of the magnetite ore in the footwall next to the granite (cf. Frietsch 1997, Hellström 2018). In the southern ores, skarn minerals are intimately associated with magnetite in a steeply dipping, 70–100 m wide zone with diopside, tremolite-actinolite and phlogopite, and more rarely serpentine and chondrodite (Fig. 14F). Magnetite is irregularly distributed, but tends to be concentrated in bands. Chalcopyrite is a minor constituent, and uranium-bearing fractures are found locally (Padget 1970, Witschard et al. 1972).

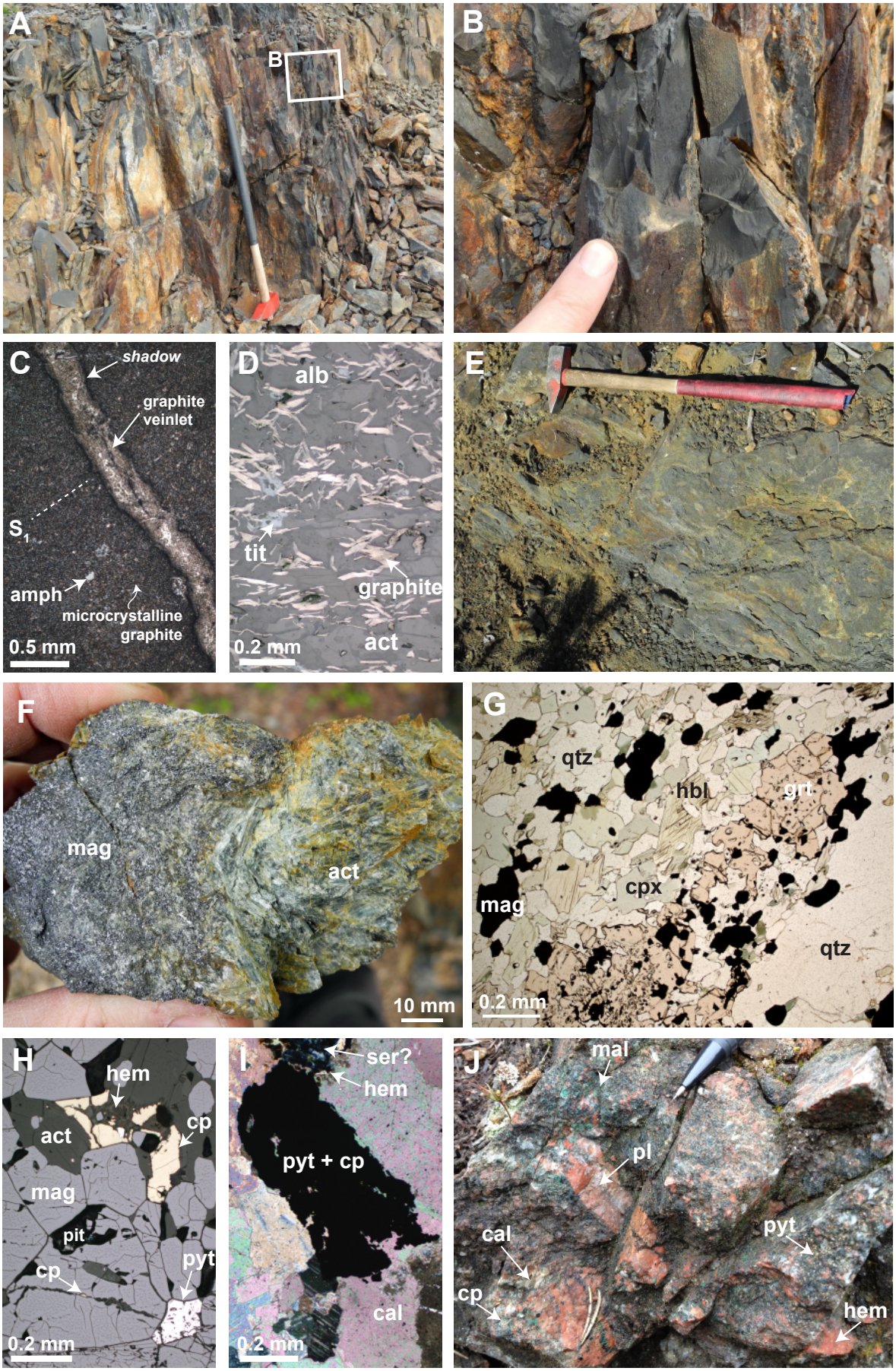
A
B
B
C
shadow
graphite veinlet
S_1
amph
microcrystalline graphite
0.5 mm
D
alb
tit
graphite
act
0.2 mm
E
F
mag
act
10 mm
G
qtz
hbl
grt
cpx
mag
qtz
0.2 mm
H
hem
act
cp
mag
pit
cp
pyt
0.2 mm
I
ser?
hem
pyt + cp
cal
0.2 mm
J
mal
pl
cal
pyt
cp
hem

◀ Figure 14. Main mineralisation types in the study areas. **A and B.** Semi-massive, stratiform graphite mineralisation at the Nunasvaara deposit. Both views are toward the southeast (i.e. along strike), and show steeply southwest-dipping, graphite-rich black schist with a well-developed, composite S_{0-1} fracture cleavage. **C.** Thin section reflected light (RL) view of a graphite veinlet crosscutting a massive, fine-grained (typically < 0.05 mm), graphite mineralisation at Nunasvaara. A weak S_1 foliation has developed in the graphite. **D.** RL view of coarser, flake graphite in amphibole-feldspar-biotite schist (Nunasvaara). **E.** Semi-massive, skarn-type, stratiform magnetite associated with amphibole + clinopyroxene (Nunasvaara). Outcrop shows abundant hematite-goethite weathering. The hammer head is 15 cm long. **F.** Skarn-type iron mineralisation (magnetite) associated with intense and pervasive amphibole alteration (Masugnsbyn). **G.** Thin section PPL view of a quartz-banded iron mineralisation at the Välivaara ore field in the northern part of the Masugnsbyn iron ores, which may represent a metamorphosed banded iron formation. Bands of quartz alternate with bands rich in clinopyroxene, hornblende, garnet, magnetite ± quartz (SWEREF99 TM: 7504207/800423). **H.** RL view of granular magnetite associated with pyrite and chalcopyrite from a skarn horizon similar to that in E and F. **I.** Thin section cross-polarised light view of a calc-silicate rock (metacarbonate), showing opaque pyrite grain with minor chalcopyrite. **J.** Example of breccia-style, hydrothermal Cu mineralisation (Nunasvaara). Feldspar grains and aggregate feldspathic clasts show 'red rock'-type hematite staining. Pencil length shown is approximately 2.5 cm. Abbreviations: act = actinolite, alb = albite, amph = amphibole, cal = calcite, cp = chalcopyrite, cpx = clinopyroxene, grt = garnet, hbl = hornblende, hem = hematite, mag = magnetite, mal = malachite, pit = polish pit, pl = plagioclase, pyt = pyrite, qtz = quartz, ser = sericite, tit = titanite.

At Nunasvaara skarn-related Fe mineralisation is spatially concentrated within amphibolitic metasedimentary sequences containing minor metacarbonate layers, and occurs close to the margins of intrusive rocks (e.g. Figs. 2 & 9). While primary mineralisation is considered to have formed through exhalative processes (e.g. Frietsch 1997; cf. Klein & Beukes 1992), the close spatial association between the Fe ± sulphide mineralisation, metacarbonate rocks and granitoid intrusions suggests that exoskarn-type magmatic-hydrothermal processes have facilitated Fe ± Cu remobilisation during later, overprinting tectonothermal events (e.g. Fig. 14I; cf. Frietsch 1997).

(3) Dolomite: A marble unit at the top of the Veikkavaara greenstone group is an important dolomite resource and is currently mined by LKAB at Masugnsbyn village. The dolomite is used as an additive in iron ore pellet production. According to Zaki (2015), the total production up to 2015 has been approximately 4 Mt, with an annual production of about 0.2 Mt. The estimated resource is 28.3 Mt of first-quality dolomite (SiO_2 ≤ 3 wt %) and 3.4 Mt of second-quality dolomite (SiO_2 3–10 wt %). Geochemically, the dolomite contains fairly constant MgO and CaO concentrations (approximately 21 wt % and 30 wt %, respectively), with variable impurities resulting in elevated amounts of SiO_2 and Fe_2O_3.

(4) Hydrothermal Cu ± Pb and Mo mineralisation: Minor hydrothermal Cu ± Pb and Mo mineralisation occurs sporadically within the greenstones. For example, at the Jälketkurkkio showing in the central Nunasvaara area an approximately 25 m wide, north-trending sodic + calcic + carbonate alteration zone at the contact between a metadolerite and black schist contains minor breccia- and vein-hosted Cu-Pb mineralisations (Fig. 2B). Here, disseminated pyrite, chalcopyrite and minor galena are found in a matrix- to clast-supported, carbonate-amphibole ± magnetite breccia. In addition, minor chalcopyrite occurs in planar carbonate-amphibole veinlets. Locally, the mineralised breccia contains reddish-pink, angular clasts (volcanic?) that are hematite-stained (Fig. 14J). The clasts are typically barren and are cut by thin amphibole-carbonate veinlets similar to the breccia matrix. Breccia clasts of a more doleritic composition are also seen. In general, the breccia has a somewhat crushed and disrupted appearance, suggesting fragmentation within a zone of higher permeability.

The Veikkavaara Cu prospect (Masugnsbyn area, Fig. 9) occurs at the western border of a 30–40 m thick mafic sill that has intruded laminated metatuff of the Tuorevaara greenstone formation. Pyrrhotite and minor chalcopyrite form disseminations and patches in a pyroxene-amphibole ± biotite ± scapolite-altered zone (Martinsson et al. 2016). In the southern Nunasvaara area, minor molybdenite ± chalcopyrite in quartz veins and pegmatitic zones occur near the margins of several Lina-type granites (e.g. Äijärova showing).

PETROGENESIS OF THE GREENSTONES: PRELIMINARY U-PB GEOCHRONOLOGY, LITHOGEOCHEMISTRY AND Sm-Nd ISOTOPIC RESULTS

This section contains preliminary analytical results relating to the greenstone successions at Nunasvaara and Masugnsbyn. New U-Pb SIMS zircon ages for two metadoleritic intrusions from both areas are presented. This dating is the first application of U-Pb SIMS geochronology to Palaeoproterozoic greenstone-related rocks in northern Sweden, and the new dates currently represent the most precise and robust absolute time constraints for "Karelian" mafic magmatism in this sector of the Fennoscandian Shield. New lithogeochemical results for the various rock units from both successions are also shown. These data facilitate preliminary rock classification and lithostratigraphic comparisons. Finally, new whole-rock Sm-Nd isotopic results for the major rock units in both study areas are presented and discussed.

U-Pb SIMS zircon geochronology

U-Pb SIMS zircon dating of greenstone-related metadolerite was conducted to establish age constraints on the formation of the greenstone sequences. At Nunasvaara, a metadolerite sample (ELH130004A) was collected from a discordant body (dyke-like) intruding hanging wall metatuff close to the Nunasvaara graphite deposit (i.e. Upper greenstone formation; e.g. Fig. 2A–B). At Masugnsbyn, a metadoleritic to metagabbroic sill intruding the Tuorevaara greenstone formation metatuff was sampled and dated (FHM140006A, Fig. 9).

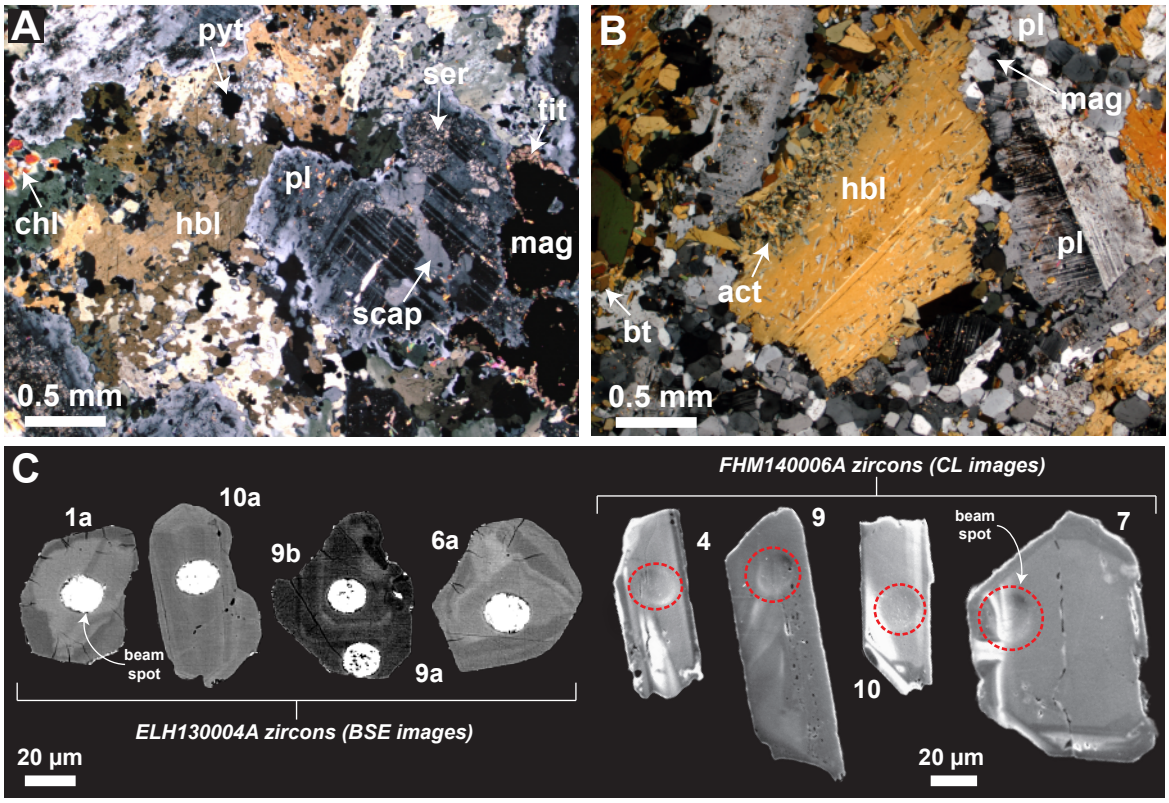

Figure 15. **A and B.** Representative thin section cross-polarised light views of metadolerite samples (ELH130004A and FHM140006A, respectively) used for U-Pb SIMS zircon dating. **C.** Back scattered electron (BSE) and cathodoluminescence (CL) images of representative zircon grains obtained from the dated samples. SIMS beam spot locations are highlighted. The adjacent numbers refer to the analytical spot numbers listed in Table 2 (final digits only). Mineral abbreviations: act = actinolite, bt = biotite, chl = chlorite, hbl = hornblende, mag = magnetite, pl = plagioclase, pyt = pyrite, scap = scapolite, ser = sericite, tit = titanite.

A summary description of the dated samples and their associated zircon fractions is presented in Table 1; representative photomicrographs and images of the dated samples and zircons are shown in Figure 15. The results of the U-Pb SIMS zircon dating are presented in Table 2, while a summary of the analytical method is presented below. Related U-Pb concordia and mean $^{207}Pb/^{206}Pb$ weighted age plots are shown in Figure 16.

Table 1. Summary descriptions of the metadolerite samples used for U-Pb SIMS zircon dating.

Sample	Setting	Brief description	Zircon characteristics
ELH130004A	Metadolerite dyke intruding mafic metatuff of the Upper greenstone formation (Vittangi greenstone group) at Nunasvaara (Fig. 2A–B).	Fine- to medium-grained (0.5–4 mm), granoblastic to blasto-ophitic, massive to weakly foliated, metadolerite. Essential minerals are plagioclase and hornblende, with minor biotite, clinopyroxene, ilmenite, zircon and magnetite (Fig. 15A–a). Alteration: (1) earlier, weak to moderate, patchy and disseminated scapolite + actinolite ± albite; and (2) later, moderate, disseminated and fracture-related amphibole + biotite + magnetite + pyrite + chalcopyrite + titanite ± K-feldspar ± carbonate alteration. Late chlorite and sericite replace hornblende and plagioclase, respectively.	Fine-grained (< 1 mm), anhedral to subhedral, tabular, colourless (Fig. 15C). Some grains show broad domainal to oscillatory zoning, and may have thin bright rims in CL images.
FHM140006A	Gabbro-pegmatitic pod in central part of 40 m wide dolerite sill intruding mafic metatuff of the Tuorevaara greenstone formation at Masugnsbyn (Fig. 9)	Relict igneous, medium-grained, isotropic texture with aggregates of green uralitic hornblende filling the interstices between randomly orientated plagioclase laths, which are in part re-crystallised into finer-grained polygonal, granoblastic texture (Fig. 15B). Minor to accessory minerals are biotite, actinolite (after hornblende), magnetite, quartz and zircon.	Subhedral to euhedral, prismatic zircon; many are fragmented (Fig. 15C). Most are metamict with inclusions. Homogeneous to oscillatory as well as patchy or irregular zoned crystals.

Table 2. SIMS U-Pb-Th zircon data for the dated metadolerite samples.

Spot #	U	Th	Pb	Th/U	^{238}U	±σ	^{207}Pb	±σ	Disc.	Disc.	^{207}Pb	±σ	^{206}Pb	±σ	$^{206}Pb/^{204}Pb$	f^{206}
	ppm	ppm	ppm	calc[1]	^{206}Pb	%	^{206}Pb	%	% conv.[2]	% 2σ lim.[3]	^{206}Pb	Ma	^{238}U	Ma	measured	%[4]
Sample ELH130004A (metadolerite, Nunasvaara)																
n5166_01a	233	215	132	0.96	2.463	1.09	0.1333	0.32	3.0	0.4	2141	6	2197	20	811639	{0.00}
n5166_02a	52	54	30	1.07	2.515	1.09	0.1332	0.68	1.0		2140	12	2158	20	80777	{0.02}
n5166_03a	318	305	181	1.00	2.480	0.96	0.1333	0.28	2.3		2143	5	2184	18	336375	{0.01}
n5166_04a	94	51	48	0.57	2.504	1.02	0.1336	0.64	1.1		2146	11	2166	19	>1e6	{0.00}
n5166_05a	79	63	43	0.81	2.535	1.13	0.1334	0.55	0.0		2144	10	2144	21	87077	{0.02}
n5166_06a	127	55	65	0.46	2.475	1.10	0.1338	0.43	2.2		2148	8	2188	20	177782	{0.01}
n5166_07a	118	125	67	1.08	2.510	1.03	0.1337	0.45	0.8		2147	8	2161	19	80717	{0.02}
n5166_08a	159	195	94	1.23	2.512	1.10	0.1335	0.39	0.9		2145	7	2160	20	70724	{0.03}
~~n5166_09a~~	~~109~~	~~3~~	~~39~~	~~0.02~~	~~3.128~~	~~1.12~~	~~0.1069~~	~~0.71~~	~~2.7~~		~~1747~~	~~13~~	~~1788~~	~~17~~	~~4852~~	~~0.39~~
~~n5166_09b~~	~~133~~	~~3~~	~~48~~	~~0.02~~	~~3.119~~	~~1.06~~	~~0.1098~~	~~0.55~~	~~-0.2~~		~~1797~~	~~10~~	~~1793~~	~~17~~	~~>1e6~~	~~{0.00}~~
~~n5166_10a~~	~~132~~	~~12~~	~~62~~	~~0.08~~	~~2.472~~	~~0.91~~	~~0.1333~~	~~0.68~~	~~2.7~~		~~2142~~	~~12~~	~~2190~~	~~17~~	~~94769~~	~~{0.02}~~
n5166_11a	268	175	147	0.72	2.426	1.06	0.1338	0.46	4.2	1.2	2149	8	2225	20	13651	0.14
SAMPLE FHM140006A (metadolerite, Masugnsbyn)																
~~n5407-01~~	~~501~~	~~1505~~	~~410~~	~~3.26~~	~~2.4662~~	~~0.90~~	~~0.1317~~	~~0.36~~	~~4.1~~	~~1.6~~	~~2121~~	~~6~~	~~2194~~	~~17~~	~~75314~~	~~0.02~~
~~n5407-02~~	~~540~~	~~2566~~	~~539~~	~~4.95~~	~~2.5196~~	~~0.90~~	~~0.1325~~	~~0.28~~	~~1.3~~		~~2131~~	~~5~~	~~2155~~	~~17~~	~~13521~~	~~0.14~~
~~n5407-03~~	~~326~~	~~141~~	~~137~~	~~0.44~~	~~2.9403~~	~~0.89~~	~~0.1145~~	~~0.38~~	~~0.9~~		~~1872~~	~~7~~	~~1887~~	~~15~~	~~78188~~	~~{0.02}~~
n5407-04	186	198	108	1.10	2.4862	0.96	0.1333	0.46	2.1		2142	8	2179	18	43476	{0.04}
n5407-05	134	143	78	1.08	2.4538	0.97	0.1331	0.55	3.5	0.4	2140	10	2204	18	34258	{0.05}
n5407-06	131	111	73	0.87	2.4786	0.97	0.1326	0.53	2.9		2133	9	2185	18	54715	{0.03}
n5407-07	143	133	80	0.93	2.5013	0.96	0.1330	0.51	1.7		2138	9	2168	18	19901	0.09
n5407-08	96	90	54	0.94	2.4958	1.04	0.1321	0.66	2.5		2126	11	2172	19	5741	0.33
~~n5407-09~~	~~454~~	~~985~~	~~318~~	~~2.21~~	~~2.4816~~	~~0.89~~	~~0.1321~~	~~0.28~~	~~3.1~~	~~0.9~~	~~2126~~	~~5~~	~~2183~~	~~17~~	~~78465~~	~~0.02~~
n5407-10	123	119	70	0.99	2.4888	0.98	0.1332	0.54	2.0		2141	9	2177	18	40051	{0.05}

Isotope values are common Pb-corrected using modern common Pb composition (Stacey & Kramers 1975) and measured ^{204}Pb.
Data rows with strikethrough lines were excluded from the concordia and mean weighted age determinations
[1] Th/U ratios calculated from $^{208}Pb/^{206}Pb$ and $^{207}Pb/^{206}Pb$ ratios, assuming a single stage of closed U-Th-Pb evolution
[2] Age discordance in conventional concordia space. Positive numbers are reverse discordant.
[3] Age discordance at closest approach of error ellipse to concordia (2σ level).
[4] Figures in curly brackets are given when no correction has been applied, and indicate a value calculated assuming present-day Stacey-Kramers common Pb.

U-Pb SIMS dating method: Zircons were obtained from a density separate of a crushed rock sample using a Wilfley water table. The magnetic minerals were removed by hand magnet. Handpicked crystals were mounted in transparent epoxy resin together with chips of reference zircon 91500. The zircon mounts were polished and, after gold coating, examined by back-scattered electron (BSE) and Cathodoluminescence (CL) imaging using electron microscopy at EBC, Uppsala University and the Swedish Museum of Natural History in Stockholm. High-spatial resolution secondary ion mass spectrometer (SIMS) analysis was carried out in November and December 2014 using the Cameca IMS 1280 at the Nordsim facility at the Swedish Museum of Natural History in Stockholm. Detailed descriptions of the analytical procedures are given in Whitehouse et al. (1997, 1999), and Whitehouse & Kamber (2005). An approximately 6 nA O^{2-} primary ion beam was used, yielding spot sizes of approximately 15 µm. U/Pb ratios, elemental concentrations and Th/U ratios were calibrated relative to the Geostandards zircon 91500 reference, which has an age of c. 1065 Ma (Wiedenbeck et al. 1995, 2004). Common Pb-corrected isotope values were calculated using modern common Pb composition (Stacey & Kramers 1975), and measured ^{204}Pb in cases of a ^{204}Pb count rate above the detection limit. Decay constants follow the recommendations of Steiger & Jäger (1977). Diagrams and age calculations of isotopic data were made using Isoplot 4.15 software (Ludwig 2012). All age uncertainties are presented at the 2σ or 95% confidence level. After recoating with carbon, electron microscopy imaging of the dated zircons was performed to confirm the spot locations.

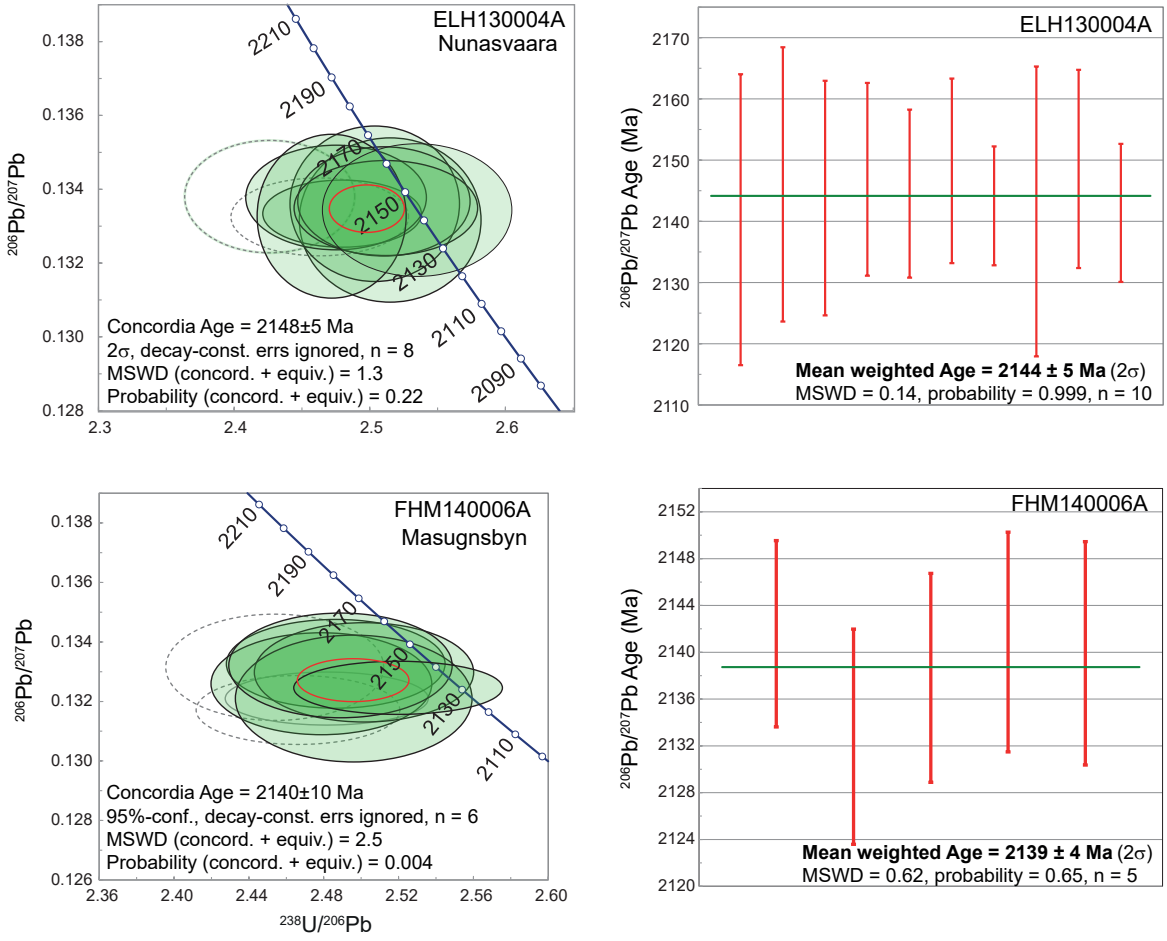

Figure 16. Tera-Wasserburg concordia diagrams (left) and mean weighted $^{207}Pb/^{206}Pb$ age plots (right) showing U-Pb SIMS zircon dating results for metadolerite samples ELH130004A (Nunasvaara) and FHM140006A (Masugnsbyn). In the concordia diagrams discordant analyses are shown with broken lines. The red ovals represent the calculated U-Pb concordia ages and associated uncertainties. See main text for discussion.

For the Nunasvaara sample (ELH130004A), 12 zircons were analysed in total. All the analyses overlap or plot close to concordia and contain fairly low amounts of uranium (52 to 318 ppm, Table 2). 10 zircons form a coherent group with apparent $^{207}Pb/^{206}Pb$ ages of 2.15–2.14 Ga and Th/U ratios of 0.46–1.23 (except spot 10a, which has a Th/U ratio of 0.08, Fig. 15C). Eight of these 10 analyses are concordant at the 2σ level and yield a U-Pb concordia age of 2 148 ± 5 Ma (2σ, *n* = 8, MSWD = 1.3, probability = 0.22, Fig. 16). Taken together, the mean $^{207}Pb/^{206}Pb$ weighted age for the 10 zircons is 2144 ± 5 Ma (2σ, *n* = 10, MSWD = 0.14, probability = 0.999). This date overlaps within error of the concordia age and is chosen as the crystallisation age of the dolerite protolith (cf. Lynch et al. 2016).

Two analyses (09a, 09b) from one of the Nunasvaara zircons record younger apparent $^{207}Pb/^{206}Pb$ ages (1.80–1.75 Ga) compared to the other 10 analyses and have relatively low Th/U ratios of 0.02 (Table 2). Analytical spot 9b is from the core domain displaying a broad oscillatory zonation, and has an apparent age of 1797 ± 20 Ma (Fig. 15C). Analytical spot 9a is from the rim domain showing a homogenous CL-grey level, and has an apparent age of 1 746 ± 26 Ma (Fig. 15C). Both dates overlap at the 2σ level. While the apparent age of the rim domain (9a) suggests a slightly younger event, this analysis yielded a relatively high amount of common lead and is thus less reliable (Table 2; e.g. Williams 1998).

The 1.80–1.75 Ga apparent ages are clearly distinct from the c. 2.14 Ga dates obtained for the rest of the zircon fraction, and may record a younger geological process. The younger ages overlap with a mixed-fraction U-Pb TIMS zircon age of 1 794 ± 24 Ma obtained from two Lina-type granites, located to the southeast of Nunasvaara (Skiöld 1988). They also coincide with 1.81–1.77 Ga U-Pb TIMS titanite ages determined for hydrothermal amphibole ± albite ± carbonate alteration in the general Nunasvaara area (Martinsson et al. 2016; cf. Smith et al. 2009).

For the metadolerite at Masugnsbyn (FMH140006A), a total of 10 zircons were analysed. These data are concordant or close to concordant at c. 2.15 Ga, except one analysis (5407-3), which records a younger age of c. 1.87 Ga (not shown in Fig. 16). This analysis has a lower Th/U ratio of 0.44, compared with 0.87 to 4.95 for the other nine spots (Table 2). Uranium concentrations for all 10 analyses range between 96 and 540 ppm (Table 2). Two analyses (5407-1, 2), placed in CL-dark grey unzoned crystals, have relatively high Th values (1 505 and 2 566 ppm, respectively), and also high Th/U ratios (3.26 and 4.95, respectively; Table 2). Additionally, analytical spot no. 9, partly placed in a CL-dark inclusion-rich domain, has a relatively high Th concentration (985 ppm). All three analyses give slightly younger $^{207}Pb/^{206}Pb$ ages (2.13–2.12 Ga) compared with the remaining six analyses, which may be attributed to Pb loss. Spots 1 and 9 also plot discordantly at the 2σ level (Fig. 16).

The six remaining zircon analyses, representing a texturally and geochemically coherent group, are concordant at the 2σ level and record a U-Pb concordia age of 2 140 ± 10 Ma (2σ, *n* = 6, MSWD of concordance + equivalence = 2.5, probability of conc. + equiv. = 0.004, Fig. 16). Three of these analyses are close to reversely discordant, plotting to the left side of the concordia line, which accounts for the rather poor MSWD of concordance. Excluding analytical spot 8, which has an elevated value for common Pb (f_{206}% = 0.33, Table 2), the mean weighted $^{207}Pb/^{206}Pb$ age for the metadolerite is 2 139 ± 4 Ma (2σ, *n* = 5, MSWD = 0.62, probability = 0.65, Fig. 16). This mean weighted age overlaps the concordia age and is chosen as the best age estimate for crystallisation of the dolerite protolith.

The new U-Pb SIMS zircon dates for the metadoleritic bodies at Nunasvaara and Masugnsbyn are geologically identical at c. 2.14 Ga, and provide minimum age constraints for the deposition of the two greenstone volcanic-sedimentary sequences. Since both successions display key lithostratigraphic similarities, are comparable in terms of their overall thicknesses, and occur relatively close to each other (based on their present-day positions), the older mean weighted age of c. 2 144 Ma represents the best estimate of a minimum age for both successions. However, the length of time between the deposition of volcanic and sedimentary material and the emplacement of the mafic hypabyssal bodies remains uncertain.

The new ages of 2 144 ± 5 Ma (Nunasvaara) and 2 139 ± 4 Ma (Masugnsbyn) for the metadolerites overlap at the 2σ precision level and thus identify a coeval mafic magmatic event in both areas. Given that the dated bodies have similar petrological, mineralogical and geochemical characteristics, the geochronology results confirm a spatially and temporally focused episode of mafic magmatism at c. 2.14 Ga in this sector of the Fennoscandian Shield (e.g. Table 1, Fig. 15A–B). This newly identified magmatic event in Norrbotten coincides with a known epoch of correlative 2.15–2.11 Ga mafic magmatism in the Finnish sector of the craton (e.g. Hanski & Huhma 2005, Huhma et al. 2013, Huhma et al. 2016). Additionally, the new dates represent the most robust and precise ages obtained thus far for greenstone-related rocks in northern Norrbotten (cf. Skiöld & Cliff 1984, Skiöld 1986). In this regard, our results highlight the utility of U-Pb SIMS zircon dating of Palaeoproterozoic hypabyssal mafic rocks to bracket volcanic and sedimentary depositional events, and its potential use in aiding stratigraphic correlations between disconnected greenstone belts in Norrbotten and across Fennoscandia.

Lithogeochemistry

Lithogeochemical analysis of representative whole-rock samples was conducted at ALS Minerals in Piteå, Sweden. Sample crushing and milling, powder digestion and measurement of major and trace element concentrations using several methods followed standard analytical procedures (see ALS methodology factsheets, www.alsglobal.com). A brief summary of the analytical techniques for the various elements is listed at the bottom of Table 3. Geochemical diagrams were plotted using GCD-Kit 3.0 (Janoušek et al. 2006).

Lithogeochemical results for visually and geochemically screened "weakly altered" greenstone-related rocks are listed in Table 3. Where more than one sample was analysed per unit, the mean value is shown. In total, 51 analyses of seven rock types from Nunasvaara and 20 analyses of nine rock units from Masugnsbyn were made. A "graphite schist" and "skarn-altered chert" sample from Masugnsbyn represent "mineralised" varieties (Table 3).

Figure 17 presents several geochemical classification plots for selected greenstone-related rock types. For the purpose of plotting, the units have been subdivided into two broad categories: coherent meta-igneous rocks (i.e. mafic metavolcanic lava, metadolerite sills and meta-ultramafic rocks), and metavolcaniclastic rocks (i.e. metatuff). Inferred metasedimentary rocks (black schist, amphibolitic pelite to schist, metacarbonate rocks, quartzite, etc.) have not been plotted.

Using the immobile trace element ratio diagram of Pearce (1996), mafic metavolcanic and metadolerite rocks from both areas form a relatively tight cluster within the sub-alkali basalt field (Fig. 17A; cf. Lager & Loberg 1990, pp. 4–5). In contrast, two meta-ultramafic rock samples fall close to the basalt-alkali basalt boundary, reflecting elevated concentrations of "incompatible" Nb relative to the other meta-igneous units (7.7 & 9.4 ppm, respectively; Table 3). For the metavolcaniclastic rocks (metatuff), all data points plot in the sub-alkali basalt field forming a relatively narrow cluster, albeit with slightly more Nb/Y variation (Fig. 17B).

► Figure 17. Lithogeochemical characteristics of Nunasvaara (green) and Masugnsbyn (blue) greenstone-type units. Data points in plots A–D represent individual analyses (not means). **A and B.** Trace element classification plot (Pearce 1996, based on Winchester and Floyd 1977) for coherent meta-igneous and metavolcaniclastic rocks, respectively. **C and D.** Jensen cation plot (Jensen 1976) for coherent meta-igneous and metavolcaniclastic rocks, respectively. **E.** Chondrite-normalised rare earth element (REE) diagram for average coherent meta-igneous rocks (cf. Table 3). Ultramafic rock patterns are based on one analysis only (as highlighted). Normalising values are from Boynton (1984). Representative REE patterns for "normal mid-ocean ridge basalt" (N-MORB) and "enriched mid-ocean ridge basalt" (E-MORB) also plotted for comparison (values from Sun & McDonough 1989). **F.** Chondrite-normalised REE diagram for average metavolcaniclastic and metasedimentary rock units. Six of the patterns from the Masugnsbyn area (highlighted) are based on one analysis only (Table 3).

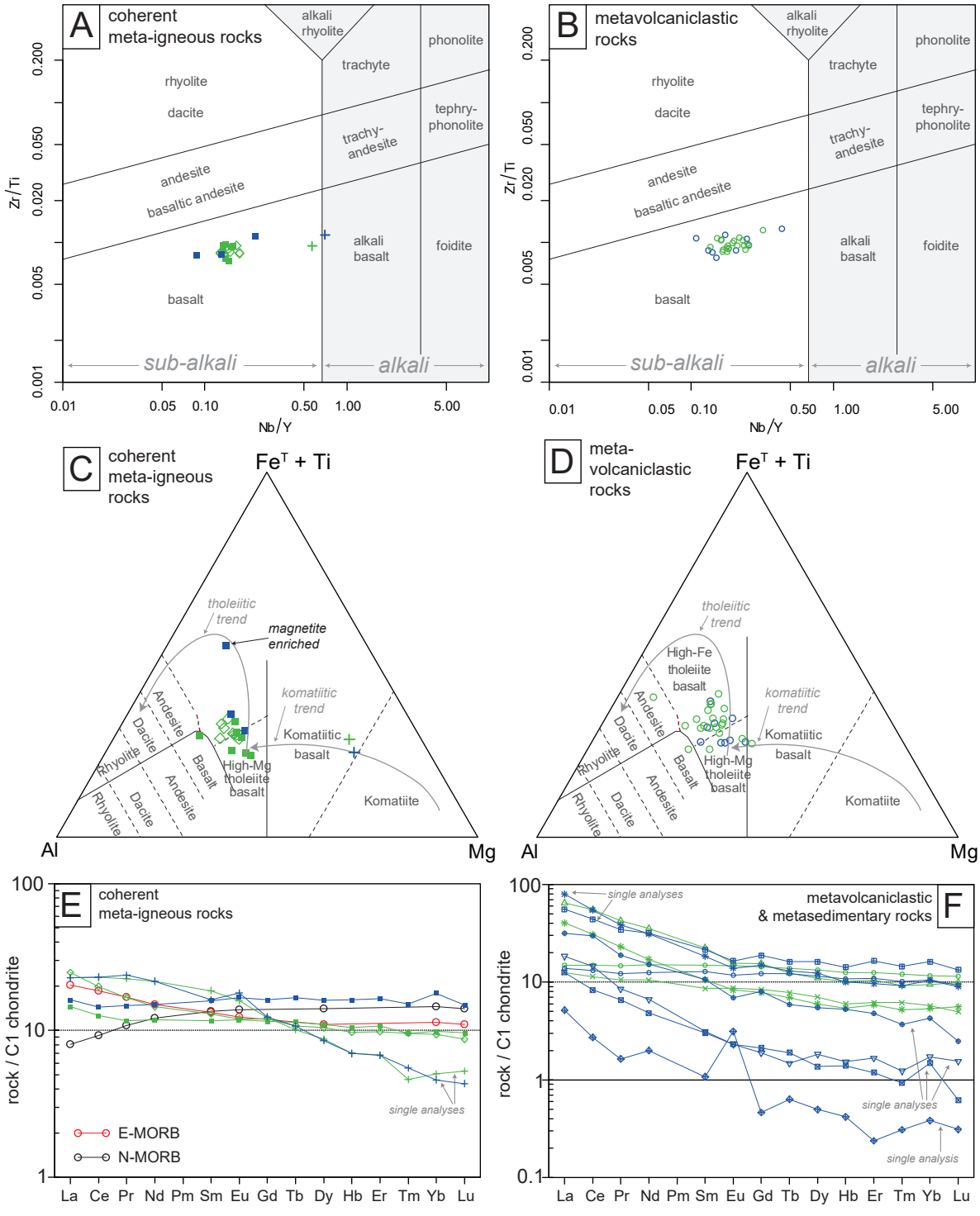

Nunasvaara greenstone units

Coherent meta-igneous rocks

- Mafic metavolcanic rock (lava)
- Meta-ultramafic rock
- Metadolerite

Metavolcaniclastic and metasedimentary rocks

- Mafic metatuff
- Meta-carbonate rock
- Graphite schist (inc. Nunasvaara deposit)
- Metasedimentary rock (mafic pelite, schist)

Masugnsbyn greenstone units

Coherent meta-igneous rocks

- Metadolerite
- Meta-ultramafic rock

Metavolcaniclastic and metasedimentary rocks

- Mafic metatuff
- Skarn-altered chert
- Quartzite
- Calcitic marble
- Dolomitic marble
- Graphite schist (Nybrännan deposit)
- Graphitic schist

Table 3. Summary of lithogeochemical data for greenstone-related rock units at Nunasvaara and Masugnsbyn.

Nunasvaara area								Masugnsbyn area								
Rock type	**Mafic metavolcanic rock** (lava)	**Graphite schist**	**Meta-tuff**	**Meta-ultramafic rock**	**Metasedimentary rock**	**Meta-carbonate rock**	**Meta-dolerite**	**Quartzite**	**Meta-tuff**	**Meta-ultramafic rock**	**Graphite schist**	**Graphitic schist**	**Skarn-banded chert**	**Calcitic marble**	**Dolomitic marble**	**Meta-dolerite**
Formation	LGF	LSF	UGF	USF	USF	USF		SF	TGF	TGF	TGF (Nybrännan)	MF	MF	MF	MF	
Quantity	*mean (n = 8)*	*mean (n = 8)*	*mean (n = 21)*	*(n = 1)*	*mean (n = 4)*	*mean (n = 2)*	*mean (n = 7)*	*(n = 1)*	*mean (n = 9)*	(n = 1)	*(n = 1)*	*(n = 1)*	*(n = 1)*	*(n = 1)*	*mean (n = 2)*	*mean (n = 3)*
wt. %																
SiO_2	47.8	45.6	50.1	42.7	59.1	33.7	47.5	98.1	51.9	41.8	26.4	62.1	64.5	5.5	0.63	48.4
Al_2O_3	13.94	11.02	13.57	6.30	16.16	6.96	14.24	0.79	14.13	7.62	6.65	14.20	2.61	1.02	0.07	12.57
Fe_2O_3t	13.19	1.86	14.30	14.05	9.49	9.66	12.19	0.55	14.31	14.05	13.35	1.23	17.45	0.91	0.88	18.05
CaO	9.22	2.98	8.26	12.75	3.12	21.58	10.97	0.03	6.08	10.20	7.39	3.97	7.56	50.80	32.30	8.70
MgO	6.59	3.00	6.61	16.30	3.93	10.73	7.42	0.99	7.87	20.00	4.43	3.56	2.85	1.58	21.20	5.86
Na_2O	4.98	3.85	3.71	0.77	4.70	1.53	3.36	0.05	3.47	0.78	1.84	1.29	1.52	0.23	0.01	3.24
K_2O	0.84	1.54	0.37	0.23	1.27	0.76	0.69	0.06	0.18	0.35	0.18	6.15	0.01	0.16	<0.01	0.66
Cr_2O_3	0.04	0.02	0.03	0.19	0.04	0.12	0.03	<0.01	0.03	0.20	0.03	0.03	0.01	0.01	<0.01	0.02
TiO_2	1.05	1.08	1.34	1.38	0.90	1.16	1.02	0.02	1.13	1.56	0.51	1.24	0.20	0.07	0.01	1.44
MnO	0.08	0.03	0.21	0.24	0.09	0.26	0.16	<0.01	0.24	0.33	0.06	0.07	1.26	0.15	0.08	0.28
P_2O_5	0.07	0.05	0.09	0.10	0.17	0.12	0.07	0.01	0.07	0.13	2.49	0.22	0.19	0.09	0.02	0.10
SrO	0.02	0.01	0.02	<0.01	0.02	<0.01	0.01	0.01	0.01	<0.01	<0.01	<0.01	<0.01	<0.01	<0.01	<0.01
BaO	0.01	0.03	0.01	0.01	0.05	0.03	0.01	<0.01	0.01	<0.01	<0.01	0.05	0.01	0.03	<0.01	0.02
LOI	0.70	28.28	1.20	1.33	0.76	13.36	0.98	1.12	0.64	2.10	36.40	4.97	2.98	38.80	46.50	0.30
Total	98.50	99.36	99.84	96.35	99.76	99.94	98.63	101.73	100.03	99.12	99.73	99.08	101.15	99.33	101.70	99.61
wt. %																
C	0.11	22.65	0.25	0.47	0.02	3.41	0.16	0.01	0.21	0.08	33.30	2.60	0.82	10.40	12.65	0.02
S	0.07	0.27	0.09	0.03	0.03	0.24	0.06	0.01	0.03	0.15	6.02	0.35	2.39	<0.01	0.09	0.03
Cl	0.75	0.25	0.17	0.04	0.07	0.03	0.61	NA	0.07	0.04	0.02	0.04	0.03	0.06	0.05	0.38
ppm																
Ag*	0.01	0.06	0.01	0.02	0.04	<0.01	<0.01	NA	NA	NA	NA	NA	NA	NA	NA	NA
As*	0.2	5.7	0.4	0.6	0.20	1.2	0.5	NA	NA	NA	NA	NA	NA	NA	NA	NA
Ba	62.7	248.0	61.2	70.7	330	138.5	85.4	4.6	47.5	23.9	14.4	392	58.1	283	9.5	120
Bi*	0.01	0.71	0.04	0.03	0.01	0.04	0.05	<0.01	NA	NA	NA	NA	NA	NA	NA	NA
Co**	42	4	46	78	27	56	41	1	48	93	77	6	69	4	5	51
Cr	283	156	210	1400	143	970	203	20	248	1530	190	230	30	20	10	93
Cs	0.32	1.70	0.29	0.02	0.46	0.13	0.70	<0.01	0.12	0.04	0.1	1.4	0.79	0.03	0.04	0.32
Cu**	46	36	61	137	56	101	55	2	78	102	372w	19	364	7	7	84
Ga	17.8	14.6	17.9	12.1	20	12.2	15.8	2.4	18.2	15.5	9.4	22.4	7.8	1.6	0.3	18.7
Hf	1.9	3.1	2.3	2.5	3.7	2.1	1.6	1.0	2.0	2.9	2.0	4.3	0.8	0.3	<0.2	2.2
Hg*	0.007	<0.005	0.014	<0.005	0.005	<0.005	0.005	NA	NA	NA	NA	NA	NA	NA	NA	NA
Mo**	<1	20	<1	<1	<1	<1	<1	<1	<1	<1	18	1	1	<1	<1	<1
Nb	2.9	8.7	4.5	7.7	8.6	6.0	2.9	0.2	3.9	9.4	4.9	10.4	3.6	0.8	0.8	4.2

Table 3. Continues.

Nunasvaara area								Masugnsbyn area								
Rock type	**Mafic metavolcanic rock** (lava)	**Graphite schist**	**Meta-tuff**	**Meta-ultramafic rock**	**Metasedimentary rock**	**Meta-carbonate rock**	**Meta-dolerite**	**Quartzite**	**Meta-tuff**	**Meta-ultramafic rock**	**Graphite schist**	**Graphitic schist**	**Skarn-banded chert**	**Calcitic marble**	**Dolomitic marble**	**Meta-dolerite**
Formation	LGF	LSF	UGF	USF	USF	USF		SF	TGF	TGF	TGF (Nybrännan)	MF	MF	MF	MF	
Quantity	*mean (n = 8)*	*mean (n = 8)*	*mean (n = 21)*	*(n = 1)*	*mean (n = 4)*	*mean (n = 2)*	*mean (n = 7)*	*(n = 1)*	*mean (n = 9)*	(n = 1)	*(n = 1)*	*(n = 1)*	*(n = 1)*	*(n = 1)*	*mean (n = 2)*	*mean (n = 3)*
Ni**	91	11	90	888	62	596	96	4	98	1040	487	16	36	5	<1	44
Rb	24.6	48.5	9.9	0.6	38.8	22.3	24.5	2.5	4.9	2.6	11.1	173.0	5.3	2.4	0.5	15.6
Sb*	0.09	0.37	0.09	0.1	0.15	0.09	0.07	NA	NA	NA	NA	NA	NA	NA	NA	NA
Sc**	40	18	41	22	21	23	41	<1	38	25	20	23	3	2	<1	44
Se*	0.5	4.0	0.7	0.3	0.4	0.5	0.4	NA	NA	NA	NA	NA	NA	NA	NA	NA
Sn	1	1	1	<1	2	1	1	<1	1.00	2.00	<1	<1	<1	<1	2	<1
Sr	138.6	96.9	89.2	42.3	171.0	40.7	113	1.8	66.2	35.9	34.7	48.7	15.5	74.3	22.9	91.8
Ta	0.2	0.6	0.3	0.5	0.5	0.4	0.2	0.1	0.33	0.70	0.6	0.8	0.20	<0.1	<0.1	0.27
Te*	0.02	0.50	0.16	0.03	0.08	0.2	0.05	NA	NA	NA	NA	NA	NA	NA	NA	NA
Th	0.29	4.06	0.55	1	5.83	0.56	0.33	1.68	0.70	0.63	3.24	7.67	1.30	0.65	0.24	0.54
Tl	<0.5	NA	<0.5	<0.5	<0.5	NA	<0.5	<0.02	0.03	0.03	0.58	0.19	0.04	<0.02	<0.02	0.12
U	0.48	6.82	0.32	0.36	1.23	0.42	0.29	0.12	0.26	0.31	7.34	3.52	0.86	0.34	1.26	0.25
V	295	260	346	213	149	169	318	5	297	211	222	215	52	15	<5	325
W	<1	3	1	<1	1	2	2	<1	4	1	1	4	<1	<1	1	<1
Y	19.0	11.7	23.3	13.5	18.4	10.8	20.5	3.8	20.8	13.4	23.8	35.1	11.0	3.5	1.2	31.5
Zn**	16	20	46	107	43	18	27	3	142	176	13	8	15	7	5	66
Zr	54	121	78	78	142	79	54	34	66	106	74	154	34	10	3	77
La	7.7	12.5	4.6	2.5	20.0	3.9	4.5	5.7	4.3	7.1	24.7	17.3	9.8	3.9	1.6	5.0
Ce	16.1	24.9	12.1	18.6	44.4	9.2	10.2	11.8	10.6	18.7	44.3	35.5	24.1	6.7	2.2	11.7
Pr	2.04	2.81	1.80	2.75	5.22	1.29	1.42	1.04	1.5	2.9	4.7	4.2	2.3	0.8	0.2	1.8
Nd	8.7	10.3	9.0	13	21.3	6.3	7.1	4	7.5	13.0	18.7	19.1	9.2	2.9	1.2	9.0
Sm	2.53	2.06	2.89	3.64	4.38	1.68	2.27	0.61	2.50	3.15	3.59	4.20	2.08	0.59	0.21	3.11
Eu	0.88	0.61	1.08	1.17	1.15	0.64	0.87	0.17	0.87	1.32	1.02	1.21	0.51	0.17	0.23	1.23
Gd	3.13	2.03	3.70	3.17	4.03	2.18	2.99	0.49	3.18	3.20	3.87	4.86	2.08	0.55	0.12	4.18
Tb	0.51	0.33	0.66	0.48	0.59	0.37	0.54	0.07	0.58	0.51	0.62	0.77	0.28	0.09	0.03	0.79
Dy	3.36	1.93	4.31	2.8	3.54	2.27	3.53	0.59	3.71	2.75	3.99	5.23	1.77	0.44	0.16	5.18
Ho	0.70	0.39	0.90	0.5	0.73	0.43	0.75	0.11	0.78	0.50	0.72	1.02	0.38	0.10	0.03	1.16
Er	2.06	1.23	2.64	1.43	2.22	1.30	2.26	0.35	2.29	1.42	2.03	3.46	1.01	0.25	0.05	3.47
Tm	0.31	0.17	0.39	0.15	0.30	0.20	0.31	0.04	0.33	0.18	0.30	0.47	0.12	0.03	0.01	0.49
Yb	1.96	1.12	2.42	1.06	1.98	1.20	2.06	0.36	2.21	0.96	2.18	3.38	0.89	0.31	0.08	3.74
Lu	0.28	0.18	0.37	0.17	0.32	0.16	0.31	0.05	0.30	0.14	0.29	0.43	0.08	0.02	0.01	0.48

Major elements analysed by ICP-AES following lithium metaborate fusion and two-acid dissolution.
S occuring as S^{2-} and total C analysed using a Leco infrared analyser. Cl analysed by KOH fusion and ion chromatography.
Trace elements analysed by ICP-AES or ICP-MS following lithium metaborate fusion and two-acid dissolution, except * = aqua regia dissolution, and ** = four- acid dissolution.

< = concentration is less than detection limit as shown. NA = not analysed.
LGF = Lower greenstone formation, LSF = Lower sedimentary formation, UGF = Upper greenstone formation, TGF = Tuorevaara greenstone formation, SF = Suinavaara formation, MF = Masugnsbyn formation.

Based on the classification diagram of Jensen (1976) for sub-alkali volcanic rocks, mafic metavolcanic and metadolerite samples plot in the high-Fe and high-Mg tholeiite basalt fields, although most of the data fall in the former (Fig. 17C; cf. Lager & Loberg 1990, pp. 4–7). One relatively magnetite-rich metadolerite sample from Masugnsbyn plots above the main group, closer to the Fe^T + Ti apex. Both meta-ultramafic samples plot in the komatiitic basalt field, consistent with their relatively high MgO concentrations (approximately 16.3 & 20.0 wt. %, Table 3). These samples also contain relatively high TiO_2 values (1.34 and 1.56 wt. %) and LREE/HREE ratios (cf. Fig. 17E). Based on the classification scheme of LeMaitre et al. (2002, p. 34), they classify as picrite and meimechite, respectively. The metatuff samples have similar compositional distributions to the basaltic metavolcanic and metadolerite rocks (i.e. mainly high-Fe tholeiite, subordinate high-Mg tholeiite), and highlight the compositional similarity between the Masugnsbyn and Nunasvaara samples (Fig. 17D).

Chondrite-normalised (Boynton 1984, subscript CN) rare earth element (REE) patterns for (1) the coherent meta-igneous rocks; and (2) combined metavolcaniclastic and metasedimentary rocks are presented in Figure 17E–F, respectively. The patterns represent the mean values from Table 3, except for those from single-value determinations (as indicated).

In general, basaltic (tholeiitic) metavolcanic and metadolerite rocks from both areas form a coherent group, with enriched REE concentrations (10–25 times chondritic) and show flat to weakly $LREE_{CN}$-enriched patterns (mean $[La/Yb]_{CN}$ = 0.9–2.7, Fig. 17E). In contrast, the meta-ultramafic units (high-Mg basalts) have identical steeply sloping patterns, showing $HREE_{CN}$-depletion relative to the other meta-igneous samples and weak positive Eu_{CN} anomalies ($[La/Yb]_{CN}$ = 4.5 & 5.0, Eu/Eu* = approximately 1.1 & 1.3, respectively, Fig. 17E). These features are consistent with incompatible element source enrichment, relatively deeper or higher temperature (asthenospheric) melting, lower-degree crystal fractionation and continental contamination of true komatiitic melts (e.g. Wilson 1989, Cattell & Taylor 1990). For comparison, mean REE_{CN} patterns for N-MORB and E-MORB oceanic crust are also plotted on Figure 17E.

For the metavolcaniclastic and metasedimentary rocks (Fig. 17F), REE relative abundances (approximately 0.5 to 80 times chondritic) and chondrite-normalised patterns are more variable. For example, mafic metatuff from both areas has identical REE_{CN} patterns (flat to very weakly $LREE_{CN}$-enriched) that broadly match the patterns for basaltic metavolcanic and metadolerite rocks shown in Figure 17E. In contrast, mafic pelite to schist at Nunasvaara and graphitic schist horizons in both study areas are LREE-enriched and have weak negative Eu anomalies (mean $[La/Yb]_{CN}$ = 3.5–7.6, mean Eu/Eu* = approximately 0.8–0.9, respectively, Fig. 17E). Likewise, skarn-altered metachert and quartzite units from Masugnsbyn have similar REE systematics (though the latter has lower abundances), which are consistent with an overall continental provenance (Fig. 17F, e.g. Taylor & McLennan 1985). Finally, metacarbonate rocks from both areas (calcitic and dolomitic marbles, metalimestone to marl) show the most variability in terms of their REE abundances and normalisation patterns. In particular, the overall lower abundances and positive europium anomaly (Eu/Eu* = approximately 4.4) seen in the dolomitic marble from Masugnsbyn is not present in a calcitic marble from the same stratigraphic unit (Masugnsbyn formation). These features may reflect local-scale primary variation of the REE budget during carbonate deposition (e.g. open marine, estuarine water or hydrothermal vent fluid inputs), or represent the effects of later hydrothermal (metasomatic) fluids overprinting a higher permeability dolomitic horizon (e.g. Kamber & Webb 2001).

In summary, igneous classification plots utilising relatively immobile major and trace elements (e.g. Rollinson 1993) highlight the basaltic, predominantly Fe-tholeiitic nature of the Palaeoproterozoic metavolcanic, metadoleritic and meta-ultramafic greenstone units. This signature is underlined by the relative abundances of other major elements, such as lower values of SiO_2 and K_2O, and elevated values of MgO, total iron and CaO, compared with intercalated metasedimentary rocks (Table 3). Mafic metavolcaniclastic rocks (metatuff) are also predominantly basaltic (Fe-tholeiitic) and compositionally

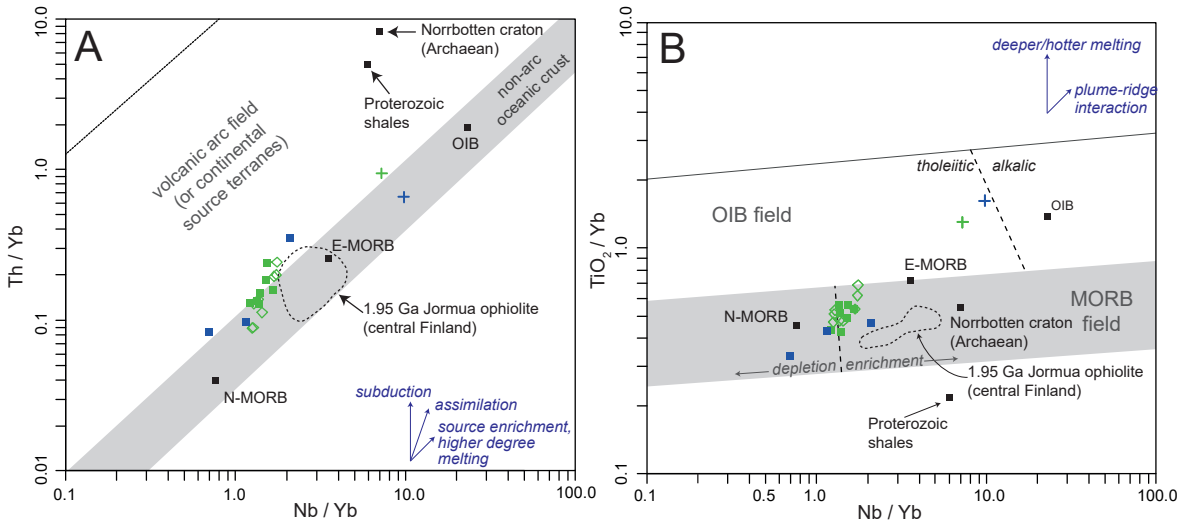

Figure 18. Nunasvaara and Masugnsbyn mafic-ultramafic meta-igneous rocks plotted on the basalt discrimination diagrams of Pearce (2008). **A.** Th/Yb versus Nb/Yb plot discriminating volcanic arc (continental) from non-arc (oceanic) basalts. See main text for discussion. **B.** TiO_2/Yb versus Nb/Yb plot discriminating spreading ridge (MORB) basalts from plume-related (OIB) basalts. See main text for discussion. Rock symbols are the same as in Figure 15. Average N-MORB, E-MORB and OIB data points are based on trace element values listed in Sun & McDonough (1989) and the TiO_2 values of Condie (1993). Average global Proterozoic shale value is from Condie (1993). Average Archaean Norrbotten craton value is based on data presented by Öhlander et al. (1987b). The dashed field for mafic rocks belonging to the 1.95 Ga Jormua ophilite (central Finland) is based on data presented by Peltonen et al. (1996).

overlap basaltic lava at Nunasvaara and the metadoleritic bodies in both study areas (e.g. Fig. 17A–B). Likewise, the weak to moderate $LREE_{CN}$-enriched REE_{CN} patterns underscore the compositional similarity between the various meta-igneous units. Given the general lithostratigraphy, the lithogeochemical results also suggest meta-igneous units in both greenstone successions may partially or wholly represent a comagmatic suite derived from a basaltic (Fe-tholeiitic) magmatic system with subordinate Mg-tholeiitic and komatiitic components (Fig. 17C–D).

Given the prevailing tectonic setting of Karelian 2.5–2.0 Ga metasupracrustal rocks in northern Fennoscandia (e.g. Laajoki 2005, Hanski 2012, Melezhik & Hanski 2012), the Pearce (2008) discrimination plot provides a means of assessing the inferred tectonic environment of the greenstone units by making a comparative assessment with major oceanic and continental crustal reservoirs (Fig. 18). In particular, the Th/Yb versus Nb/Yb plot acts as a useful first-order discriminator between compositionally variable oceanic realm (non-arc) basalts and subduction-related (arc) volcanic suites (Fig. 18A). It may also allow for less ambiguous inferences when compared with other tectonic discrimination diagrams containing superimposed or overlapping oceanic ("MORB") and volcanic arc fields (e.g. Pearce & Cann 1973, Meschede 1986; cf. Martinsson 2004).

Data points for greenstone-related basaltic metavolcanic and metadoleritic rocks mainly fall within the non-arc oceanic field between average N-MORB and E-MORB values, while a subset trends diagonally into the volcanic arc field (Fig. 18A). These data also plot close to the circular field for c. 1.95 Ga Jormua ophiolitic rocks in central Finland, which have general E-MORB geochemical signatures (Peltonen et al. 1996). If extended to the top of the diagram, the diagonal trend for the Norrbotten greenstone units intersects with the approximate positions of average Proterozoic shale and the Archaean Norrbotten craton. The latter value is a proxy for a major continental terrane underlying northern Norrbotten metasupracrustal successions. Unlike the metavolcanic and metadoleritic rocks, the meta-ultramafic samples plot within or close to the boundary of the oceanic field between average E-MORB and OIB values.

Pearce (2008) equates diagonal trends in the Th/Yb-Nb/Yb plot (Fig. 18A), extending from the oceanic to volcanic arc fields, to bulk assimilation (or contamination) by continental crustal material, primarily reflected by variable Th (and LREE) enrichment. Such assimilation may chiefly develop either when viscous magma ascends through attenuated continental lithosphere or within subduction zones. In the absence of petrological and geochemical proxies for subduction systems (e.g. general absence of calc-alkaline-type volcanic and plutonic rocks, subordinate to absent intermediate to felsic suites, no strong negative Nb or Th geochemical anomalies), and given the general tectonic regime of the Fennoscandian Shield at c. 2.1 Ga, rifting-related crustal contamination is considered a feasible explanation for the observed trend.

Figure 18B shows that data points for basaltic metavolcanic and metadoleritic rocks all fall within the oceanic (MORB) field, mostly with an enriched (E-MORB) signature close to that from Jormua ophiolite-related basaltic rocks. In contrast, both meta-ultramafic samples plot in the OIB array defined by ridge-distal oceanic island volcanism (Pearce 2008) consistent with their ultrabasic (low silica, high-Mg) geochemical signatures (cf. Fig. 17C). A weakly developed diagonal trend between all the data points is also evident. Pearce (2008) suggests that such diagonal trends in TiO_2/Yb-Nb/Yb space may result when rocks have formed during plume-ridge interactions.

Sm-Nd isotopic analysis

Whole-rock Sm-Nd isotopic analysis of 18 greenstone-related samples was conducted at the Geological Survey of Finland (GTK), Espoo, Finland. Trace element concentrations and Sm-Nd isotopic ratios were determined using the ID-TIMS method and followed the analytical procedure outlined in Huhma et al. (2012). Initial εNd values (relative to present day CHUR; Jacobsen & Wasserburg 1980) have been calculated at 2.14 Ga for the Nunasvaara samples (n = 11) and 2.14 Ga for the Masugnsbyn samples (n = 7; see Table 4, footnote No. 5). Initial εNd values are based on $^{147}Sm/^{144}Nd$ = 0.1966, $^{143}Nd/^{144}Nd$ = 0.512640 for present day CHUR (Jacobsen & Wasserburg 1980) and the decay constant $\lambda^{147}Sm = 6.54 \times 10^{-12}yr^{-1}$ (Lugmair & Marti 1978). Estimated precision for initial εNd values is ± 0.4 ε-units (2σ), except for the altered sample ELH130023D (± 2.0 ε-units, Table 4). Where listed, depleted mantle model ages (T_{DM}) utilise the Nd evolution curve of DePaolo (1981).

The results of the Sm-Nd isotopic analysis are listed in Table 4. For the Nunasvaara samples (n = 11), $\varepsilon Nd_{(2.14\ Ga)}$ values range from +0.4 to +4.0, with the majority (n = 9) falling between +1.4 and +4.0. Based on rock type, the range of $\varepsilon Nd_{(2.14\ Ga)}$ values are: basaltic metavolcanic rocks (Lower greenstone formation) = +1.4 to +4.0 (n = 4); basaltic metatuff (Upper greenstone formation) = +2.3 to +2.9 (n = 3); a sodic-altered metatuff (Upper greenstone formation) = +0.4 (n = 1); and metadolerite = +0.5 to +3.8 (n = 3). Four Nunasvaara samples with relatively high Sm/Nd values (0.26–0.30) yielded depleted mantle model ages (T_{DM}) ranging from 2.8–2.4 Ga (Table 4). For the Masugnsbyn samples (n = 7), $\varepsilon Nd_{(2.14\ Ga)}$ values range from +0.4 to +3.7. The range of values by rock type are: basaltic metatuff (Veikkavaara upper greenstone formation) = +0.4 to +3.7 (n = 5); metadolerite = +1.6 (n = 1); and meta-ultramafic rock = +2.2 (n = 1). Two Masugnsbyn samples with lower Sm/Nd yielded T_{DM} ages of c. 2.2 and 2.3 Ga (Table 4).

Overall, the Sm-Nd results indicate that greenstone-related units have consistently positive initial εNd signatures lying between the CHUR reference value (εNd = 0) and a LREE-depleted mantle model (εNd = approximately +3 to +4.5 at c. 2.14 Ga, Fig. 19). These signatures are characteristic of lithologic material derived from "juvenile" melts (either directly or indirectly), with a relatively short crustal residence time (e.g. Faure & Mensing 2005). However, the spread in the data and trend toward less positive initial εNd values may partly reflect the influence of overprinting metasomatic fluids, as evidenced by an $\varepsilon Nd_{(2.14\ Ga)}$ value of +0.4 for a moderate to intensely sodic-altered metatuff at Nunasvaara (Table 4).

Table 4. Whole-rock Sm-Nd results for greenstone rocks at Nunasvaara (n = 11) and Masugnsbyn (n = 7).

Sample[1]	Rock type (and unit)[2]	Sm (ppm)	Nd (ppm)	Sm/Nd	$^{147}Sm/^{144}Nd$[3]	$^{143}Nd/^{144}Nd$[4]	$\varepsilon Nd_{(t = 0\ Ga)}$	$\varepsilon Nd_{(t = 2.14)}$	T_{DM} (Ga)[5]
Nunasvaara area (t = 2.14 Ga)									
ELH130016A	Metabasalt (VGG, LGF)	2.36	6.81	0.347	0.2096 (± 8)	0.512994 (± 10)	6.9	3.4	n/a
ELH130011A	Metabasalt (VGG, LGF)	2.02	6.24	0.334	0.1962 (± 8)	0.512839 (± 25)	3.9	4.0	n/a
ELH130014D	Metabasalt (VGG, LGF)	2.74	9.02	0.303	0.1834 (± 7)	0.512601 (± 10)	-0.8	2.9	2.75
ELH130061C	Metabasalt (VGG, LGF)	2.8	10.69	0.262	0.1581 (± 6)	0.512167 (± 10)	-9.2	1.4	2.68
ELH130030A	Metatuff (VGG, UGF)	3.76	12.7	0.296	0.1793 (± 7)	0.512531 (± 10)	-2.1	2.7	2.73
ELH130010A	Metatuff (VGG, UGF)	2.93	8.2	0.245	0.2205 (± 9)	0.513092 (± 10)	8.8	2.3	n/a
ELH130006A	Metatuff (VGG, UGF)	2.82	8.53	0.331	0.2000 (± 8)	0.512838 (± 10)	3.9	2.9	n/a
ELH130023D	Metatuff (VGG, UGF)	2	6.65	0.301	0.1820 (± 7)	0.512455 (± 72)	-3.6	0.4	3.32
ELH130020D	Metadolerite	2.61	7.98	0.327	0.1981 (± 8)	0.512686 (± 10)	0.9	0.5	n/a
ELH130121A	Metadolerite	5.33	18.4	0.29	0.1750 (± 7)	0.512530 (± 10)	-2.2	3.8	2.43
ELH130025A	Metadolerite	2.11	5.31	0.397	0.2409 (± 10)	0.513434 (± 10)	15.5	3.3	n/a
Masugnsbyn area (t = 2.14 Ga)									
FHM140001B	Metatuff (VeiGG, TGF)	5.54	24.71	0.224	0.1355 (± 8)	0.511908 (± 10)	-14.3	2.5	2.21
FHM140008A	Metatuff (VeiGG, TGF)	3.5	9.27	0.379	0.2290 (± 14)	0.513115 (± 28)	9.3	0.4	n/a
FHM140009A	Metatuff (VeiGG, TGF)	2.97	8.73	0.34	0.2058 (± 12)	0.512810 (± 18)	3.3	0.8	n/a
FHM140011A	Metatuff (VeiGG, TGF)	1.73	5.23	0.332	0.2007 (± 12)	0.512873 (± 11)	4.5	3.4	n/a
FHM140018A	Metatuff (VeiGG, TGF)	2.23	7.54	0.295	0.1786 (± 11)	0.512576 (± 26)	-1.2	3.7	n/a
FHM140006A	Metadolerite	2.85	8.02	0.355	0.2147 (± 20)	0.512978 (± 16)	6.6	1.6	n/a
FHM140007A	Meta-ultra-mafic rock	3.25	12.94	0.251	0.1520 (± 9)	0.512123 (± 10)	-10.1	2.2	2.27

[1]Sample ELH130023D is an intensely scapolite-altered metatuff and the precision of the calculated $\varepsilon Nd_{2.14\ Ga}$ value is ± 2 ε-units (see main text for discussion).
[2]VGG, LGF = Vittangi greenstone group, Lower greenstone formation. VGG, UGF = Vittangi greenstone group, Upper greenstone formation. VeiGG, TGF = Veikkavaara greenstone group, Tuorevaara greenstone formation
[3]Uncertainty refers to the last digit at 2σ level.
[4]Uncertainty refers to the last two digits at 2σ level.
[5]T_{DM} = Depleted mantle model age (based on general assumptions outlined in Murphy & Nance 2002). Where n/a is shown, the evolution path does not intersect the DePaolo (1981) depleted mantle model curve. No uncertainties are reported for T_{DM} values, and any interpretation should be tentative.

Figure 19 shows initial εNd values versus $^{147}Sm/^{144}Nd$ for the greenstone units analysed (cf. Table 4). In general, the former parameter is a proxy for crustal (continental) signature, with increasing negative values (and by extension increasing crustal residence time), whereas the latter may highlight LREE enrichment or depletion characteristics of source region(s), relative degrees of fractionation in comagmatic suites, potential influence of crustal assimilation and effects of metasomatism (e.g. Beck & Murthy 1991). Figure 19 also shows Sm-Nd characteristics (shaded fields) for the depleted mantle (DM) and Archaean Norrbotten craton (ANC) calculated at c. 2.14 Ga (cf. Fig. 20). These domains represent potential source end-members for Palaeoproterozoic mafic magmatism in the northern Fennoscandian Shield.

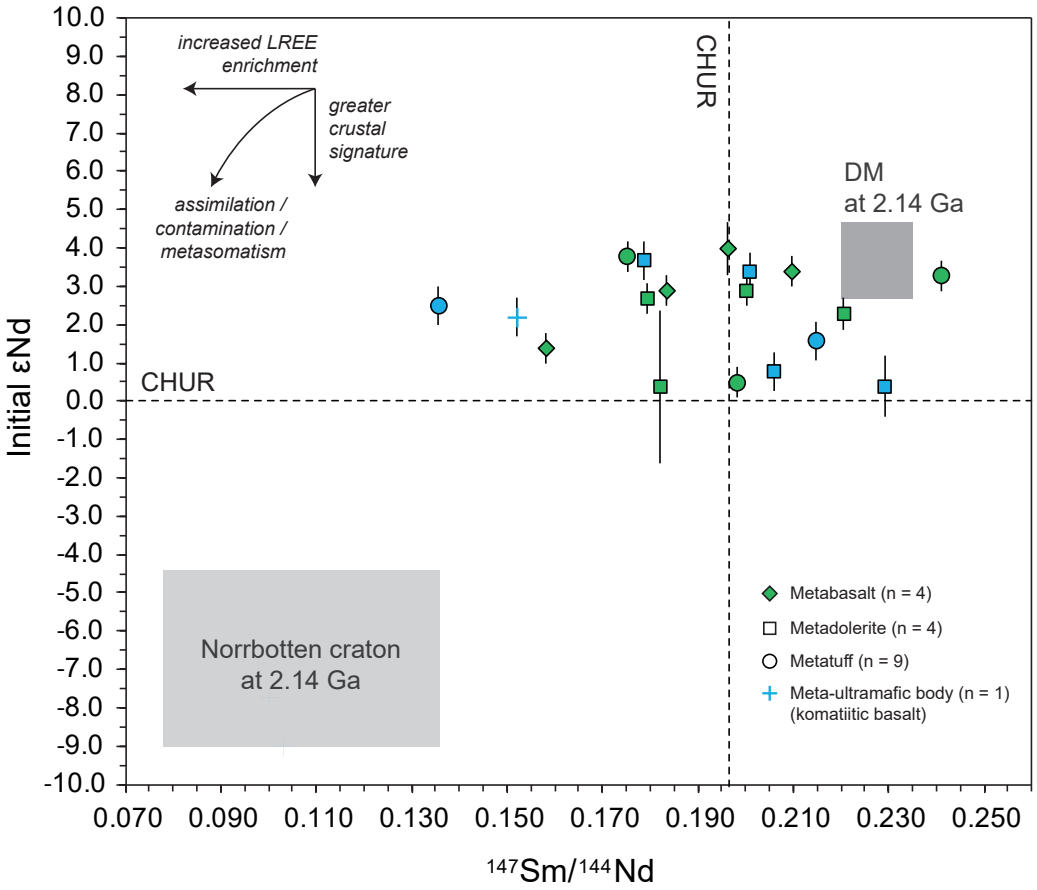

Figure 19. Initial εNd versus $^{147}Sm/^{144}Nd$ for greenstone units at Nunasvaara (green symbols) and Masugnsbyn (blue symbols). Error bars for $^{147}Sm/^{144}Nd$ not visible at the plot scale. Shaded data range (2σ spread) for a depleted mantle (DM) reservoir at c. 2.14 Ga is from Huang et al. (2013). Shaded data range for a Norrbotten craton reservoir is based on initial εNd values for Archaean orthogneisses and metagranitoids from Öhlander et al. (1987b) and Mellqvist (1999), recalculated for 2.14 Ga. The CHUR reference lines are based on $^{147}Sm/^{144}Nd$ = 0.1967 (Jacobsen & Wasserburg 1980) and εNd = 0.

Greenstone-related units generally plot as a fairly coherent group, with the majority (12) having initial εNd values that overlap the εNd signature of the DM at 2.14 Ga (Fig. 19). The remainder (6) plot between the DM and CHUR reference values. The dataset displays a broader spread in terms of $^{147}Sm/^{144}Nd$, which mainly falls between the DM range and the least evolved margin of the ANC (i.e. the higher $^{147}Sm/^{144}Nd$ margin). Overall, a somewhat indistinct mixing trend or zone of assimilation/contamination between the DM and ANC source regions is apparent. A clearer delineation of such a feature (if geologically valid) may be limited by the small number of samples, a degree of sampling bias (i.e. lack of metasedimentary units), and the relatively inadequate geochemical and isotopic constraints for the Norrbotten craton in northernmost Sweden.

In general, geological factors that may account for the observed Sm-Nd systematics of the greenstone units include (1) magma source region and corresponding LREE abundance variability (e.g. asthenospheric mantle versus sub-continental lithospheric mantle); (2) single-source LREE heterogeneity (e.g. along-axis E-MORB versus N-MORB variants); (3) melt contamination during ascent and crystallisation (i.e. assimilation of Archaean continental material); (4) magma series differentiation (affecting Sm/Nd), and (5) overprinting metasomatic-hydrothermal events, leading to LREE variability or mobility and potential disturbance of the Sm-Nd isotopic systematics (cf. Huhma et al. 1990).

The effects of metasomatic-hydrothermal fluids in the Nunasvaara and Masugnsbyn areas have been documented in this study and elsewhere (e.g. Smith et al. 2009). The ability of such overprinting events

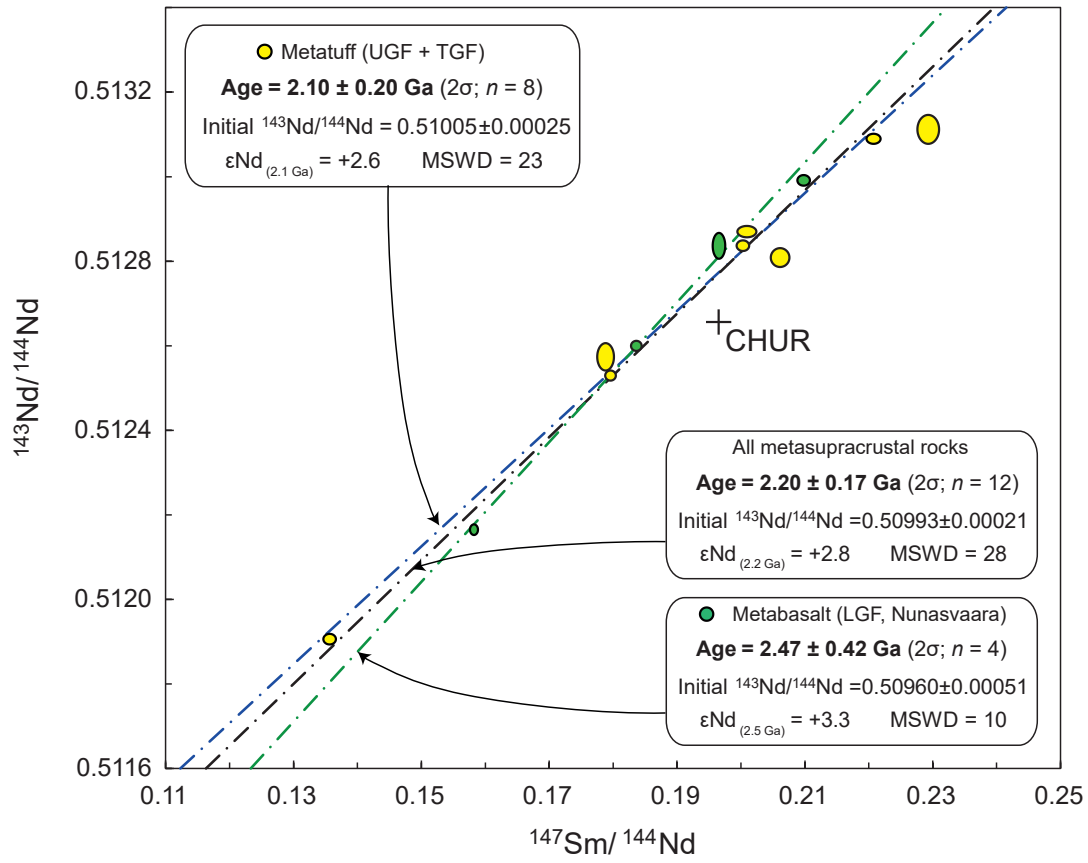

Figure 20. Sm-Nd "errorchrons" for greenstone-related metasupracrustal rocks at Nunasvaara and Masugnsbyn. The regressed ages should be regarded as statistically non-robust reference ages only, due to the large mean squares of weighted deviate (MSWD) values, narrow $^{147}Sm/^{144}Nd$ range of the samples and low precision at the 2σ level. The errorchron "age" of 2.10 ± 0.20 Ga is based on Sm-Nd results for metatuff samples from both study areas, but excludes altered metatuff sample ELH130023D (see Table 4). The errorchron "age" of 2.47 ± 0.42 Ga is for Nunasvaara metabasalt only. The errorchron "age" of 2.20 ± 0.17 Ga is for all samples. CHUR represents the present-day value for a bulk silicate Earth (Jacobson & Wasserburg 1980). Plot created in Isoplot 4.16 (Ludwig 2012). LGF = Lower greenstone formation (at Nunasvaara), TGF = Tuorevaara greenstone formation (Veikkavaara greenstone group, Masugnsbyn).

to disturb the Sm-Nd systematics of the greenstones may be partly assessed using a whole-rock Sm-Nd isochron plot as shown in Figure 20. In this plot, the slopes of three "errorchron" regression lines yield imprecise "reference ages" of c. 2.45 Ga (Nunasvaara metabasalt only), c. 2.10 Ga (metatuff from Nunasvaara and Masugnsbyn) and c. 2.20 Ga (i.e. all metasupracrustal units from both areas). Additionally, the regressed data provide $^{143}Nd/^{144}Nd$ intercepts, corresponding to initial εNd values of approximately +2.6, +3.3 and +2.8 for the three reference ages, respectively.

While the imprecise reference ages preclude any meaningful interpretation, either individually or as a whole, the age of c. 2.20 Ga through all the greenstone metasupracrustal rocks is relatively consistent with the minimum formational age of c. 2.14 Ga determined by U-Pb zircon dating. Likewise, the $\varepsilon Nd_{(2.2\,Ga)}$ value of +2.8 based on the equivalent $^{143}Nd/^{144}Nd$ intercept generally conforms to the spread of initial εNd values determined for the individual metasupracrustal samples (Table 4, Fig. 19). Thus, while some variation may be attributed to secondary metasomatic effects, on the whole the Sm-Nd systematics appear to have remained relatively robust during subsequent tectonothermal events, since a younger Sm-Nd age (i.e. < c. 2.0 Ga) is not preserved. This confirms that LREE variability as illustrated in Figure 19 may best be explained by primary geological factors as previously described.

One such factor may be melt fractionation during ascent and crystallisation, leading to a differentiated

magma series. However, the predominantly tholeiitic basaltic nature of both greenstone successions and the apparent absence of intercalated intermediate and felsic units suggest that the greenstones represent a relatively homogenous geochemical suite. Likewise, the compositional overlap between the basaltic metasupracrustal units and the metadoleritic bodies suggests that a phase of relatively consistent mafic magmatism may have occurred. Thus, any local differentiation effects during magma ascent and storage cannot account for the LREE variability seen in the greenstone units. Consequently, source region variability and the assimilation of older continental material (i.e. the Norrbotten craton) were probably major factors in determining the generally positive εNd character and the relatively LREE-enriched geochemical composition of the greenstones.

A preliminary petrogenetic model

Potential source regions and precursor material for Palaeoproterozoic greenstone-type magmatism in northern Norrbotten include (1) a REE-depleted asthenospheric mantle (e.g. DM curve, Fig. 21); (2) a REE-enriched (plume-modified?) asthenospheric mantle (e.g. CHUR line, Fig. 21); (3) a REE-enriched sub-continental lithospheric mantle (e.g. adjacent to the CHUR line); (4) a depleted mantle plus assimilated Norrbotten craton mixed source; (5) a depleted mantle plus assimilated older supracrustal rocks mixed source (e.g. rift-related *Kovo group* in northern Norrbotten); and (6) a combination of 1 to 5. The initial εNd versus time plot shown in Figure 21 provides a means of assessing the contribution of potential source terranes and crustal assimilation effects, and summarises the petrogenesis of the greenstone successions as part of the broader tectonic evolution of northern Norrbotten.

In Figure 21, initial εNd values of the c. 2.14 Ga greenstone units are plotted relative to values for (1) 2.83–2.67 Ga basement rocks of the Norrbotten craton (and their projected Nd evolution field); (2) 1.90–1.80 Ga syn- to late-orogenic volcanic and plutonic rocks located in the interior part of the craton (i.e. distal from the Knaften-Skellefte arc to the south; cf. Weihed et al. 2005, Lahtinen et al. 2009); and (3) 1.92–1.78 Ga syn- to late-orogenic plutonic rocks located at the southern margin of the craton (i.e. proximal to the Knaften-Skellefte arc). Vertical time lines highlight the beginning of key tectonothermal events affecting the northern Fennoscandian Shield. These include plume-induced break-up of composite Fennoscandia at c. 2.45 Ga, eventually leading to separation of the Karelian and Norrbotten cratons (e.g. Walker et al. 1997, Melezhik & Hanski 2012), and initial subduction-related magmatism at c. 2.02 and c. 1.95–1.89 Ga on the eastern and southern margins of the Norrbotten craton, forming the Kittilä and Knaften-Skellefte arcs, respectively (Hanski & Huhma 2005, Wasström 2005, Lahtinen et al. 2009).

Based on its spatial distribution and projected Nd evolution characteristics (Fig. 21), the Meso- to Neoarchaean Norrbotten craton represents a major continental source terrane for Palaeoproterozoic magmatism in northernmost Sweden (cf. Witschard 1984). For example, studies of Svecokarelian plutonic and volcanic rocks formed within the thick interior of the craton (i.e. Knaften–Skellefte retroarc hinterland) indicate that continental anatexis contributed to syn-orogenic melt generation, producing extensive calc-alkaline to alkaline, mafic to felsic volcanic-plutonic suites with negative initial εNd values (approximately -1 to -9, Fig. 21, e.g. Öhlander et al. 1987a, Skiöld et al. 1988, Mellqvist et al. 1999). This signature partly reflects a REE budget inherited from the cratonic reservoir, which by c. 1.9 Ga had acquired a distinctly negative εNd character of between approximately -7 and -12 (Fig. 21). Conversely, contemporaneous syn-orogenic mafic to intermediate plutonic suites emplaced along the southern margin of the craton (Knaften–Skellefte arc foreland) have markedly more juvenile εNd characteristics (approximately -2 to +4), reflecting increased slab or mantle wedge-derived inputs and a lesser contribution from isotopically mature, continental source rocks. Thus, the REE budget of the arc-proximal magmas was less influenced by a relatively thinner basement margin, which by c. 1.9 Ga formed part of the upper plate of the north-directed subduction zone (Fig. 21, e.g. Nironen 1997, Lahtinen et al. 2005, Weihed et al. 2005).

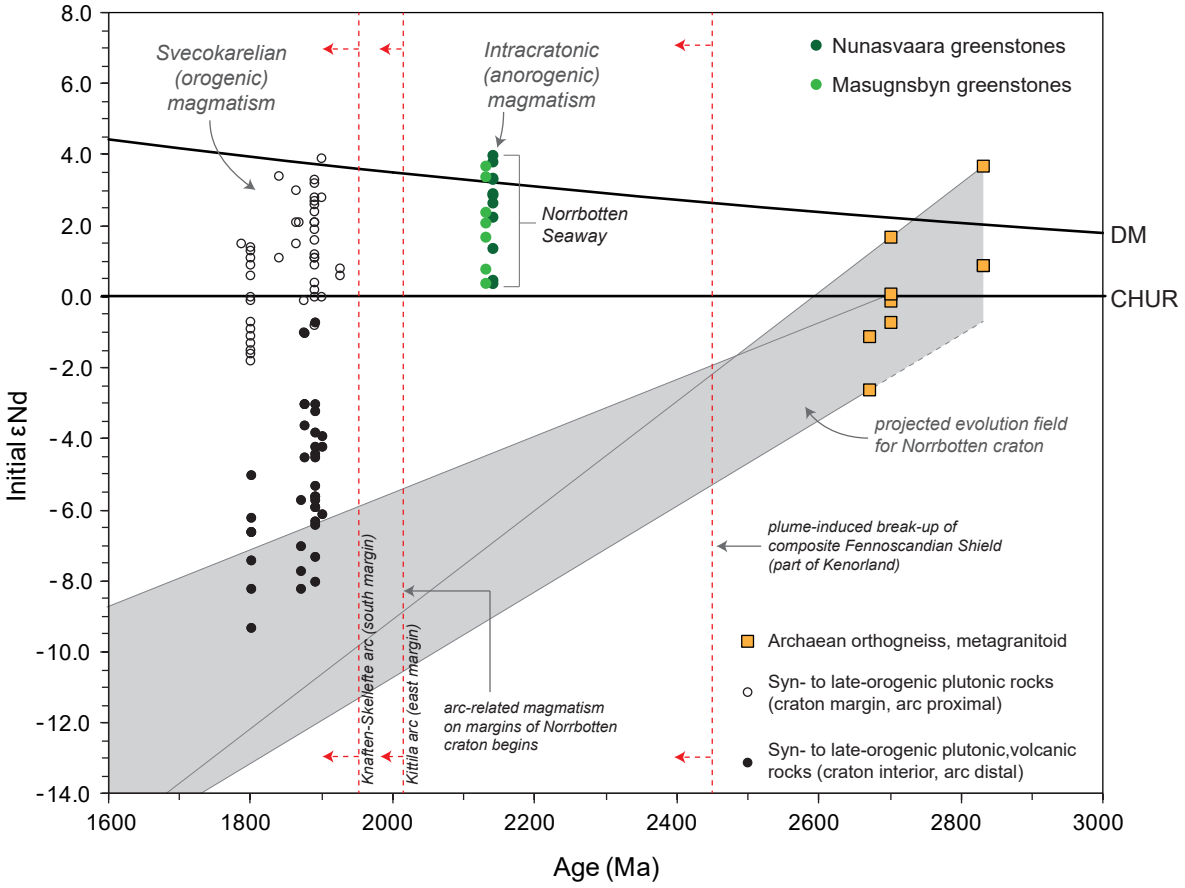

Figure 21. Initial εNd versus time plot for greenstone units at Nunasvaara and Masugnsbyn (green dots) in relation to other Norrbotten craton and Svecokarelian-related rocks. Initial εNd values are calculated at 2.14 Ga (Nunasvaara) and 2.13 Ga (Masugnsbyn) to aid data visualisation in figure and do not alter the geological interpretation from that which would have been made if all values had been calculated at 2.14 Ga. See main text for discussion. DM = depleted mantle model curve (DePaolo 1981), CHUR = chondrite uniform reservoir (e.g. DePaolo & Wasserburg 1976). Archaean data points (squares) are from Öhlander et al. 1987b, Mellqvist 1999 and Mellqvist et al. 1999. Svecokarelian-related data points (black dots and circles) are from Wilson et al. 1985, Öhlander et al. 1987a, Öhlander et al. 1987b, Skiöld et al. 1988, Cliff et al. 1990, Öhlander et al. 1993, Öhlander & Skiöld 1994, Mellqvist et al. 1999 and Mellqvist et al. 2003. Major time lines (broken red lines) are from Hanski & Huhma (2005) and Wasström (2005).

In general, the Nd isotopic characteristics of the c. 2.14 Ga greenstones indicate a mainly juvenile, depleted to enriched mantle-like signature that extends from the DM model towards the CHUR reference (Fig. 21). By c. 2.14 Ga, the bulk εNd signature of the Norrbotten craton had evolved to moderately negative εNd values of between approximately -4 and -9 (Fig. 21). Thus, the distinct continental crustal signature of the cratonic terrane is not strongly reflected in the εNd values of the greenstones and suggests that the assimilation of continental material had a minor modifying effect during primitive melt ascent and storage. Moreover, if crustal assimilation had played a significant role, a mixed initial εNd signature similar to that for Svecokarelian igneous rocks formed in the craton interior (i.e. arc distal setting) may be expected for the greenstone units formed in the same cratonic setting (Fig. 21).

The involvement of a depleted asthenospheric mantle in the petrogenesis of the greenstones is somewhat contradicted by the trace element systematics. Specifically, the chondrite-normalised REE patterns and Th/Nb ratios reveal a relatively enriched signature, more consistent with E-MORB-type oceanic crust (cf. Fig. 18). Given the regional tectonic setting at c. 2.14 Ga (e.g. Melezhik & Hanski 2012), three

preferred petrogenetic scenarios may account for the geochemical and isotopic characteristics: (1) deeply sourced light REE-enriched asthenospheric melts (plume-modified?) ascended through the continental lithosphere during regional rifting and extension; (2) relatively enriched sub-continental lithospheric mantle melts ascended through the continental lithosphere during rifting and extension; or (3) N-MORB-like depleted mantle magmas partially assimilated continental material, resulting in a "mixed" light REE-enriched plus isotopically juvenile (positive initial εNd) signature. All three scenarios presuppose some degree of assimilation of continental crust.

Regional geological and tectonic reconstructions of northern Fennoscandia 2.5–2.0 Ga emphasise a major phase of lithospheric-scale continental rifting and dispersion (e.g. Smolkin 1997, Hanski & Huhma 2005, Hanski 2012, Melezhik & Hanski 2012). The c. 2.14 Ga greenstone successions at Nunasvaara and Masugnsbyn developed as part of this protracted rift-to-drift episode. In north-central Norrbotten, volcanosedimentary depocentres developed within an epieric sea, which we here name the *Norrbotten Seaway* (cf. Fig. 21). Deposition and extrusion of sedimentary and volcanic material was probably controlled by extensional tectonics and half-graben structures during relatively high rates of sedimentation and volcanism (e.g. Melezhik & Fallick 2010).

The apparent lack of Svecokarelian-cycle arc-type magmatism in the Norrbotten craton interior with juvenile Nd isotope characteristics (i.e. equivalent to arc-proximal rocks along its southern margin; cf. Fig. 21) suggests that the Norrbotten Seaway remained a relatively narrow, aulacogen-type, intracontinental basin, and did not mature into a wide oceanic plateau. Thus, the greenstone successions at Nunasvaara and Masugnsbyn probably represent authothonous or parautothonous fragments of this fully or partially closed marginal sea. By c. 2.14 Ga the Norrbotten Seaway lay adjacent to a developing oceanic basin to the northeast (Kittilä Ocean), which was spreading and maturing at that time (e.g. Melezhik & Hanski 2012).

SUMMARY AND CONCLUSIONS

New field mapping, U-Pb SIMS zircon geochronology, lithogeochemistry and Sm-Nd isotopic analysis have been integrated to investigate two Palaeoproterozoic greenstone successions in north-central Norrbotten, northern Sweden. The conclusions from this work are:

1. The greenstone succession at Nunasvaara (*Vittangi greenstone group*) consists of a partly conformable, polydeformed sequence divisible into four formations, with a minimum total thickness of approximately 2.4 km. The basal *Lower greenstone formation* (LGF) contains effusive basaltic metavolcanic rocks that locally display amygdaloidal and pillowed forms. The overlying *Lower sedimentary formation* contains a distinctive black schist horizon at the top (Nunasvaara member, NM), which locally contains significant disseminated and vein graphite mineralisation (Nunasvaara deposit). Pyrite and pyrrhotite associated with the graphite suggest a relatively reduced (anoxic to euxinic) depositional environment. The overlying *Upper greenstone formation* (UGF) comprises laminated basaltic metatuff. The uppermost unit, called the *Upper sedimentary formation* (USF), consists of pelite, black schist, minor intercalated metacarbonate layers and rare meta-ironstone and komatiitic metabasalt horizons. Locally, the USF hosts stratiform–stratabound iron mineralisation associated with variable sodic-calcic (skarn-type) alteration and sulphides.

2. At Masugnsbyn (*Veikkavaara greenstone group*), the greenstones form a relatively conformable sequence divisible into four formations, with a minimum total thickness of 3.4 km. The lowermost *Tuorevaara greenstone formation* is poorly exposed and is inferred to consist mainly of effusive basaltic metavolcanic rocks similar to the LGF at Nunasvaara. The overlying *Suinavaara formation* (SF) is a relatively thin horizon consisting of intercalated quartzite, graphitic pelite and metacarbonate rocks. The stratigraphic position of the SF remains uncertain, and correlation with a Nunasvaara unit is not proposed. The Tuorevaara greenstone formation (TGF) mainly consists of laminated basaltic metatuff.

A correlation between the TGF and the UGF at Nunasvaara is permissible based on petrographic and geochemical comparisons. Additionally, an approximately 50 m thick graphitic schist horizon at the base of the NGF correlates with the *Nunasvaara member* and further supports a stratigraphic link between the NGF and UGF (i.e. both metatuff sequences conformably overlie a distinctive black schist horizon). The uppermost *Masugnsbyn formation* (MF) consists of skarn-banded metachert (ironstone), graphitic schist and metacarbonate layers. The MF correlates with the USF at Nunasvaara and contains abundant skarn-style Fe mineralisation (e.g. the Junosuando deposit).

3. At Nunasvaara and Masugnsbyn new U-Pb SIMS zircon ages of 2144 ± 5 Ma and 2139 ± 4 Ma, respectively, obtained for metadolerite bodies intruding the greenstone successions constrain the timing of sub-volcanic mafic magmatism and provide a new minimum age of c. 2.14 Ga for the deposition of both greenstone sequences. The geochronology results identify a new c. 2.14 Ga episode of tholeiitic mafic magmatism in this sector of the Fennoscandian Shield and provide a temporal framework for greenstone-type volcanic-sedimentary depositional processes in north-central Norrbotten.

4. Major and trace element systematics in greenstone-related meta-igneous units indicate predominantly sub-alkali basaltic compositions corresponding to high-Fe and high-Mg tholeiitic rocks. Rare meta-ultramafic horizons have low silica, high-Mg (picritic to meimechitic) compositions. Metasedimentary units have mainly mafic to intermediate compositions. Chondrite-normalised rare earth element (REE) patterns for the mafic meta-igneous units are flat to light REE-enriched. Metabasalts at Nunasvaara (LGF) have REE patterns that overlap those of average E-MORB signatures. The patterns also overlap those for the metatuff and metadolerite, suggesting a potential comagmatic suite. Metasedimentary units from both areas display moderately light REE-enrichment patterns indicating evolved, upper continental crust-type signatures (cf. Taylor & McLennan 1985).

5. Sm-Nd isotopic results show initial εNd values between +0.4 and +4.0 for the greenstone units that fall between the depleted mantle and CHUR reference models. While metasomatic overprinting may partly account for some of the variation, these data, combined with the trace element systematics, suggest that juvenile melts from a geochemically enriched mantle were a major source component for the greenstones. Assimilation of older continental crust (e.g. the Norrbotten craton) may also have played a minor role.

6. The greenstone successions are interpreted to have formed within a rifted continental setting, in which crustal extension facilitated upwelling of tholeiitic magmas and provided sub-aqueous depositional sites for volcanic and sedimentary material. From a broader perspective, the Norrbotten greenstone belts evolved within an immature marginal sea or oceanic basin named the Norrbotten Seaway.

7. Overprinting geological processes recorded at Nunasvaara and Masugnsbyn, including amphibolite facies metamorphism, polyphase ductile-brittle deformation, graphitisation and hydrothermal metasomatism are attributed to subsequent tectonothermal events at 1.90–1.78 Ga.

ACKNOWLEDGEMENTS

We thank James Kilgannon for able field assistance at Nunasvaara, and Cecilia Jönsson for conducting ground geophysical measurements at Masugnbyn. Laboratory assistance by Leena Järvinen and Arto Pulkkinen at the Geological Survey of Finland (GTK) is gratefully acknowledged. U-Pb zircon dating at the Nordsim facility was performed in cooperation with the Laboratory for Isotope Geology, Swedish Museum of Natural History (NRM), Stockholm. We express our gratitude to Martin Whitehouse, Lev Ilyinsky and Kerstin Lindén at Nordsim for their analytical support. Martin Whitehouse reduced the zircon analytical data, Lev Ilyinsky assisted during SIMS analyses, while Kerstin Lindén prepared the zircon mounts and assisted with zircon imaging. Jaroslaw Majka at the Department of Earth Sciences, Uppsala University, is also thanked for his assistance during zircon imaging.

REFERENCES

Ahl, M., Bergman, S., Bergström, U., Eliasson, T., Ripa, M. & Weihed, P., 2001: Geochemical classification of plutonic rocks in central and northern Sweden. *Sveriges geologiska undersökning Rapporter och meddelanden 106*, Uppsala, 86 p.

Ambros, M., 1980: Description of the geological maps Laanavaara NV, NO, SV, SO and Karesuando SV, SO with geophysical interpretation by Herbert Henkel. *Sveriges geologiska undersökning Af 25–30*, 111 pp.

Beck, W. & Murthy, V.R., 1991: Evidence for continental crustal assimilation in the Hemlock Formation flood basalts of the early Proterozoic Penokean Orogen, Lake Superior Region. *In:* P.K. Sims & L.M.H. Carter (eds.) Contributions to Precambrian Geology of the Lake Superior Region. *United States Geological Survey Bulletin 1904-1*, 13–125.

Bergman, S., Kübler, L. & Martinsson, O., 2001: Description of regional geological and geophysical maps of northern Norbotten County. *Sveriges geologiska undersökning Ba 56*, 110 pp.

Bergman, S., Billström, K., Persson, P.-O., Skiöld, T. & Evins, P., 2006: U-Pb age evidence for repeated Paleoproterozoic metamorphism and deformation near the Pajala shear zone in the northern Fennoscandian Shield. *GFF 128*, 7–20.

Bergman, S., Stephens, M.B., Andersson, J., Kathol, B. & Bergman, T., 2012: Bedrock map of Sweden, 1:1 000 000 scale. *Sveriges geologiska undersökning K 423*.

Bergström, R., 1987. Nunasvaara grafitfyndinghet. Unpublished company report for LKAB, *K 87-4,* 98 p.

Bida, J., 1979: Hietajoki dolomitförekomst. Slutrapport. *Sveriges geologiska undersökning PRO79-38*, 19 pp.

Billström, K., Bergman, S. & Martinsson, O., 2002: Post-1.9 Ga metamorphic, mineralization and hydrothermal events in northern Sweden. *GFF 124*, p. 228.

Billström, K., Eilu, P., Martinsson, O., Niiranen, T., Broman, C., Weihed, P., Wanhainen, C. & Ojala, J., 2010: IOCG and related mineral deposits of the northern Fennoscandian Shield. *In:* T.M. Porter (ed.): *Hydrothermal iron oxide–copper–gold & related deposits: a global perspective, vol. 3*. Advances in the Understanding of IOCG deposits. PGC Publishing, Adelaide, 381–414.

Bingen, B., Solli, A., Viola, G., Torgersen, E., Sandstad, J.-S., Whitehouse, M.J., Røhr, T.S., Ganerød, M. & Nasuti, A. 2016: Geochronology of the Palaeoproterozoic Kautokeino Greenstone Belt, Finnmark, Norway: Tectonic implications in a Fennoscandia context. *Norwegian Journal of Geology 95,* 1–32.

Blake, K., 1990. *The petrology, geochemistry and association to ore formation of the host rocks of the Kiirunavaara magnetite-apatite deposit, northern Sweden*. Ph.D. thesis, University of Wales, Cardiff, UK.

Boynton, W.V., 1984. Geochemistry of the rare earth elements: meteorite studies. *In:* P. Henderson (ed.) *Rare earth element geochemistry*. Elsevier, 63–114.

Buseck, P.R. & Beyssac, O., 2014: From organic matter to graphite: Graphitization. *Elements 10*, 421–426.

Cattell, A.C. & Taylor, R.N., 1990: Archaean basic magmas. *In:* R.P. Hall & D.J. Hughes (eds) *Early Precambrian Basic Magmatism*. Blackie, Glasgow, UK, 11–39.

Cliff, R.A., Rickard, D. & Blake, K., 1990: Isotope systematics of the Kiruna magnetite ores, Sweden: Part 1. Age of the ore. *Economic Geology 85*, 1770–1776.

Condie, K.C., 1993: Chemical composition and evolution of the upper continental crust: contrasting results from surface samples and shales. *Chemical Geology 104,* 1–37.

Condie, K.C., Des Marais, D.J. & Abbott, D., 2001: Precambrian superplumes and supercontinents: a record in black shales, carbon isotopes, and paleoclimates? *Precambrian Research 106*, 239–260.

Damberg, K., Nylund, B. & Mannström, B., 1974: Tornefors järnmalmsfyndighet. Rapport rörande resultaten av Sveriges geologiska undersökning: undersökningar 1949, 1966, 1970. *Sveriges geologiska undersökning BRAP 736*, 24 pp.

DePaolo, D.J., 1981: Neodymium isotopes in the Colorado Front Range and crust-mantle evolution in the Proterozoic. *Nature 291*, 684–687.

DePaolo, D.J. & Wasserburg, G.J., 1976: Nd isotopic variations and petrogenetic models. *Geophysical Research Letters 3*, 249–252.

Edfelt, Å., Armstrong, R.N., Smith, M. & Martinsson, O., 2005: Alteration paragenesis and mineral chemistry of the Tjårrojåkka apatite–iron and Cu (-Au) occurrences, Kiruna area, northern Sweden. *Mineralium Deposita 40*, 409–434.

Edfelt, Å., Sandrin, A., Evins, P., Jeffries, T., Storey C., Elming, S.-Å. & Martinsson, O., 2006: Stratigraphy and tectonic setting of the host rocks at the Tjårrojåkka Fe-oxide Cu-Au deposits. *GFF 128,* 221–232.

Eilu, P. (ed.) 2012: Mineral deposits and metallogeny of Fennoscandia. *Geological Survey of Finland, Special Paper 53*. 401 pp.

Eriksson, B., 1969: Berggrunden inom det central Vittangifältet, dess petrografi, stratigrafi och tektonisk. *Sveriges geologiska undersökning Brap 881*, 181 pp.

Eriksson, B. & Hallgren, U., 1975: Beskrivning till berggrundskartbladen Vittangi NV, NO, SV, SO. *Sveriges geologiska undersökning Af 13–16*, 203 pp. (with summary in English).

Faure, G. & Mensing, T.M., 2005: *Isotopes. Principles and Applications*. John Wiley & Sons, Inc., Hoboken, NJ, USA. 897 pp.

Frietsch, R., 1984: Petrochemistry of the iron ore-bearing metavolcanics in Norrbotten County northern Sweden. *Sveriges geologiska undersökning C 802,* 62 pp.

Frietsch, R., 1997: The iron ore inventory programme 1963 to 1972 in Norrbotten County. *Sveriges geologiska undersökning Rapporter och meddelanden 92*, 77 pp.

Frietsch, R., Tuisku, P., Martinsson, O. & Perdahl, J-A., 1997: Early Proterozoic Cu-(Au) and Fe ore deposits associated with regional Na–Cl metasomatism in northern Fennoscandia. *Ore Geology Reviews 12*, 1–34.

Gavelin, S., 1957: Variations in isotopic composition of carbon from metamorphic rocks in northern Sweden and their geological significance. *Geochimica et Cosmochimica Acta 12*, 297–314.

Geijer, P., 1929: Masugnsbyfältens geologi. *Sveriges geologiska undersökning C 351*, 39 pp.

Gerdin, P., Johansson, L., Hansson, K.E., Holmqvist, A. & Ottosson, D., 1990: Grafit uppslagsgenerering i Norrbotten 1990. *Sveriges geologiska undersökning Prap 90068*, 100 pp.

Grigull, S., Berggren, R., Jönberger, J., Jönsson, C., Hellström, F.A. & Luth, S., 2018: Folding observed in Palaeoproterozoic supracrustal rocks in northern Sweden. *In:* Bergman, S. (ed): Geology of the Northern Norrbotten ore province, northern Sweden. *Rapporter och Meddelanden 141,* Sveriges geologiska undersökning. This volume pp 205–257.

Grip, E. & Frietsch, R., 1973: *Malm i Sverige 2. Norra Sverige*. Almqvist & Wiksell, 295 pp.

Gustafsson, B., 1993. *The Swedish Norrbotten greenstone belt. A compilation of available information concerning exploration*. Unpublished company report for the State Mining Property Commission (NSG). 52 pp.

Hanski, E.J. & Huhma, H., 2005: Central Lapland greenstone belt. *In:* R. Lehtinen, P.A. Nurmi, O.T. Rämö (eds.) *Precambrian Geology of Finland – key to the evolution of the Fennoscandian Shield*. Elsevier, Amsterdam, 139–194.

Hanski, E.J., 2012: Evolution of the Paleoproterozoic (2.5–1.95 Ga) non-orogenic magmatism in the eastern part of the Fennoscandian Shield. *In:* V.A. Melezhik, A.R. Prave, E.J. Hanski, A.E. Fallick, A. Lepland, L.R. Kump & H. Strauss (eds.) *Reading the archive of Earth's oxygenation*, Volume 1, Springer, Berlin, 179–245.

Hellström, F. & Jönsson, C., 2014: Barents project 2014: Summary of geological and geophysical information of the Masugnsbyn key area. *Sveriges geologiska undersökning 2014:21, 84 pp.*

Hellström, F. & Jönsson C., 2015: Summary of geological and geophysical field investigations in the Masugnsbyn key area, northern Norrbotten. *Sveriges geologiska undersökning 2015:04*, 31 pp.

Hellström, F.A., Kumpulainen, R., Jönsson, C., Thomsen, T.B., Huhma, H. & Martinsson, O., 2018: Age and lithostratigraphy of Svecofennian volcanosedimentary rocks at Masugnsbyn, northernmost Sweden – host rocks to Zn-Pb-Cu- and Cu ±Au sulphide mineralisations. *In:* Bergman, S. (ed): Geology of the Northern Norrbotten ore province, northern Sweden. *Rapporter och Meddelanden 141,* Sveriges geologiska undersökning. This volume pp 151–203.

Hellström, F.A., 2018: Early Svecokarelian migmatisation west of the Pajala Deformation Belt, northeastern Norrbotten Province, northern Sweden. *In:* Bergman, S. (ed): Geology of the Northern Norrbotten ore province, northern Sweden. *Rapporter och Meddelanden 141,* Sveriges geologiska undersökning. This volume pp 361–379.

Henderson, I. & Kendrik, M., 2003: Structural controls on graphite mineralisation, Senja, Troms. *Norges geologiske undersökelse (NGU) Report 2003.011*, 105 pp.
Huang, S, Jacobsen, S.B. & Mukhopadhyay, S., 2013: ^{147}Sm-^{143}Nd systematics of Earth are inconsistent with a superchondritic Sm/Nd ratio. *Proceedings of the National Academy of Sciences 110*, 4929–4934.
Huhma, H., Cliff, R.A., Perttunen, V. & Sakko, M., 1990: Sm-Nd and Pb isotopic study of mafic rocks associated with early Proterozoic continental rifting: the Peräpohja schist belt in northern Finalnd. *Contributions to Mineralogy and Petrology 104*, 369–379.
Huhma, H., Kontinen, A., Mikkola, P., Halkoaho, T., Hokkanen, T., Hölttä, P., Juopperi, H., Konnunaho, J., Luukkonen, E., Mutanen, T., Peltonen, P., Pietikäinen,K. & Pulkkinen, A. 2012: Nd isotopic evidence for Archaean crustal growth in Finland. *In*: P. Hölttä (ed.) *The Archaean of the Karelia Province in Finland*. *Geological Survey of Finland (GTK) Special Paper 54*, 176–213.
Huhma, H., Hanski, E., Vuollo, J., Kontinen, A. & Mutanen, T., 2013: Sm-Nd isotopes and age of Paleoproterozoic mafic rocks in Finland – evidence for rifting of Archaean lithosphere and multiple mantle sources. *Geological Survey of Finland (GTK) Report 198*, 45–48.
Huhma, H., Hanski, E., Vuollo, J. & Kontinen, A., 2016: Age and Sm-Nd isotopes of Paleoproterozoic mafic rocks in Finland – evidence for rifting stages and magma sources. *Bulletin of the Geological Society of Finland Special Volume 1*, p. 155
Jacobsen S.B. & Wasserburg G.J., 1980: Sm-Nd isotopic evolution of chondrites. *Earth and Planetary Science Letters* 50, 139–155.
Janoušek, V., Farrow, C.M. & Erban, V., 2006: Interpretation of whole-rock geochemical data in igneous geochemistry: introducing Geochemical Data Toolkit (GCDkit). *Journal of Petrology 47*, 1255–1259.
Jensen, L.S., 1976: A new cation plot for classifying subalkalic volcanic rocks. *Ontario Division of Mines Miscellaneous Paper 66*, 22 pp.
Kamber, B.S. & Webb, G.E., 2001: The geochemistry of late Archaean microbial carbonate: implications for ocean chemistry and continental erosion history. *Geochimica et Cosmochimica Acta 65*, 2509–2525.
Klein, C. & Beukes, N.J., 1992: Proterozoic iron formations. *In:* K.C. Condie (ed.) *Proterozoic Crustal Evolution*. *Developments in Precambrian Geology 10*, Elsevier, 383–418.
Koistinen, T., Stephens, M.B., Bogatchev, V., Nordgulen, O., Wenneström, M. & Korhonen, J., 2001: *Geology of the Fennoscandian Shield. 1:2 000 000-scale map*. Geological Survey of Finland (GTK), Geological Survey of Sweden (SGU), Geological Survey of Norway (NGU), DNRR.
Kumpulainen, R.A., 2000: *The Paleoproterozoic sedimentary record of northernmost Norrbotten, Sweden*. Unpublished report for the Geological Survey of Sweden (SGU). 45 pp.
Laajoki, K., 2005: Karelian supracrustal rocks. *In:* M. Lehtinen, P.A. Nurmi, O.T. Rämö (eds.), *Precambrian Geology of Finland – key to the evolution of the Fennoscandian Shield*. Elsevier, Amsterdam, 279–341.
Ladenberger, A., Andersson, M., Gonzalez, J., Lax, K., Carlsson, M., Olsson, S-Å. & Jelinek, C., 2012: Till geochemistry in northern Norrbotten. *Sveriges geologiska undersökning K410*, 112 pp (In Swedish).
Lager, I. & Loberg, B., 1990: *Sedimentologisk bassänganalytisk malmprospekteringsmetodik inom norrbottniska grönstensbälten*. Unpublished report for STU project 86-03967P, Luleå College, Luleå, 131 pp.
Lahtinen, R., Korja, A. & Nironen, M., 2005: Proterozoic tectonic evolution. *In:* R. Lehtinen, P.A. Nurmi, O.T. Rämö (eds.) *Precambrian Geology of Finland – key to the evolution of the Fennoscandian Shield*. Elsevier, Amsterdam, 481–532.
Lahtinen, R., Garde, A.A. & Melezhik, V.A., 2008: Paleoproterozoic evolution of Fennoscandia and Greenland. *Episodes 31*, 1–9.
Lahtinen, R., Korja, A., Nironen, M. & Heikkinen, P., 2009: Paleoproterozoic accretionary processes in Fennoscandia. *Geological Society, London, Special Publications 318*, 237–259.
Lahtinen, R., Huhma, H., Lahaye, L., Jonsson, E., Manninen, M., Lauri, L.S., Bergman, S., Hellström, F., Niiranen, T. & Nironen, M., 2015: New geochronological and Sm-Nd constraints across the Pajala shear zone of northern Fennoscandia: reactivation of a Paleoproterozoic suture. *Precambrian Research 256*, 102–119.

Le Maitre, R.W., Streckeisen, A., Zanettin, B., Le Bas, M., Bonin, B. & Bateman, P., 2002: *Igneous rocks: a classification and glossary of terms: recommendations of the International Union of Geological Sciences Subcommission on the Systematics of Igneous Rocks*. Cambridge University Press, 236 pp.

Lugmair, G.W. & Marti, K., 1978: Lunar initial $^{143}Nd/^{144}Nd$: Differential evolution of the lunar crust and mantle. *Earth and Planetary Science Letters*, v.39, p. 349–357.

Ludwig, K.R., 2012: User's manual for Isoplot 3.75. A geochronological toolkit for Microsoft Excel. *Berkeley Geochronology Center Special Publication No. 5,* 75 pp.

Luque, F.J., Crespo-Feo, E., Barrenechea, J.F. & Ortega, L., 2012: Carbon isotopes of graphite: Implications on fluid history. *Geoscience Frontiers 3*, 197–207.

Lynch, E.P., Jönberger, J., Luth, S., Grigull, S. & Martinsson, O., 2014. Geological and geophysical studies in the Nunasvaara, Saarijärvi and Tjårrojåkka areas, northern Norrbotten. *Sveriges geologiska undersökning 2014:04*, 48 pp.

Lynch, E.P., Jönberger, J., Bauer, T.E., Sarlus, Z. & Martinsson, O., 2015: Meta-volcanosedimentary rocks in the Nautanen area, Norrbotten: Preliminary lithological and deformation characteristics. *Sveriges geologiska undersökning 2015:30*, 51 pp.

Lynch, E.P., Hellström, F., & Huhma, H., 2016: The Nunasvaara graphite deposit, northern Sweden: New geochemical and U-Pb zircon age results for the host greenstones. *Bulletin of the Geological Society of Finland Special Volume 1*, 112–113.

Martinsson, O., 1993: Stratigraphy of the greenstones in the eastern part of northern Norrbotten. *In:* Martinsson, O., Perdahl, J.-A. & Bergman, J. (eds): *Greenstone and porphyry hosted ore deposits in northern Norrbotten*. Unpublished report for PIM/NUTEK project, no. 1, 77 p.

Martinsson, O., 1997: *Tectonic setting and metallogeny of the Kiruna greenstones*. Ph.D. thesis, Luleå University of Technology, Luleå, Sweden, 165 p.

Martinsson, O., Hallberg, A., Broman, C., Godin-Jonasson, L., Kisiel, T. & Fallick, A.E., 1997: Viscaria – a syngenetic exhalative Cu-deposit in the Paleoproterozoic greenstones. *In:* Martinsson, O., 1997: *Tectonic setting and metallogeny of the Kiruna greenstones*. Ph.D. thesis, Luleå University of Technology, Luleå, Sweden. 1–57.

Martinsson, O., 2004: Geology and metallogeny of the northern Norrbotten Fe–Cu–Au province. *In:* R.L. Allen, O. Martinsson & P. Weihed (eds.): Svecofennian ore-forming environments of northern Sweden – volcanic-associated Zn-Cu-Au-Ag, intrusion-associated Cu-Au, sediment-hosted Pb-Zn, and magnetite-apatite deposits in northern Sweden. *Society of Economic Geologists, guidebook series 33*, 131–148.

Martinsson, O., Van der Stilj, I., Debras, C. & Thompson, M., 2013: Day 3. The Masugnsbyn, Gruvberget and Mertainen iron deposits. *In:* O. Martinsson & C. Wanhainen (eds.): 12th Biennial SGA Meeting, Uppsala, Sweden. *Society of Geology Applied to Mineral Deposits, excursion guidebook SWE5*, 37–44.

Martinsson, O., Billström, K., Broman C., Weihed, P. & Wanhainen C., 2016: Metallogeny of the Northern Norrbotten ore province, northern Fennoscandian Shield with emphasis on IOCG and apatite-iron ore deposits. *Ore Geology Reviews 78*, 447–492.

Masurel, Q., 2011: *Volcanic and volcano-sedimentary facies analysis of the Viscaria D-zone Fe-Cu occurrence, Kiruna District, Northern Sweden*. M.Sc. thesis, Luleå University of Technology, Luleå, Sweden. 125 pp.

McClay, K.R., 1987: *The mapping of geological structures*. Geological Society, London, Field Guide Series. John Wiley & Sons, Chichester, UK. 161 pp.

Melezhik, V.A. & Fallick, A.E., 2010: On the Lomagundi-Jatuli carbon isotopic event: The evidence from the Kalix Greenstone Belt, Sweden. *Precambrian Research 179*, 165–190.

Melezhik, V.A. & Hanski, E.J., 2012: The early Paleoproterozoic of Fennoscandia: Geological and tectonic settings. *In:* V.A. Melezhik, A.R. Prave, E.J. Hanski, A.E. Fallick, A. Lepland, L.R. Kump & H. Strauss (eds.): *Reading the archive of Earth's oxygenation*, Volume 1, Springer, Berlin. 33–38.

Melezhik, V.A., Kump, L.R., Hanski, E.J., Fallick, A.E. & Prave, A.R., 2012: Tectonic evolution and major global Earth-surface palaeoenvironmental events in the Palaeoproterozoic. *In:* V.A. Melezhik, A.R. Prave, E.J. Hanski, A.E. Fallick, A. Lepland, L.R. Kump & H. Strauss (eds.): *Reading the archive of Earth's oxygenation*, Volume 1, Springer, Berlin, 3–21.

Mellqvist, C., 1999. *Proterozoic crustal growth along the Archaean continental margin in the Luleå and Jokkmokk areas, northern Sweden*. Ph.D. thesis, Luleå University of Technology, Luleå, 140 pp.
Mellqvist, C., Öhlander, B., Skiöld, T. & Wikström, A., 1999: The Archaean-Proterozoic paleoboundary in the Luleå area, northern Sweden: field and isotope geochemical evidence for a sharp terrane boundary. *Precambrian Research 96*, 225–243.
Mellqvist, C., Öhlander, B., Weihed, P. & Schöberg, H., 2003: Some aspects on the subdivision of the Haparanda and Jörn intrusive suites in northern Sweden. *GFF 125,* 77–85.
Meschede, M., 1986: A method for discriminating between different types of mid-ocean ridge basalts and continental tholeiites with the Nb-Zr-Y diagram. *Chemical Geology 56*, 207–218.
Mitchell, C.J., 1993: Industrial Minerals Laboratory Manual: Flake graphite. *British Geological Survey Technical Report WG/92/30*, 31 pp.
Murphy, J.B. & Nance, R.D., 2002: Sm–Nd isotopic systematics as tectonic tracers: an example from West Avalonia in the Canadian Appalachians. *Earth Science Reviews 59*, 77–100.
Niiniskorpi, V., 1986: En Zn-Pb-Cu-mineralisering i norra Sverige, en case-studie. Licenciate thesis., geological department of Åba Akademi, 74 pp.
Nironen, M., 1997. The Svecofennian Orogen: a tectonic model. *Precambrian Research 86*, 21–44.
Nordstrand, J., 2012: *Mineral chemistry of gangue minerals in the Kiirunavaara iron ore*. M.Sc. thesis, Luleå University of Technology, Luleå, Sweden. 46 pp.
Öhlander, B. & Skiöld, T., 1994: Diversity of 1.8 Ga potassic granitoids along the edge of the Archaean craton in northern Scandinavia: a result of melt formation at various depths and from various sources. *Lithos 33*, 265–283.
Öhlander, B., Hamilton, P.J., Fallick, A.E. & Wilson, M.R., 1987a: Crustal reactivation in northern Sweden: the Vettasjärvi granite. *Precambrian Research 35*, 277–293.
Öhlander, B., Skiöld, T., Hamilton, P.J. & Claesson, L-Å., 1987b: The western border of the Archaean province of the Baltic Shield: evidence from northern Sweden. *Contributions to Mineralogy and Petrology 95*, 437–450.
Öhlander, B., Lager, I., Loberg, B.E.H. & Schöberg, H., 1992. Stratigraphical position and Pb-Pb age of the Lower Proterozoic carbonate rocks from the Kalix Greenstone Belt, northern Sweden. *GFF 114*, 317–322.
Öhlander, B., Skiöld, T., Elming, S.-Å., BABEL Working Group, Claesson, S., & Nisca, D.H., 1993: Delineation and character of the Archaean-Proterozoic boundary in northern Sweden. *Precambrian Research 64*, 67–84.
Öhlander, B., Mellqvist, C., & Skiöld, T., 1999: Sm–Nd isotope evidence of a collisional event in the Precambrian of northern Sweden. *Precambrian Research 93*, 105–117.
Oze C. & Winter J.D., 2005. The occurrence, vesiculation and solidification of dense blue glassy pahoehoe. *Journal of Volcanology and Geothermal Research 142***,** 285–301.
Padget, P., 1970. Description of the geological maps Tärendö NW, NE, SW, SE with an appendix on geophysical aspects by J.D. Cornwell. *Sveriges geologiska undersökning Af 5–8*, 95 pp.
Pearce, J.A., 1996: A user's guide to basalt discrimination diagrams. *In:* D.A. Wyman (ed.) Trace element geochemistry of volcanic rocks: Applications for massive sulphide exploration. Geological Association of Canada, Short Course Notes 12, 79–113.
Pearce, J.A., 2008: Geochemical fingerprinting of oceanic basalts with applications to ophiolite classification and the search for Archean oceanic crust. *Lithos 100*, 14–48.
Pearce, J.A. & Cann, J.R., 1973: Tectonic setting of basic volcanic rocks determined using trace element analysis. *Earth and Planetary Science Letters 19*, 290–300.
Pearce, M., Godel, B.M., & Thompson, M., 2015: Microstructures and mineralogy of a world-class graphite deposit. *Society of Economic Geologists, Annual Conference 2015, Hobart, Australia. Program and abstracts*.
Peltonen, P., Kontinen, A., & Huhma, H., 1996: Petrology and geochemistry of metabasalts from the 1.95 Ga Jormua ophiolite, northeastern Finland. *Journal of Petrology 37*, 1359–1383.
Pharaoh, T.C. & Brewer, T.S., 1990: Spatial and temporal diversity of early Proterozoic volcanic sequences – comparisons between the Baltic and Laurentian shields. *Precambrian Research 47*, 169–189.

Pharaoh, T.C. & Pearce, J.A., 1984: Geochemical evidence for the geotectonic setting of early Proterozoic metavolcanic sequences in Lapland. *Precambrian Research 25*, 283–308.
Pharaoh, T.C., Warren, A., & Walsh, N.J., 1987: Early Proterozoic volcanic suites of the northernmost Baltic Shield. *Geological Society, London, Special Publication 33*, 41–58.
Reddy, S.M. & Evans, D.A.D., 2009: Palaeoproterozoic supercontinents and global evolution: correlations from core to atmosphere. *In:* S.M. Reddy, R. Mazumdr, D.A.D. Evans, A.S. Collins (eds): *Paleoproterozoic supercontinents and global evolution*. *Geological Society, London, Special Publication 323*, 1–26.
Rollinson, H., 1993: *Using geochemical data: evaluation, presentation, interpretation*. Longman Scientific & Technical, Harlow, UK, 352 pp.
Romer, R.L. & Boundy, T.M., 1988: Interpretation of lead isotope data from the uraniferous Cu-Fe-sulfide mineralizations in the Proterozoic greenstone belt at Kopparåsen, northern Sweden. *Mineralium Deposita 23*, 256–261.
Romer, R.L., Martinsson, O., & Perdahl, J.-A., 1994: Geochronology of the Kiruna iron ores and hydrothermal alterations. *Economic Geology 89*, 1249–1261.
Salvador, A. (ed.), 1994: *International stratigraphic guide. A guide to stratigraphic classification, terminology, and procedure*. International Union of Geological Sciences and Geological Society of America, 2nd edition, 214 pp.
Sandstad, J.S., Bjerkgård, T., Boyd, R., Ihlen, P., Korneliussen, A., Nlsson, J.-A., Often, M., Eilu, P., & Hallberg, A., 2012: Metallogenic areas in Norway. *In:* P. Eilu (ed) Mineral deposits and metallogeny of Fennoscandia. *Geological Survey of Finland, Special Paper 53,* 35–138.
Sarapää, O., Lauri, L.S., Ahtola, T., Al-Ani, T., Grönholm, S., Kärkkäinen, N., Lintinen, P., Torppa, A. & Turunen, P., 2015: *Discovery potential of hi-tech metals and critical minerals in Finland. Geological Survey of Finalnd, Report of Investigation 219*, 54 pp.
Scogings, A., Chesters, J. & Shaw, B., 2015: Rank and file: Assessing graphite projects on credentials. *Industrial Minerals Magazine,* August 2015, 50–55.
Self, S., Keszthelyi, L. & Thordarson, T., 1998: The importance of pāhoehoe. *Annual Reviews in Earth and Planetary Science 26*, 81–110.
Shaikh, N.A., 1972: Sammanställning over grafitförkomsterna i det centrala Vittangifältet, Norrbottens län. *Sveriges geologiska undersökning Brap 876,* 19 pp.
Skiöld, T., 1981: Radiometric ages of plutonic and hypabyssal rocks from the Vittangi–Karesuando area, northern Sweden. *GFF 103*, 317–329.
Skiöld, T., 1986. On the age of the Kiruna Greenstones, northern Sweden. *Precambrian Research 32*, 35– 44.
Skiöld, T., 1988: Implications of new U–Pb zircon chronology to early Proterozoic crustal accretion in northern Sweden. *Precambrian Research 38*, 147–164.
Skiöld, T. & Cliff, R.A., 1984: Sm–Nd and U–Pb dating of Early Proterozoic mafic–felsic volcanism in northernmost Sweden. *Precambrian Research 26*, 1–13.
Skiöld, T., Öhlander, B., Markkula, H., Widenfalk, L., & Claesson, L.-Å., 1993: Chronology of Proterozoic orogenic processes at the Archaean continental margin in northern Sweden. *Precambrian Research 64*, 225–238.
Skiöld, T., Öhlander, B., Vocke, Jr, R.D., & Hamilton P.J., 1988: Chemistry of proterozoic orogenic processes at a continental margin in Northern Sweden. *Chemical Geology 69,* 193–207.
Smith, M., Coppard, J., Herrington, R., & Stein, H., 2007: The geology of the Rakkurijärvi Cu–(Au) prospect, Norrbotten: A new iron-oxide–copper–gold deposit in northern Sweden. *Economic Geology 102*, 393–414.
Smith, M.P., Storey, C.D., Jefferies, T.E. & Ryan, C., 2009: In situ U–Pb and trace element analysis of accessory minerals in the Kiruna district, Norrbotten, Sweden: New constraints on the timing and origin of mineralization. *Journal of Petrology 50*, 2063–2094.
Smith, M.P., Gleeson, S.A. & Yardley, B.W.D., 2013: Hydrothermal fluid evolution and metal transport in the Kiruna District, Sweden: Contrasting metal behaviour in aqueous and aqueous–carbonic brines. *Geochimica et Cosmochimica Acta 102*, 89–112.

Smolkin, V.F., 1997: The Paleoproterozoic (2.5–1.7 Ga) midcontinent rift system of the northeastern Fennoscandian Shield. *Canadian Journal of Earth Sciences 34*, 426–443.

Stacey, J.S. & Kramers, J.D., 1975: Approximation of terrestrial lead isotope evolution by a two-stage model. *Earth and Planetary Science Letters 26*, 207–221.

Steiger, R.H. & Jäger, E., 1977: Convention on the use of decay constants in geo- and cosmochronology. *Earth and Planetary Science Letters 36*, 359–362.

Sun, S.-S. & McDonough, W.F., 1989: Chemical and isotopic systematics of oceanic basalts: implication for mantle composition and processes. *Journal of the Geological Society of London Special Publication 42*, 313–345.

Talbot, C.J., 2001: Weak zones in Precambrian Sweden. *Geological Society, London, Special Publications 186*, 287–304.

Talbot, C.J., & Koyi, H., 1995: Palaeoproterozoic intraplating exposed by resultant gravity overturn near Kiruna, northern Sweden. *Precambrian Research 72*, 199–225.

Talga Resources Ltd, 2014: *Annual report to shareholders*. www.talgaresources.com. 73 pp.

Talga Resources Ltd, 2016: *Vittangi graphite resource upgrade*. Press release from Talga Resources Ltd, May 2016. www.talgaresources.com.

Taylor, H.A., Jr., 2006: Graphite. *In:* J.E. Kogel, N.C. Trivedi, J.M. Barker & S.T. Krukowski (eds.): *Industrial Minerals and Rocks*, Society for Mining, Metallurgy and Exploration, 507–518.

Taylor, S.R. & McLennan S.M., 1985: *The Continental Crust: Its Composition and Evolution*. Blackwell Scientific Publications, Oxford. 312 pp.

Thiessien, R., 1986: Two-dimensional refold interference patterns. *Journal of Structural Geology 8*, 563–573.

Tice, M.M. & Lowe, D.R., 2006: The origin of carbonaceous matter in pre-3.0 Ga greenstone terrains: A review and new evidence from the 3.42 Ga Buck Reef Chert. *Earth Science Reviews 76*, 259–300.

Walker, R.J., Morgan, J.W., Hanski, E.J. & Smolkin, V.F., 1997: Re–Os systematics of Early Proterozoic ferropicrites, Pechenga Complex, northwestern Russia: evidence for ancient ^{187}Os-enriched plumes. *Geochimica et Cosmochimica Acta 61*, 3145–3160.

Wanhainen, C., Billström, K. & Martinsson, O., 2006: Age, petrology and geochemistry of the porphyritic Aitik intrusion, and its relation to the disseminated Aitik Cu-Au-Ag deposit, northern Sweden. *GFF 128*, 273–286.

Wanhainen, C., Broman, C., Martinsson, O. & Magnor, B., 2012: Modification of a Palaeoproterozoic porphyry-like system: Integration of structural, geochemical, petrographic, and fluid inclusion data from the Aitik Cu–Au–Ag deposit, northern Sweden. *Ore Geology Reviews 48*, 306–331.

Wanke, A., & Melezhik, V., 2005: Sedimentary and volcanic facies recording the Neoarchaean continent breakup and decline of the positive $\delta^{13}C_{carb}$ excursion. *Precambrian Research 140*, 1–35.

Wasström, A., 2005: Petrology of a 1.95 Ga granite–granodiorite–tonalite–trondhjemite complex and associated extrusive rocks in the Knaften area, northern Sweden. *GFF 127*, 67–82.

Weihed, P., Arndt, N., Billström, K., Duchese, J.-C., Eilu, P., Martinsson, O., Papunen, H. & Lahtinen, R., 2005: Precambrian geodynamics and ore formation: The Fennoscandian Shield. *Ore Geology Reviews 27*, 273–322.

Welin, E., 1987: The depositional evolution of the Svecofennian supracrustal sequence in Finland and Sweden. *Precambrian Research 35*, 95–113.

Wiedenbeck, M., Allé, P., Corfu, F., Griffin, W.L., Meier, M., Oberli, F., Quadt, A.V., Roddick, J.C. & Spiegel, W., 1995: Three natural zircon standards for U-Th-Pb, Lu-Hf, trace element and REE analyses. *Geostandards Newsletter 19*, 1–23.

Wiedenbeck, M., Hanchar, J.M., Peck, W.H., Sylvester, P., Valley, J., Whitehouse, M., Kronz, A., Morishita, Y., Nasdala, L., Fiebig, J., Franchi, I., Girard, J.P., Greenwood, R.C., Hinton, R., Kita, N., Mason, P.R.D., Norman, M., Ogasawara, M., Piccoli, P.M., Rhede, D., Satoh, H., Schulz-Dobrick, B., Skår, O., Spicuzza, M.J., Terada, K., Tindle, A., Togashi, S., Vennemann, T., Xie, Q. & Zheng, Y.F., 2004: Further characterisation of the 91500 zircon crystal. *Geostandards and Geoanalytical Research 28*, 9–39.

Whitehouse, M.J., Claesson, S., Sunde, T. & Vestin, J., 1997: Ion-microprobe U–Pb zircon geochronology and correlation of Archaean gneisses from the Lewisian Complex of Gruinard Bay, north-west Scotland. *Geochimica et Cosmochimica Acta 61*, 4429–4438.

Whitehouse, M.J., Kamber, B.S. & Moorbath, S., 1999: Age significance of U–Th–Pb zircon data from Early Archaean rocks of west Greenland: a reassessment based on combined ion-microprobe and imaging studies. *Chemical Geology 160*, 201–224.

Whitehouse, M.J. & Kamber, B.S., 2005: Assigning dates to thin gneissic veins in high-grade metamorphic terranes: a cautionary tale from Akilia, southwest Greenland. *Journal of Petrology 46*, 291–318.

Wikström, A., Skiöld, T., & Öhlander, B., 1996: The relationship between 1.88 Ga old magmatism and the Baltic-Bothnian shear zone in northern Sweden. *Geological Society, London, Special Publication 112*, 249–259

Williams, I.S., 1998: U-Th-Pb geochronology by ion microprobe. *In:* M.A. McKibben, W.C. Shanks III & W.I. Ridley (eds.): Applications of microanaytical techniques to understanding mineralizing processes. *Reviews in Economic Geology 7*, 1–35.

Wilson, M., 1989: *Igneous Petrogenesis. A Global Tectonic approach*. Unwin Hyman, London, 466 pp.

Wilson, M.R., Hamilton, P.J., Fallick, A.E., Aftalion, M. & Michard, A., 1985: Granites and early Proterozoic crustal evolution in Sweden: evidence from Sm-Nd, U-Pb and O isotope systematics. *Earth and Planetary Science Letters 72*, 376–388.

Winchester, J.A. & Floyd, P.A., 1977: Geochemical discrimination of different magma series and their differentiation products using immobile elements. *Chemical Geology 20*, 325–343.

Witschard, F., Nylund, B. & Mannström, B. 1972: Masugnsbyn iron ore. Report concerning the results of Sveriges geologiska undersökning:s investigations in the years 1965-1970. *Sveriges geologiska undersökning Brap 734*, 95 pp.

Witschard, F., 1984: The geological and tectonic evolution of the Precambrian of northern Sweden – A case for basement reactivation? *Precambrian Research 23*, 273–315.

Zaki, N., 2015: Masugnsbyns dolomitbrott, redovisning av dolomittillgång. Unpublished *LKAB report 15-20003*, 30 pp.

Geological Survey of Sweden
Box 670
SE-751 28 Uppsala
Phone: +46 18 17 90 00
Fax: +46 18 17 92 10
www.sgu.se

Uppsala 2018
ISSN 0349-2176
ISBN 978-91-7403-393-9
Tryck: Elanders Sverige AB